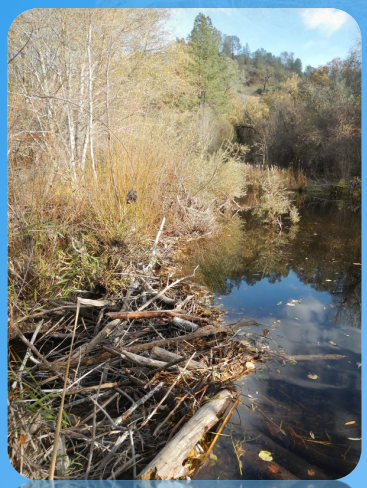

Long-Term Streamflow and Precipitation Trends in the Eel River Basin

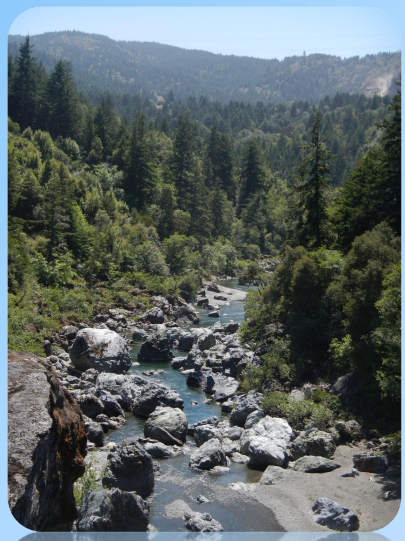

J. Eli Asarian
Riverbend Sciences

October 2015

Riverbend Sciences

Prepared for:

FRIENDS OF THE EEL RIVER

Working for the recovery of our Wild & Scenic River, its fisheries and communities

Long-Term Streamflow and Precipitation Trends in the Eel River Basin

J. Eli Asarian
Riverbend Sciences
P.O. Box 2874
Weaverville, CA 96093

Prepared for:
Friends of the Eel River
P.O. Box 4945
Arcata, CA 95518

October 2015

Suggested citation:

Asarian, J.E. 2015. Long-Term Streamflow and Precipitation Trends in the Eel River Basin. Prepared by Riverbend Sciences for Friends of the Eel River, Arcata, CA. 30p. + appendices.

Photo credits for cover page:

All photos by Eli Asarian

EXECUTIVE SUMMARY

This report analyzes long-term (1953-2014 in most cases, but some analyses span back as far as 1910) trends in streamflow and precipitation in the Eel River Basin, located on California's North Coast. I evaluated trends in streamflow and precipitation-adjusted streamflow separately for each of the 365 days of the year, providing greater temporal detail than a previous analysis (Asarian and Walker *in press*) that used similar methods but a monthly time step.

I obtained daily streamflow data for ten long-term stream gages from the U.S. Geological Survey. The mainstem and South Fork of the Eel River have multiple streamflow gages, allowing for the calculation (i.e., downstream flow minus upstream flow) of "accretions" between gages, which represents the net contributions of all tributaries, springs, and groundwater, minus any diversions. I combined data from several nearby precipitation stations to calculate a time series of Antecedent Precipitation Index (API) for the watershed contributing to each streamflow site. API is a time-weighted summary of precipitation which provides high weight to recent precipitation and low weight to precipitation that occurred many months ago. I used a regression model of the relationship between API and streamflow to calculate "precipitation-adjusted streamflow", which statistically reduced the year-to-year fluctuations caused by variable precipitation and allowed evaluation of the underlying streamflow trend.

For the five long-term benchmark precipitation stations closest to the Eel River Basin (there are none within the Basin), there were no statistically significant trends in annual total precipitation for 1880-2014 or any shorter period ending in 2014; however, decadal and multi-decadal cycles are evident. Monthly trends included decreased January precipitation since the mid-20th century at all five stations and increased March precipitation since the early 20th century at Orleans, Eureka, and Fort Bragg. Only one benchmark station (Weaverville) had decreasing September precipitation for 1953-2014, contrary to a previous analysis (Asarian and Walker *in press*) which found geographically widespread declines in September precipitation for 1953-2012.

I characterized trends by both their duration (i.e., the number of days with a statistically significant decreasing or increasing trend) and their magnitude (i.e., slope, the amount of change that occurred across the 1953-2014 trend period). For each day of the year, I express magnitude in three ways:
1) absolute trend magnitude (i.e., annual slope of the trend) in units of cubic feet per second per year,
2) relative trend magnitude (i.e., annual slope of the trend relative to 1953-2014 median flow) in units of percent per year, and
3) trend magnitude normalized to watershed area (i.e., absolute trend magnitude divided by watershed area) in units of cubic meters per day per square kilometer of watershed area.

Both streamflow and precipitation-adjusted streamflow declined at most tributary sites in the Eel River Basin during the low-flow season over the 1953-2014 period, especially from July through mid-October when streamflows are lowest. At most tributary sites, the number of days of the year with a declining trend was higher for precipitation-adjusted streamflow than streamflow (Figure ES-1), likely because accounting for precipitation reduces inter-annual fluctuations that can impair statistical detection of streamflow trends. The relative magnitude of declines (i.e., the slope of the trend) was higher for streamflow than for precipitation-adjusted streamflow, indicating that precipitation patterns are contributing to streamflow declines (i.e., dry years are more frequent in recent years than in the early decades of the 1953-2014 trend period).

The number of days of the year with a declining streamflow trend for the 1953-2014 period varied among tributary sites (Figure ES-1), with the fewest number of days at Elder Creek, Middle Fork Eel River, and accretions between Fort Seward and Scotia, followed by the South Fork Eel at Leggett. The relative magnitude (i.e., annual trend slope as a percent of 1953-2014 median flow) of declining trends were steepest (up to 6% per year for late August and September) for accretions to the mainstem Eel River from Van Arsdale to Fort Seward, but when normalized to watershed area (i.e., absolute trend magnitude divided by watershed area) the declines were actually among the least steep. The relative magnitude of declining trends were also steep (greater than 2% per year for late August and September) at Bull Creek and accretions to the South Fork Eel between Leggett and Miranda. The relative magnitude of declines at the Van Duzen River and the combined accretions from Van Arsdale to Scotia (includes the entire South, Middle, and North forks of the Eel River) were ~1% in August through mid-October; compared to Bull Creek and accretions to the South Fork Eel between Leggett and Miranda, the relative magnitude of declines is lower but the numbers of days with declines is similar.

Trends in streamflow and precipitation-adjusted streamflow at mainstem Eel River stations for the 1953-2014 period show a clear upstream/downstream pattern, with large increases directly below Van Arsdale Dam (2-15% per year during April through December), almost no trends at Fort Seward (the next mainstem gage) as decreased contributions from the tributaries and/or increased diversions from the mainstem offset increased Van Arsdale releases, and then declines at Scotia (the furthest downstream gage) of similar magnitude/duration as those of the tributaries (Figure ES-1).

With the exception of precipitation quantity, the methods used in this analysis do not allow individual quantification of the factors contributing to streamflow declines. However, the long-term streamflow gages include a diverse range of watershed and climate conditions. Thus, we can hypothesize about causal mechanisms by carefully examining the trends that have occurred in watersheds with different conditions/histories. Potential factors include increased water diversions and/or increased evapotranspiration by vegetation/forests. Increased evapotranspiration could be due to climate (i.e., air temperature, wind, humidity, or precipitation shifting from snow to rain) and/or structure/composition of vegetation.

Elder Creek is one of the most pristine watersheds within the Eel River Basin, with almost no diversions, roads, or history of timber harvest. Elder Creek had declining trends in streamflow but not precipitation-adjusted streamflow. In other words, Elder Creek maintained its relationship between precipitation and streamflow through the 1953-2014 period, in contrast to most other sites where the relationship diverged. This suggests that streamflow decreases at other sites are more likely the result of increased water withdrawals and/or vegetation structure/composition changes than other (i.e., aside from precipitation quantity) climate factors. As the planet continues to warm, even pristine watersheds like Elder Creek will likely experience streamflow declines due to the increased evapotranspiration resulting from increased temperatures.

This study did not quantify water diversions but precipitation-adjusted streamflow trends from the previous analysis (Asarian and Walker *in press*), and to a lesser extent this study[1], suggest that diversions are an important factor influencing summer streamflow declines. California Department of Fish and Wildlife estimates for marijuana-related water use within five Northwest California watersheds

[1]There are only two stream gages not affected by diversions, so the sample size is small.

range from approximately 1 to 10 cubic meters of water per day per square kilometer of watershed area. In comparison, the total magnitude of the decline in precipitation-adjusted streamflows across the entire 62 year period 1953-2014 (i.e., annual trend magnitude multiplied by 62 years) during the months of July-October in this study was in the range of 30 to 100 cubic meters of water per day per square kilometer of watershed area for most tributary sites, indicating that water diversions for marijuana cultivation likely explain only a relatively small fraction (i.e., roughly 1% to 33%) of the total declines. These results do not mean that water diversions for marijuana cultivation do not have serious, even catastrophic, effects on streamflows in many Eel River Basin streams, including those with the highest value salmonid habitats, it just means that these diversions are only a partial explanation for basin-scale declines in streamflow. Despite being responsible for only a portion of streamflow declines, recent increases in diversions are a key additional impact compounding with previous impacts. Furthermore, diversions are perhaps the only factor causing streamflow declines that could actually be substantively addressed in the near-term (i.e., water can be stored in tanks and ponds when it is abundant during winter and early spring, offsetting the need for summer diversions).

Because evapotranspiration is such a large portion of the annual water budget, small changes in evapotranspiration have the potential for large effects on summer streamflows. The Eel River Basin's forests have undergone substantial changes in the past century as a result of timber harvest and fire suppression. Without fire or mechanical intervention, Douglas-fir trees are invading prairies and oak woodlands, potentially increasing evapotranspiration. The young dense forests of the Eel River Basin may be in a state of maximum evapotranspiration. Bull Creek provides evidence supporting the hypothesis that vegetation change is contributing to streamflow declines, because despite lacking water diversions it had the largest number of days (and nearly the greatest magnitude of declines) with declining precipitation-adjusted streamflow (Figure ES-1), coinciding with the regeneration of its forests following intensive logging that occurred prior to installation of the stream gage in 1960.

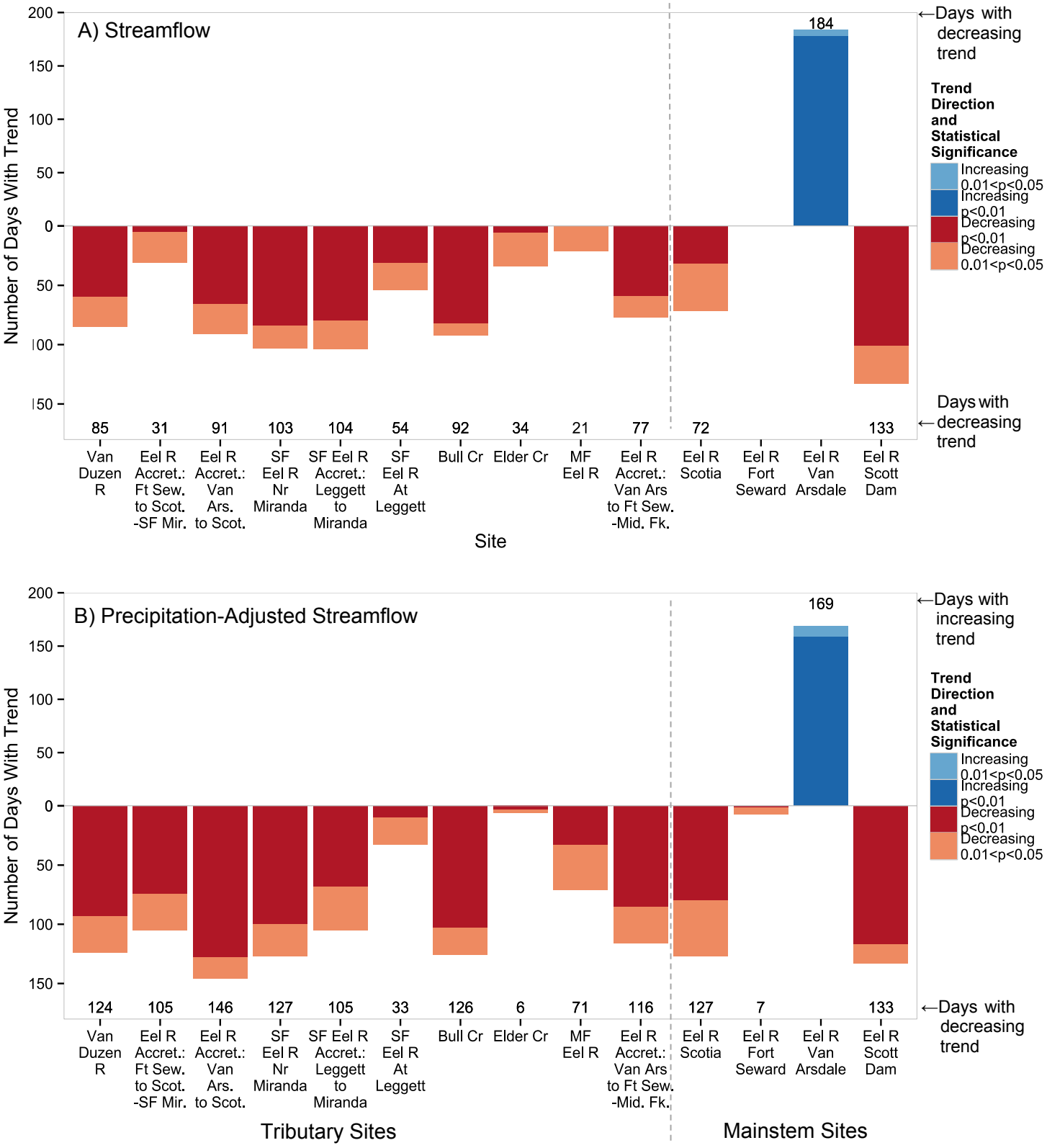

Figure ES-1. The number of days in May through October (184 possible days) with increasing or decreasing trends in (A) streamflow and (B) precipitation-adjusted streamflow at mainstem and tributary sites for WY1953-2014. Bars are stacked with colors indicating statistical significance and labels indicating the total number of days with an increasing or decreasing trend.

TABLE OF CONTENTS

LIST OF FIGURES

LIST OF TABLES

1 INTRODUCTION

1.1 DESCRIPTION OF STUDY AREA

The Eel River Basin is located on the North Coast of California (Figure 1). The area has a Mediterranean climate with primarily mountainous terrain. Vegetation includes conifer forests, oak woodlands, and grasslands. Streamflows vary strongly by season, with streamflows during the rainy winter several orders of magnitude higher than during the dry summer and early fall (Power et al. 2015). The Basin is home to four species of salmonid fishes: chinook salmon (*Oncorhynchus tshawytscha*), coho salmon (*Oncorhynchus kisutch*), steelhead trout (*Oncorhynchus mykiss*), and coastal cutthroat trout (*Oncorhynchus clarki clarki*). Chinook, coho, and steelhead are protected under the federal Endangered Species Act and all have declined greatly from historical levels (Yoshiyama and Moyle 2010).

The only significant dams in the Eel River Basin are Scott Dam and Cape Horn Dam on the upper mainstem, which are part of the Potter Valley Project and form Lake Pillsbury and Van Arsdale Reservoir, respectively (NMFS 2014). The largest water diversion in the Basin is from Van Arsdale Reservoir though a tunnel into the adjacent Russian River Basin (NMFS 2002). There are many smaller surface water diversions and groundwater wells associated with rural residences and marijuana cultivation sites throughout the Basin (Bauer et al. 2015, Power et al. 2015); pastures and forage crops in the Eel River Delta (Ferndale/Loleta), Little Lake Valley (Willits), Round Valley (Covelo), Long Valley (Laytonville); and municipal water systems including the communities of Willits, Scotia, Fortuna, Loleta, Ferndale, Laytonville, Redway, and Garberville.

Since California legalized medical marijuana in 1995, marijuana cultivation has expanded dramatically in the Basin, with associated increases in water diversions (Bauer et al. 2015). Inadequate summer streamflow has been identified as a primary contributor to declining populations of coho salmon in the Basin (NMFS 2014, Bauer et al. 2015).

1.2 PREVIOUS EEL RIVER BASIN STREAMFLOW TREND STUDIES

U.S. Geological Survey (USGS) has operated a network of streamflow gages within the Eel River Basin for many decades, providing data which can be used to assess long-term trends. Most previous analyses of streamflow trends at these gages (Kim and Jain 2010, Madej 2011, and Sawaske and Freyberg 2014) were intended to assess regional climate change and thus only examined streams that were relatively un-impacted by human activities. These studies did detect summer streamflow declines at many sites within the Basin.

As part of the development of an Endangered Species Act recovery plan for coho salmon, the National Marine Fisheries Service (NMFS) commissioned an analysis of streamflow trends for all long-term streamflow gages within the range of the Southern Oregon/Northern California Coast (SONCC) Evolutionarily Significant Unit (ESU) of coho salmon for the period 1953-2012 (Asarian 2014). The study was subsequently reformatted for submission to a peer-reviewed journal and is currently undergoing review (Asarian and Walker *in press*). The study included a statistical model to account for the variability in streamflow due to precipitation, so that underlying trends in "precipitation-adjusted streamflow" could be assessed. Most analyses in that study, including the streamflow/precipitation model, were conducted on a monthly timestep.

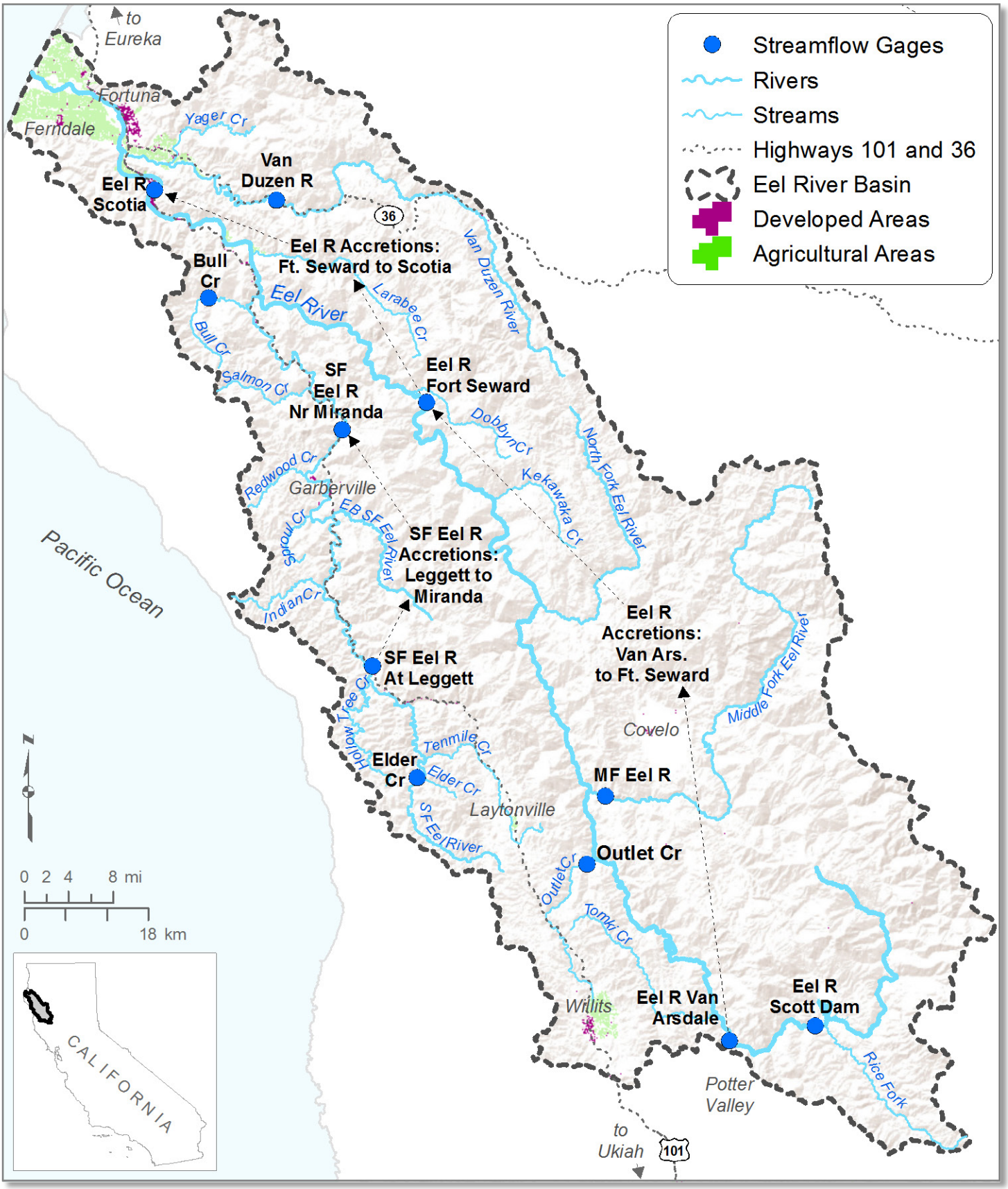

Figure 1. Location of USGS long-term streamflow gages in the Eel River Basin of California, as well as calculated accretions between stream gages (see Section 2.2 for description of accretions).

1.3 STUDY GOALS

The goal of this study is to assess long-term trends in precipitation, streamflow, and precipitation-adjusted streamflow in the Eel River Basin. This study employs similar methods as Asarian (2014), but differs by: 1) analyzing data on a daily rather than monthly basis, 2) includes additional years (2013, 2014, and part of 2015), 3) is restricted to Eel River Basin rather than the entire Southern Oregon/ Northern California Coast region, and 4) does not include estimates of human water consumption.

2 METHODS

2.1 STREAMFLOW DATA

Streamflow data for eleven gages were downloaded from the U.S. Geological Survey (USGS) National Water Information System[2] (NWIS) (Figure 1, Table 1). Most of the gages are on the larger rivers, but there are two smaller tributaries (Bull Creek and Elder Creek).

Table 1. Site information for streamflow gages (first eleven rows) and calculated accretions between streamflow gages (bottom four rows).

Gage Name (Abbreviated)	Gage ID	Basin Area (km^2)	Mean Elev. (m)	Max Elev. (m)	Annual Precip. (cm)	Flow Reg.	Streamflow Period of Record
Eel R. Scotia	11477000	8062	786	2306	159	Y	1911-1914, 1917-2014
Eel R. Fort Seward	11475000	5457	922	2306	154	Y	1956-2014
Eel R. Van Arsdale	11471500	904	1070	2140	138	Y	1911-1926, 1928-2014
Eel R. Scott Dam	11470500	750	1111	2140	138	Y	1923-2014
Van Duzen R.[1,2]	11478500	572	923	1788	166	N	1951-2014
South Fork Eel R. At Leggett[1]	11475800	642	626	1289	192	N	1966-94, 2000-04, 2008-14
South Fork Eel R. Nr Miranda	11476500	1390	526	1289	185	N	1940-2014
Bull Cr.[1,2]	11476600	72	473	1023	182	N	1961-2014
Elder Cr.[1,2]	11475560	17	848	1277	247	N	1968-2014
Outlet Creek	11472200	419	598	1042	143	Y	1957-1994
Middle Fork Eel R.[1,2]	11473900	1925	1122	2306	154	N	1966-2014
Eel R. Accretions: Ft Seward - Van Ars. – M. Fork		2628	725	1882	159	N	1966-2014
Eel R. Accretions: Scotia – Ft. Seward – S. Miranda		1215	470	1710	155	N	1956-2014
Eel R. Accretions: Scotia - Van Arsdale		7158	750	2306	162	N	1911-1926, 1928-2014
South Fork Eel R. Accretions: Miranda - Leggett		748	440	1245	179	N	1966-94, 2000-04, 2008-14

Notes: Basin elevation, area, and precipitation were computed for the catchment area contributing to site. Sites were classified as regulated if combined volume of reservoir(s) is >0.5% of watershed precipitation if mainstem reservoirs present or >2% if mainstem reservoirs absent.
[1]Site listed as "reference" by GAGES-II (Falcone 2011).
[2]Site included in USGS HydroClimatic Data Network (HCDN) 2009 (Lins 2012).

2.2 ESTIMATED ACCRETIONS BETWEEN GAGES

The mainstem Eel River and South Fork Eel River have multiple gages, allowing for the calculation of accretions between gages. The calculated accretion represents the net contributions of all tributaries, springs, and groundwater, minus any diversions.

[2] http://waterdata.usgs.gov/nwis

Because they are derived from multiple (two or three) gages, the calculated accretions also inherently include the combined measurement error of all the component gages and are therefore substantially less accurate than flows measured at individual gages. Interpretations of accretion calculations must take into account this decreased accuracy. Despite the increased uncertainty, the four calculated accretions provide valuable data to supplement the relatively sparse network of streamflow gages within the study area (Figure 1, Table 1). These accretions are calculated as the downstream flow minus the upstream flow minus any additional gaged tributaries. The accretions were calculated on a daily basis and then smoothed with a 7-day average to reduce the frequency of negative values. Negative values can result from a number of factors including: measurement error, water diversions, and downstream transit of high flood peaks.

2.3 CALCULATION OF STREAMFLOW METRICS

Key streamflow metrics were selected based on a review of previous hydrologic analyses (Poff 1996, Madej 2011, Mayer and Naman 2011, Chang et al. 2012, Asarian 2015) and calculated for each gage and year, including: minimum flow, the minimum 7-day average flow, minimum 30-day average flow, minimum 90-day average flow, average flow for each month, annual mean flow, and center of timing of streamflow (the date by which 50 percent of the runoff in a water year has occurred). Minimum flow and minimum 7-day average flow were not calculated for accretions between gages due to the increased uncertainty at shorter time scales. Metrics were calculated using R (R Core Team 2012).

2.4 PRECIPITATION DATA SOURCES

I used three precipitation datasets for this analysis. I used the monthly U.S. Historical Climatology Network (USHCN) to assess long-term regional trends in monthly and annual precipitation because it is the highest quality dataset available, with stations selected by the National Oceanic and Atmospheric Administration's (NOAA) National Centers for Environmental Information (NCEI) and Department of Energy's Carbon Dioxide Information Analysis Center (CDIAC) based on record longevity, percentage of missing values, and other factors that affect data reliability (Menne et al. 2015). Quality control review by NCEI and CDIAC includes estimation of some gaps, so the resulting dataset is generally continuous (Menne et al. 2015). There are no USHCN stations within the Eel River basin, but nearby stations span back to the mid/late 19th century, with the oldest record being 1871 in Weaverville (Figure 2). The dataset is only updated once annually, so the most recent data is December 31, 2014.

To make statistical comparisons with streamflow data, I primarily used daily precipitation data from the Global Historical Climatology Network (GHCN), which is also maintained by NOAA's NCEI. Data were downloaded directly into R using the rnoaa package (Edmund et al. 2014). There are many GHCN stations within the Eel River Basin and nearby areas (Figure 2), but also many gaps in the records for most stations (Appendix A). I also used some data from the California Data Exchange Center (CDEC) automated rain gages.

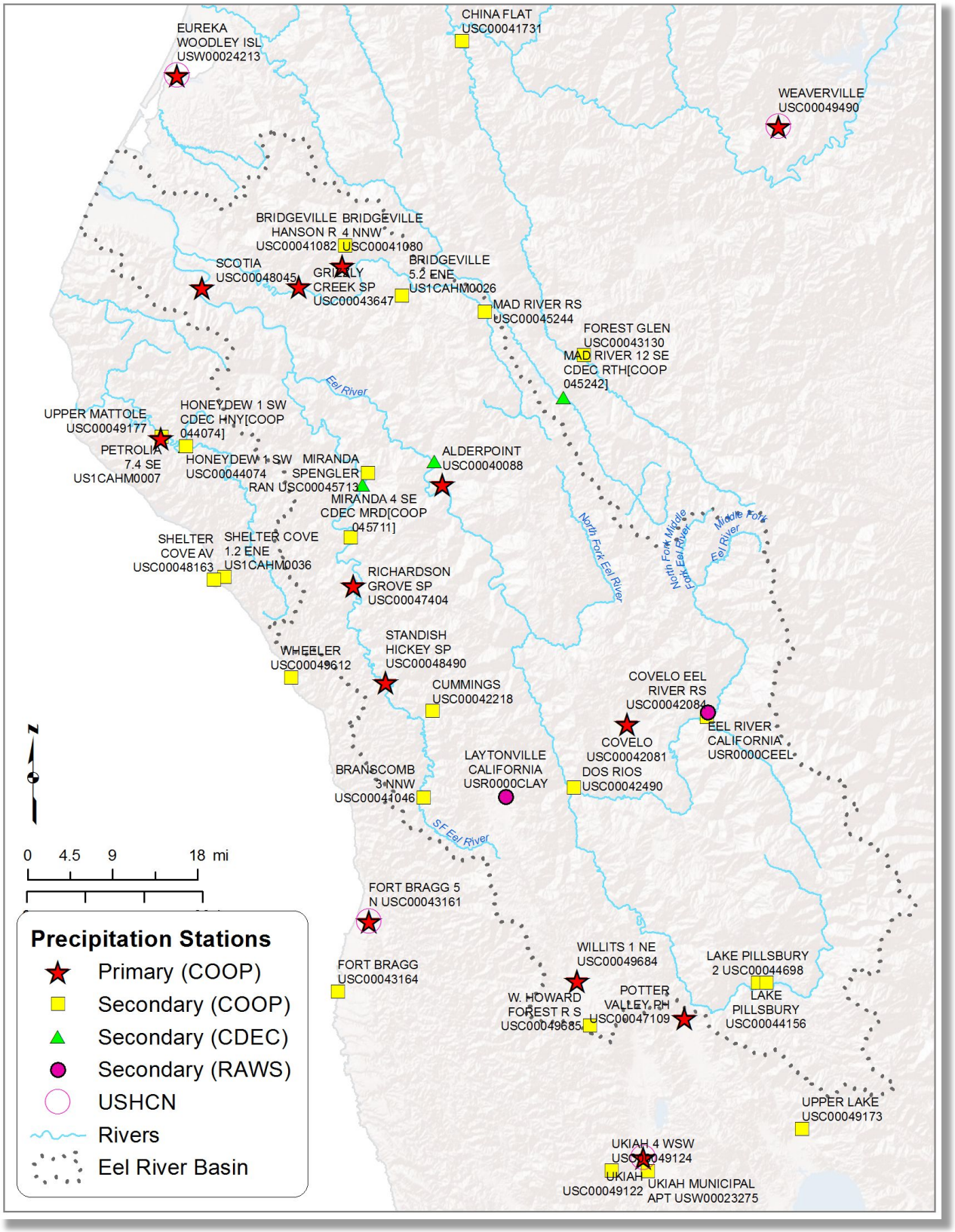

Figure 2. Location of selected precipitation stations in the Eel River Basin and adjacent areas from the Global Historical Climatology Network (GHCN) database, U.S. Historical Climatology Network (USHCN), and the California Data Exchange Center (CDEC).

2.5 QUALITY CONTROL AND FILLING GAPS IN PRECIPITATION DATA

Temporally continuous precipitation records were required for this project, so gaps in primary precipitation gages were filled through linear regression of data from a nearby station. A station was only used to fill gaps if there was a minimum of 36 months of overlapping data upon which a regression could be constructed. Regression equations were developed from monthly totals, but applied to daily data. The gaps were typically filled using the nearby station with the highest correlation (Figure 3), although in some cases stations with longer-term datasets were given priority so that the number of nearby stations used to fill gaps was minimized. A matrix showing which gages were used to fill gaps in records for primary precipitation gages is available in Appendix A.

The CDEC daily summaries are calculated from 24-hour periods ending at midnight, whereas the GHCN data reporting periods generally ended at another time of day (e.g., 6pm). The CDEC data are published as preliminary and not quality-controlled, so I spent considerable time reviewing the data and removing high outlier values. In spite of that effort, the correlation[3] between the CDEC data and GHCN data was lower than expected even for stations located within a few miles of each other, and therefore the only CDEC station I ended up using was Bridgeville (BGV).

Before settling on filling gaps using linear regression from a nearby station, I experimented with more complex modern statistical approaches[4], but was unsuccessful due to the extremely large size of the dataset. In retrospect, rather than using data from individual stations and then having to fill gaps, it would have been better (possibly more accurate and certainly much more time efficient), to use existing spatially and temporally continuous modeled daily precipitation datasets such as Livneh et al. (2013 and 2014) and PRISM (Parameter-elevation Relationships on Independent Slopes Model) AN81d (Di Luzio et al. 2008)[5]; however, it is unlikely that using these alternative precipitation datasets would substantially alter the overall results or conclusions of this study. The Livneh dataset is available[6] for 1915-2011 but the PRISM AN81d dataset is only available[7] for 1981-present and updated continuously, so it should be possible to use the overlapping 1981-2011 period to develop regressions between the two datasets for each geographic area of interest and derive a continuous record for 1915-present[8]. Livneh and colleagues have also developed a 1950-2013 daily dataset[9].

2.6 ASSIGNING PRECIPITATION STATIONS TO STREAMFLOW SITES

After gaps were filled, I initially[10] assigned one to five precipitation stations to each streamflow site based on proximity (priority was given to precipitation stations located within the watershed contributing the streamflow site, but some stations in adjacent watershed were also used) and long-term consistency (priority given to stations with few gaps). Precipitation values were then averaged across stations to obtain a daily time series of precipitation for each streamflow station.

---

[3] i.e., how similar precipitation values were between two stations for a shared time period (days or months).
[4] Examples include k-Nearest Neighbour Imputation ("kNN" function in "VIM" R package, Templ et al. 2013) and Multivariate Imputation by Chained Equations ("mice" R package, van Buuren 2011).
[5] http://www.prism.oregonstate.edu/documents/PRISM_datasets.pdf
[6] Online at ftp://ftp.hydro.washington.edu/pub/blivneh/CONUS/
[7] Online at http://www.prism.oregonstate.edu/recent/ and http://www.prism.oregonstate.edu/6month/
[8] The Livneh and PRISM datasets use different spatial interpolation methods. Grid resolution also differs (~4km [1/24 degree] for PRISM, ~6km [1/16 degree] for Livneh). In addition, precipitation values for each grid cell in the Livneh dataset were scaled so that the 1915-2011 mean matches the long-term normals from the 1961–1990 PRISM climatology. The most recent version of the PRISM AN81d uses the long-term normals from the 1981-2010 PRISM climatology.
[9] ftp://gdo-dcp.ucllnl.org/pub/dcp/archive/OBS/livneh2014.1_16deg/
[10] As described in section 2.7.3 below, the assignment of precipitation stations to streamflow sites was also refined based on how well each precipitation station could predict the observed streaflow.

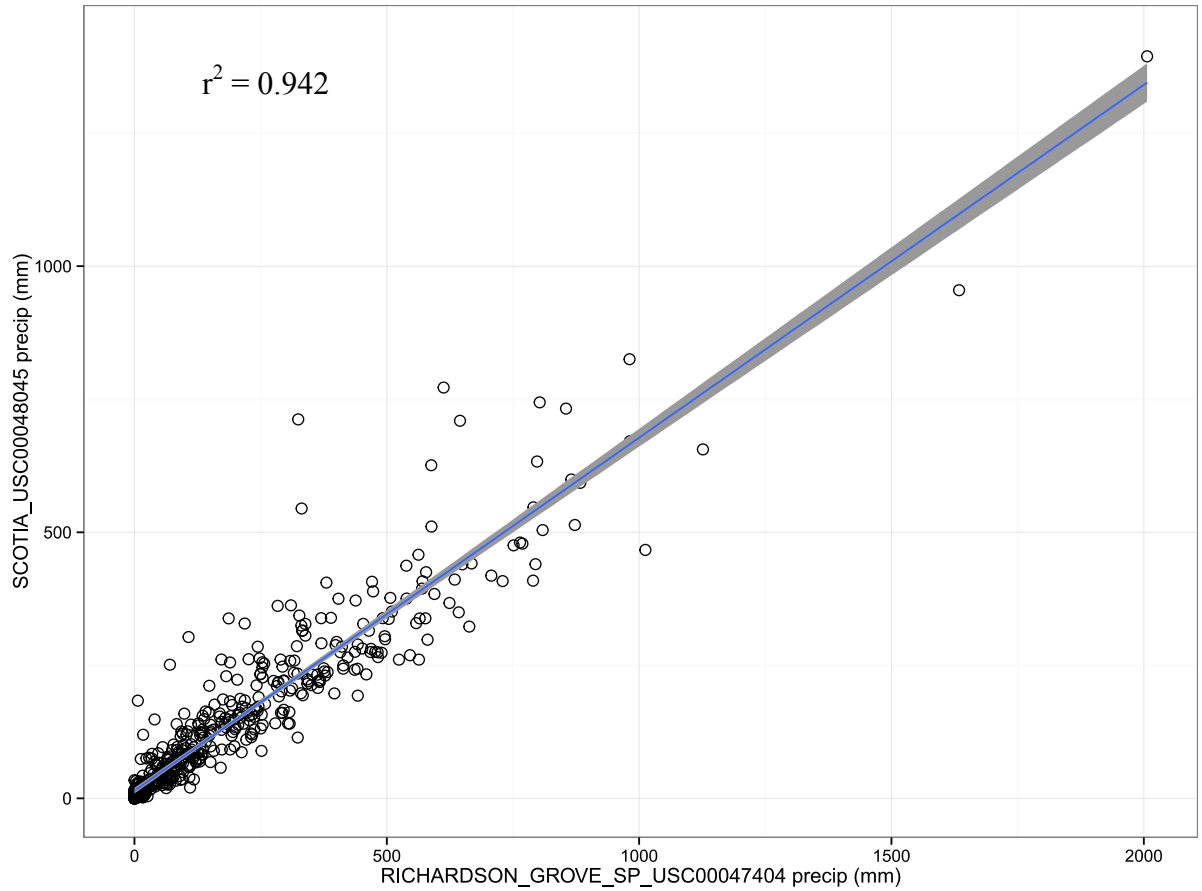

Figure 3. Regression of monthly precipitation at Scotia (GHCND:USC00048045) versus monthly precipitation at Richardson's Grove (GHCND:USC00047404), with the r^2 value of 0.942 indicating an excellent correlation between the two sites.[11]

2.7 CALCULATION OF "PRECIPITATION-ADJUSTED STREAMFLOW" TO ACCOUNT FOR PRECIPITATION VARIABILITY

Precipitation is the source of streamflow and is therefore highly correlated with streamflow. Precipitation is highly variable between years, which can obscure underlying trends in streamflow that result from changes in other climate factors aside from precipitation (e.g., air temperature, wind, humidity, coastal fog, etc.), water consumption by vegetation, or extraction of water by people. When the variation in streamflow due to precipitation is removed, the underlying trends in streamflow become more visible (Helsel and Hirsch 2002).

[11] r^2 is the "coefficient of determination", which is a measure of how linear the relationship between the two variables is. An r^2 value of 1 indicates that the regression line data fits the data perfectly, while an r^2 value of 0 indicates the regression line does not fit the data at all.

2.7.1 ANTECEDENT PRECIPITATION INDEX (API)

To remove the variability in streamflow due to precipitation, I used a statistical model which relates streamflow to Antecedent Precipitation Index (API).

API is a time-weighted summary of precipitation, with precipitation in the current period assigned full weight and each preceding period assigned a successively lower weight. API is a proxy for soil moisture and can be used to predict streamflow (Figure 4) (Reid and Lewis 2011, Klein 2012, Asarian and Walker *in press*). I calculated API for each site at a daily timestep by combining the precipitation on a given day with a weighted sum of precipitation in the preceding 364 days according to the following formulas:

$$API_i = (P_i) + (P_{i-1})(k^1) + (P_{i-2})(k^2) + (P_{i-3})(k^3) + \ldots + (P_{i-364})(k^{364})$$

Where API_i is Antecedent Precipitation Index for month *i* in units millimeters, P*i* is precipitation for month *I* in units of millimeters, and k is a dimensionless recession coefficient ranging from 0 to 1 which is specific to the gage and day. The recession coefficient k governs how heavily previous precipitation is discounted[12] . I adjusted the recession coefficient k separately for each site and day to maximize the fit between precipitation and streamflow.[13] Figure 4 provides an example illustration of a daily time series of precipitation, antecedent precipitation index (API), and streamflow.

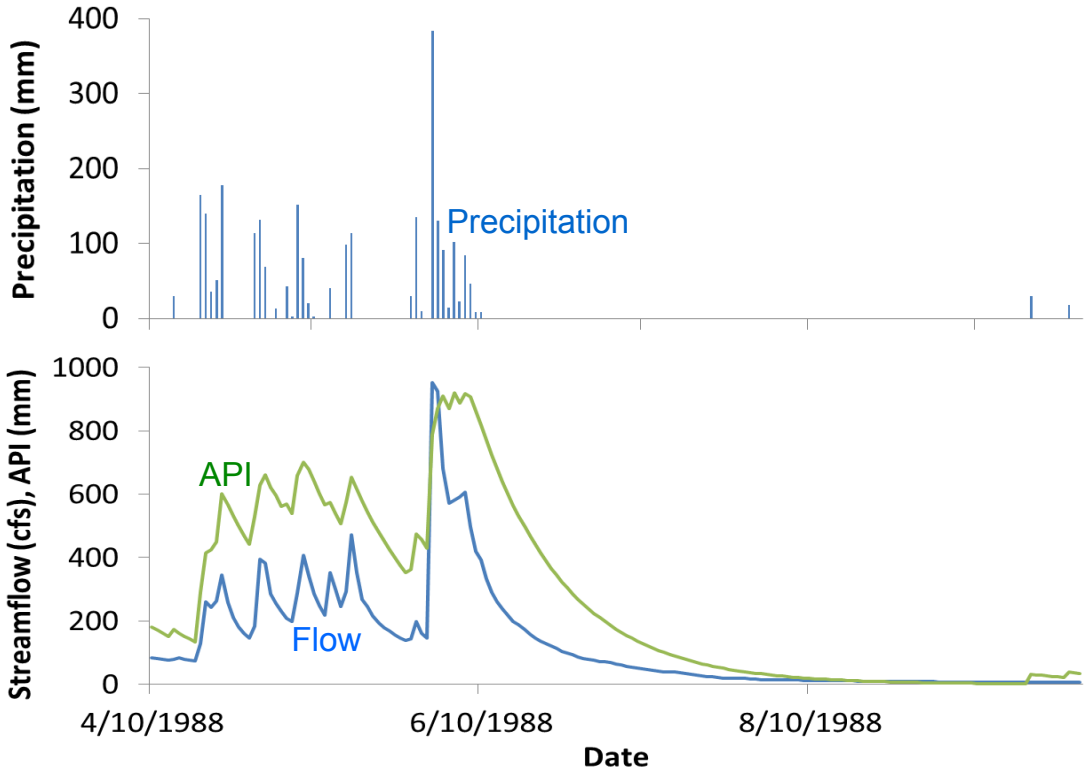

Figure 4. Daily time series of precipitation, antecedent precipitation index (API), and streamflow at an example site.

[12] k value of 0 means precipitation from previous days is discounted to zero, while a k value of 1 means that precipitation from previous days receives equal weight to precipitation from the current day)

[13] In technical terms: I calibrated k to maximize the Spearman's rank correlation coefficient (Spearman's rho) between observed streamflow and API.

2.7.2 STATISTICAL MODEL OF RELATIONSHIP BETWEEN STREAMFLOW AND API

For each streamflow site and day, I constructed a scatterplot of daily streamflow vs API (Figure 5) and then fit a Locally Estimated Scatterplot Smoothing (LOESS) regression curve (Helsel and Hirsch 2002). The LOESS curve in the flow versus API model is a quantitative description of the overall (i.e., best fit) relationship between flow and precipitation across the entire period of record of streamflow; however, the observed values for any given year rarely lie exactly on the LOESS curve (Figure 5). The difference between the observed value (i.e., daily measured streamflow for a particular day and year) and the expected value (i.e., the modeled streamflow for a particular day and year, based on the LOESS relationship between API and flow across the period of record [all years] for that particular day) is referred to as the "residual"[14] (Figure 5). These residuals represent the variability in streamflow that is not explained by the variability in precipitation and are referred to in this report as "precipitation-adjusted streamflow" (Helsel and Hirsch 2002).

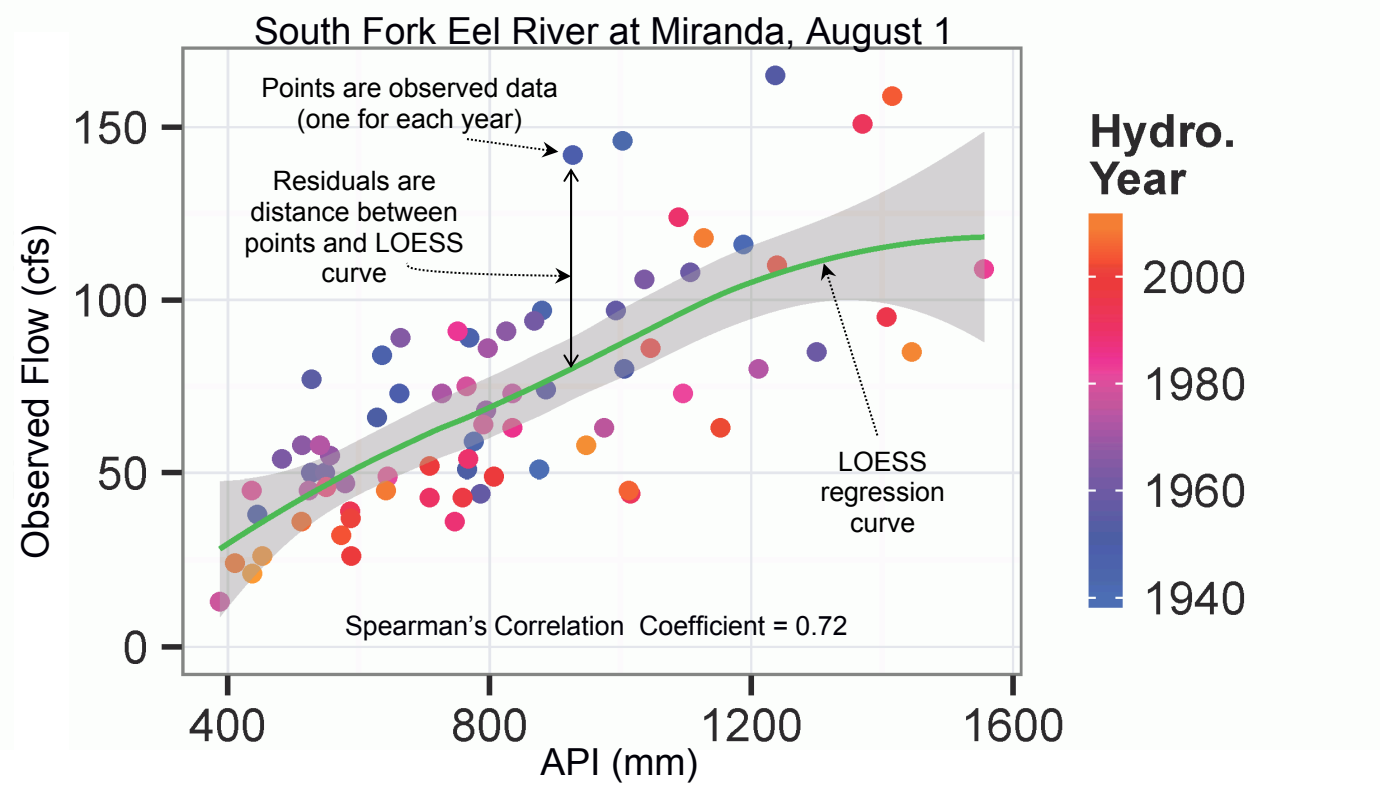

Figure 5. Observed streamflow in South Fork Eel River at Miranda for August 1 vs. API. Each point is a different year in the period of record. Green line is LOESS (Locally Estimated Scatterplot Smoothing) smoother.

[14] The residual is calculated as observed minus expected. Thus, a negative residual means the model over-estimated, while a positive residual means the model under-estimated.

2.7.3 ASSIGNMENT OF PRECIPITATION STATIONS REFINED USING CORRELATION WITH STREAMFLOW

I chose precipitation stations for streamflow sites by comparing the correlation between streamflow and API (i.e., how well precipitation from a particular station predicted streamflow). If a precipitation station resulted in a markedly lower correlation with streamflow than did other precipitation stations, then I excluded that station and mean precipitation was re-calculated. For example, Figure 6 shows that precipitation at the Grizzly Creek station resulted substantially weaker correlation with Van Duzen River streamflow than did other nearby precipitation stations (Bridgeville, Scotia, Richardson's Grove, and Eureka Woodley Island), particularly during summer and early fall; therefore, I replaced Grizzly Creek with Eureka Woodley Island.

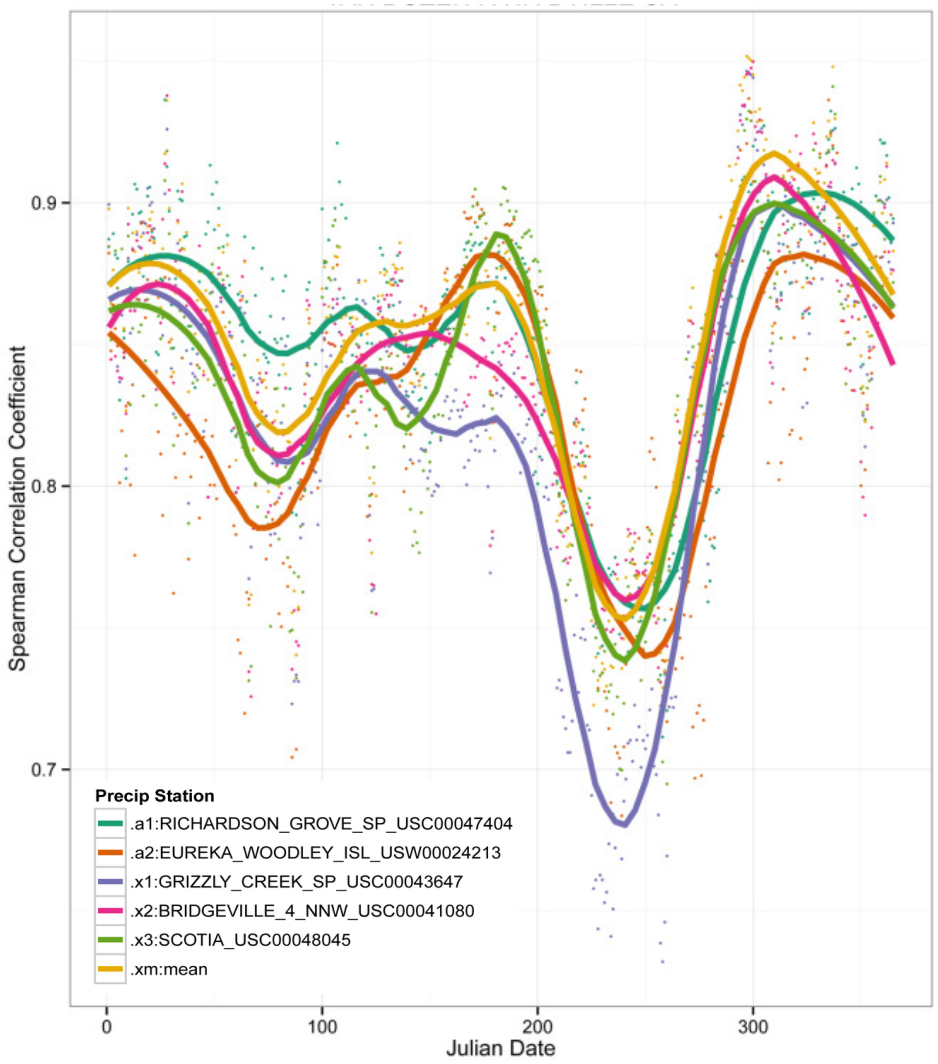

Figure 6. Correlation between streamflow in Van Duzen near Bridgeville and API calculated from five different precipitation stations (as well as the mean of three primary stations, labelled as ".xm") for each day of the 365 days of the year. Solid lines are Locally Estimated Scatterplot Smoothing (LOESS) curves which are provided as visual aids to indicate the overall seasonal pattern while dots show individual data points. Julian Day 200 is July 19 in a non-leap year and July 18 in a leap year.

2.8 LONG-TERM TRENDS IN PRECIPITATION, STREAMFLOW, AND PRECIPITATION-ADJUSTED STREAMFLOW

Long-term trends in streamflow quantity (average for each day of the year; monthly average; annual average; and minimum 7-day, 30-day, and 90-day averages), streamflow timing (date of calendar year on which minimum 7-day, 30-day, and 90-day average streamflow occurs), precipitation (monthly and annual), and precipitation-adjusted streamflow (average for each day of the year) were analyzed using the Mann–Kendall test (Helsel and Hirsch 2002, Yue et al. 2002) which is a nonparametric[15] test commonly utilized to assess hydrologic trends (Clark 2010, Mayer and Naman 2011, Chang et al. 2012).

Tests were performed in R 3.1.2 (R Core Team 2014) using the WQ package (Jassby and Cloern 2012). A p-value of 0.05 was used as the threshold for statistical significance for summaries, but values of 0.05-0.10 are also differentiated in some figures. To facilitate comparison of trends between sites, trend tests were run on the 62-year period 1953–2014, with some gaps allowed. Following guidance from Helsel and Hirsch (2002), sites that did not have at least 20% coverage (4 years) in each third (1953–1973, 1974–1994, 1993–2014) of the 62-year period were excluded. Trend slopes were calculated using the non-parametric Sen slope estimator method (Helsel and Hirsch 2002). An additional set of trend tests were also run for the entire period of record[16] and are included in Appendix F but not discussed in the main text of this report.

I characterized trends by both their duration (i.e., the number of days with a statistically significant decreasing or increasing trend) and their magnitude (i.e., slope, the amount of change that occurred across the 1953-2014 trend period). For each day of the year, I express magnitude in three ways:
1) absolute trend magnitude (i.e., annual slope of the trend) in units of cubic feet per second per year,
2) relative trend magnitude (i.e., annual slope of the trend relative to 1953-2014 median flow) in units of percent per year, and
3) trend magnitude normalized to watershed area (i.e., absolute trend magnitude divided by watershed area) in units of cubic meters per day per square kilometer of watershed area.

[15] Non-parametric statistical techniques require less assumptions than parametric statistical techniques, so are well-suited for analysis of large datasets where it would be cumbersome to verify that all assumptions are met. For example the Mann-Kendall test does not rely on assumptions of normality of residuals, constant variance and linearity.
[16] The term period of record means all years with available data (which varies by gage); however, if a site had just a few years early in the record and then a long gap, the early years were excluded from the trend test.

3 RESULTS AND DISCUSSION

3.1 LONG-TERM TRENDS IN PRECIPITATION

Precipitation records for U.S. Historical Climatology Network (USHCN, Menne et al. 2015) stations near the Eel River Basin span back to the mid/late 19th century with the oldest record being 1871 in Weaverville (Figure 7). There is considerable variability from year to year, but decadal and multi-decadal cycles are also evident (e.g., wetter in 1890s, 1900s, 1910s, drier in the 1920s and 1930s, wetter in mid-1940s to mid-1970s, dry in the late-1980s and early 1990s, wet in mid-1990s to mid-2000s, and dry in the most recent decade). For the five USHCN closest to the Eel River Basin, there are no statistically significant trends in annual total precipitation for 1880-2014 or any shorter period ending in 2014 (Figure 8). There are some monthly trends including decreased January precipitation since the mid-20th century at all five stations, increased March precipitation since the early 20th century at Orleans, Eureka, and Fort Bragg, increased July/August precipitation since the late 19th century and early 20th century at Eureka and Fort Bragg, and decreased August precipitation since the mid-20th century at Fort Bragg and Ukiah; however, these summer trends may not have much effect on streamflow because precipitation is so low during the summer.

Asarian and Walker (*in press*) noted decreasing trends in September precipitation for 1953-2012 for portions of the Eel River Basin as well as much of the area north of the Eel River Basin into Oregon. Substantial September rains then occurred in 2013 and 2014. The current analysis found only one USHCN station (Weaverville) with September precipitation decreasing since 1950, and statistical significance is lower for 1953-2014 than for 1953-2012 (Figure 8).

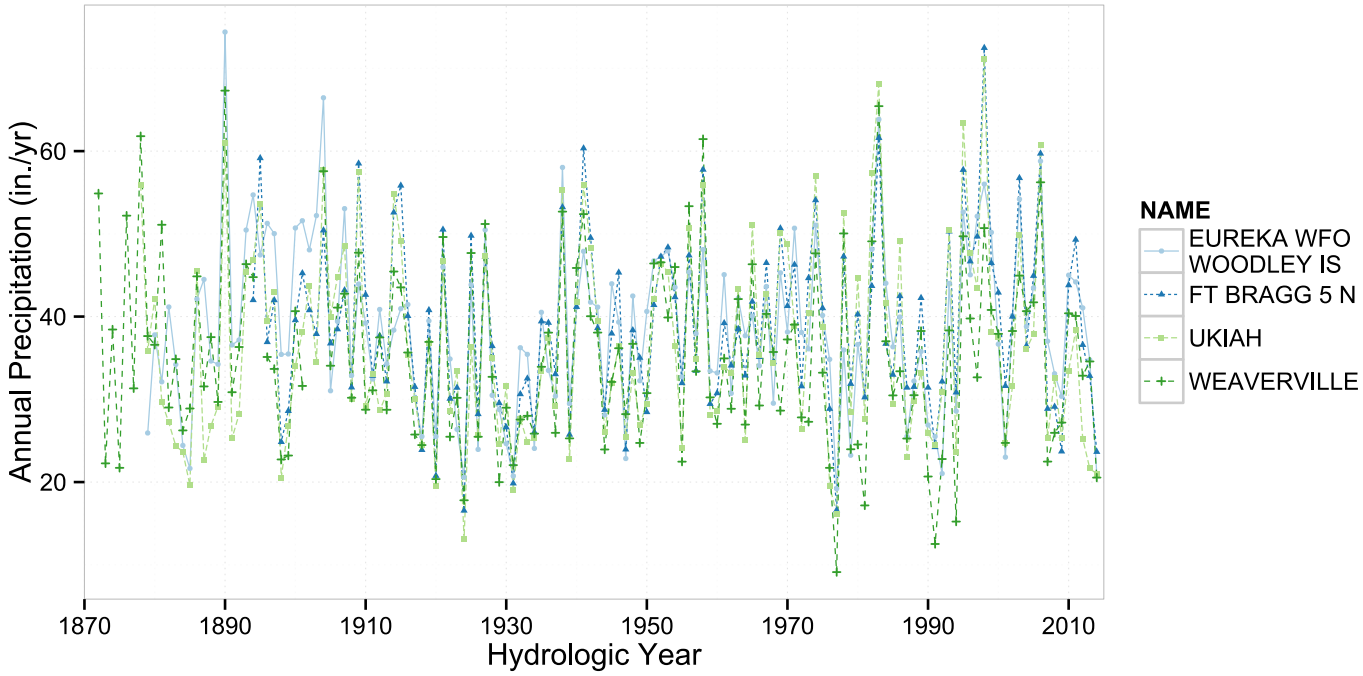

Figure 7. Annual precipitation for hydrologic years 1871-2014 at U.S. Historical Climatology Network (USHCN) stations near the Eel River Basin. Hydrologic year totals were calculated by summing monthly values, some of which were estimated by Menne et al. (2015).

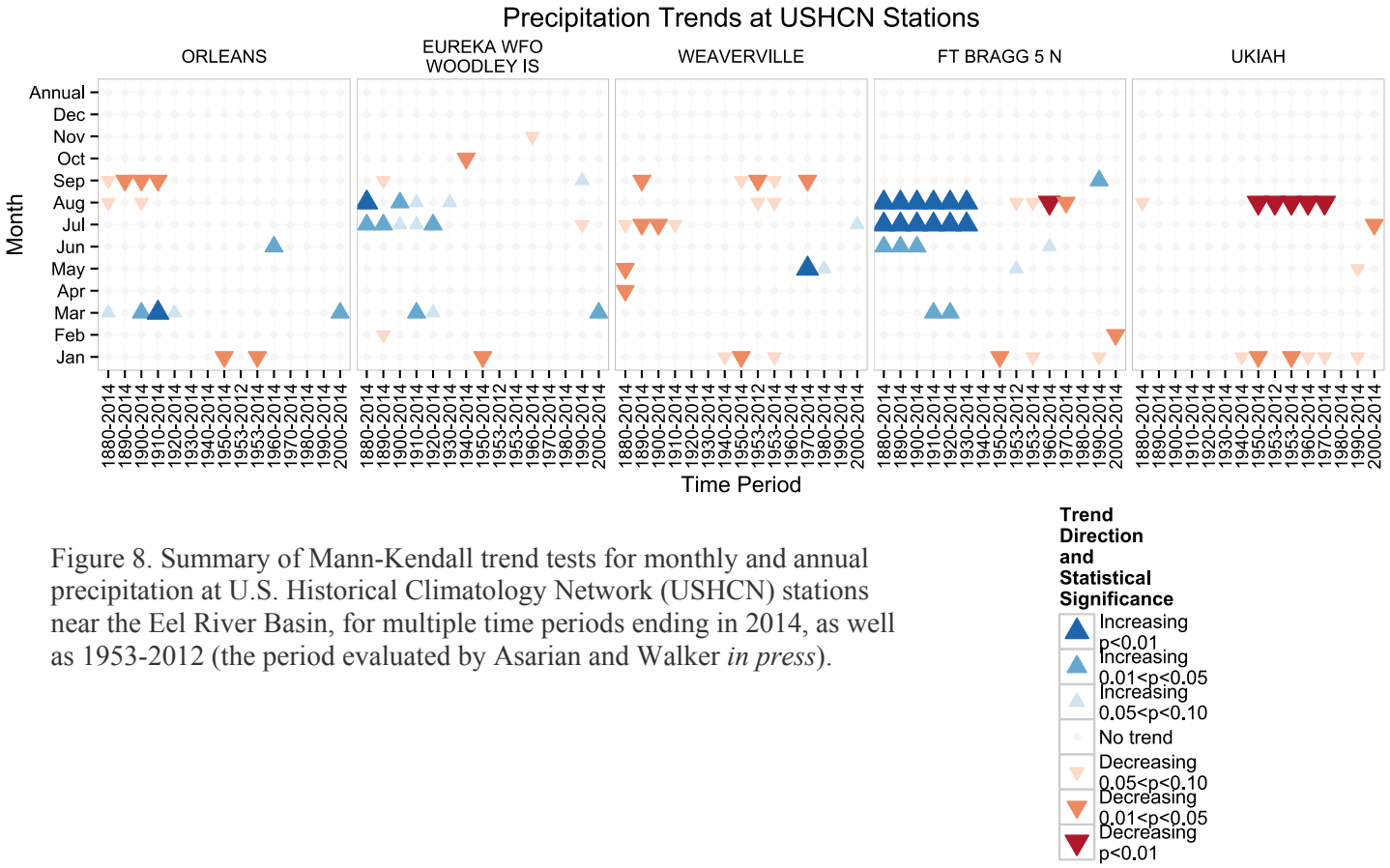

Figure 8. Summary of Mann-Kendall trend tests for monthly and annual precipitation at U.S. Historical Climatology Network (USHCN) stations near the Eel River Basin, for multiple time periods ending in 2014, as well as 1953-2012 (the period evaluated by Asarian and Walker *in press*).

3.2 API MODEL TO CALCULATE PRECIPITATION-ADJUSTED STREAMFLOW

The statistical model of streamflow vs. Antecedent Precipitation Index (API) performed well at tributary and lower mainstem sites, as indicated by correlation coefficients of 0.5 to 0.9 (Figure B2 in Appendix B). The model performed better (i.e., correlation coefficients were higher) during the high flow season of November through June than in the lower flow season of July through October (Figure B2). At upper mainstem sites (i.e., below Scott Dam and below Van Arsdale Dam) correlation coefficients were much lower than at tributary sites and downstream mainstem sites (Figure B2) especially in the summer months, because streamflows at the upper mainstem sites were highly influenced by dam releases which were not closely tied to precipitation patterns and were substantially increased following implementation of the NMFS (2002) Biological Opinion.

Optimal recession coefficients in the streamflow vs. API model followed expected patterns reflecting physical processes according to day of the year (i.e., higher recession coefficients in summer than winter and spring, because summer precipitation is rare and therefore summer flows are more influenced by the precipitation that occurred during previous months whereas winter streamflows are most influenced by recent precipitation) (Figure B1 in Appendix B).

3.3 LONG-TERM TRENDS IN STREAMFLOW

Streamflows declined at most tributary sites in the Eel River Basin during the low-flow season over the 1953-2014 period. Declines were especially prevalent from July through mid-October, when streamflows are lowest (Figure 9a, Figure 10a). The number of days with a declining streamflow trend varied among tributary sites. The sites with the fewest number of days with declining streamflow were Elder Creek, Middle Fork Eel River, and accretions[17] between Fort Seward and Scotia (Figure 11a). The relative magnitude (i.e., annual trend slope as a percent of 1953-2014 median flow) of declining trends were steepest (up to 6% per year for late August and September) for accretions to the mainstem Eel River from Van Arsdale to Fort Seward (Figure 9a), but when normalized to watershed area (i.e., absolute trend magnitude divided by watershed area) the declines were actually among the least steep (Figure 12c). The relative magnitude of declining trends were also steep (greater than 2% per year for late August and September) at Bull Creek and accretions to the South Fork Eel between Leggett and Miranda (Figure 9a). The relative magnitude of declines at the Van Duzen River and the combined accretions from Van Arsdale to Scotia (includes the entire South, Middle, and North forks of the Eel River) were ~1% in August through mid-October; compared to Bull Creek and accretions to the South Fork Eel between Leggett and Miranda, the relative magnitude of declines is lower but the numbers of days with declines is similar. Magnitude and duration of streamflow declines in the South Fork Eel at Leggett were intermediate relative to other tributary stations, with declines largely confined to mid-August through mid-October.

Streamflow declines were much less common at mainstem Eel River sites than at tributary sites (Figure 11a). Streamflow trends in the mainstem Eel River below Van Arsdale Dam show large increases (2-15% per year) during April through December (Figure 10a). Streamflow increases at Van Arsdale Dam began in 2003 (Figure D3a in Appendix D) due to increased instream flow releases from the Potter Valley Project required under the Reasonable and Prudent Alternative (RPA) in National Marine Fisheries Service's 2002 Biological Opinion (NMFS 2002) which was issued after NMFS determined that the previous flow regime was jeopardizing the continued existence of Eel River salmon. Given the streamflow increases at Van Arsdale, I had expected that streamflows would also be increasing at Fort Seward (the next mainstem gage downstream). In fact, Fort Seward had zero days with increasing or decreasing streamflow trends (Figure 10a, Figure 11a) because increased Van Arsdale releases were offset by declining accretions between Van Arsdale and Fort Seward (Figure 9a, Figure 11a). At Scotia, the lowermost mainstem gage, these declines in tributary contributions (and/or increased diversions) overcome the increased releases from Van Arsdale Dam, resulting in a moderate number of days and magnitude of streamflow decline (Figure 9a, Figure 10a, Figure 11a).

Multiplying the annual trend rates by the length of the 1953-2014 time period (62 years) yields the total magnitude of the declines for the entire period for streamflow (Figure 12a). Dividing the total magnitude by watershed area facilitates even comparisons between sites that have different sized watersheds (Figure 12c).

[17] The mainstem Eel River and South Fork Eel River have multiple streamflow gages, allowing for the calculation of accretions between gages. Accretions are calculated as the flow at the downstream gage minus the flow at the upstream gage minus any additional gaged tributaries. Accretions represent the net contributions of all tributaries, springs, and groundwater, minus any diversions.

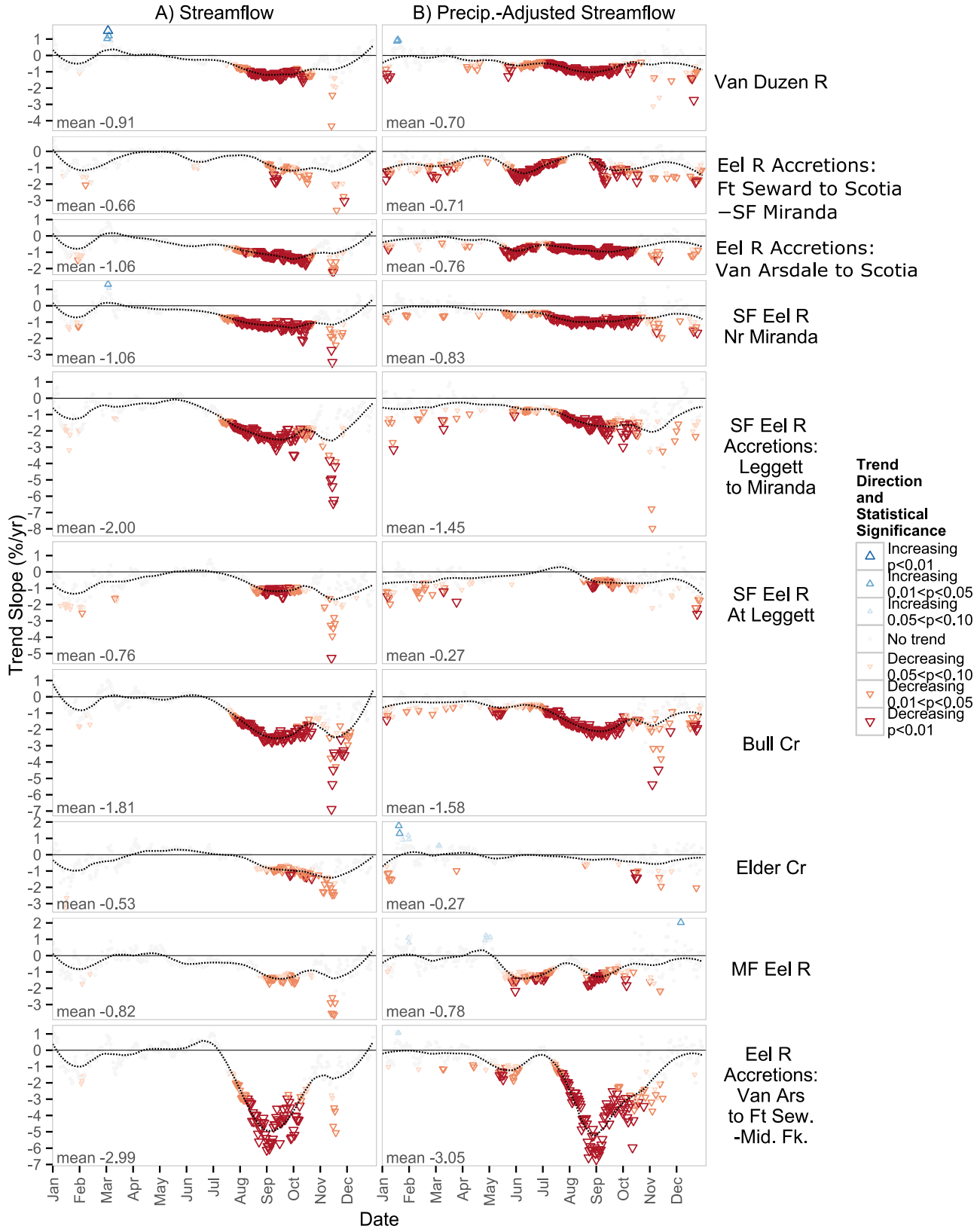

Figure 9. Summary of WY1953-2014 Mann-Kendall trend tests for each (365) day of the year for (A) streamflow and (B) precipitation-adjusted streamflow at Eel River tributaries. Symbols are color-coded by direction and statistical significance of the trend. Dashed lines are LOESS curves provided as visual aids to indicate the overall seasonal pattern. A horizontal line is placed at zero in each panel, so declining days are below the line and increasing days are above the line. Average (mean) of all July-October days is shown in lower-left corner of each panel. Y-axis scale is proportional in all panels (i.e., panel for Eel River Accretions from Van Arsdale to Fort Seward is provided additional height but each Y-unit is same height as other panels in this figure.

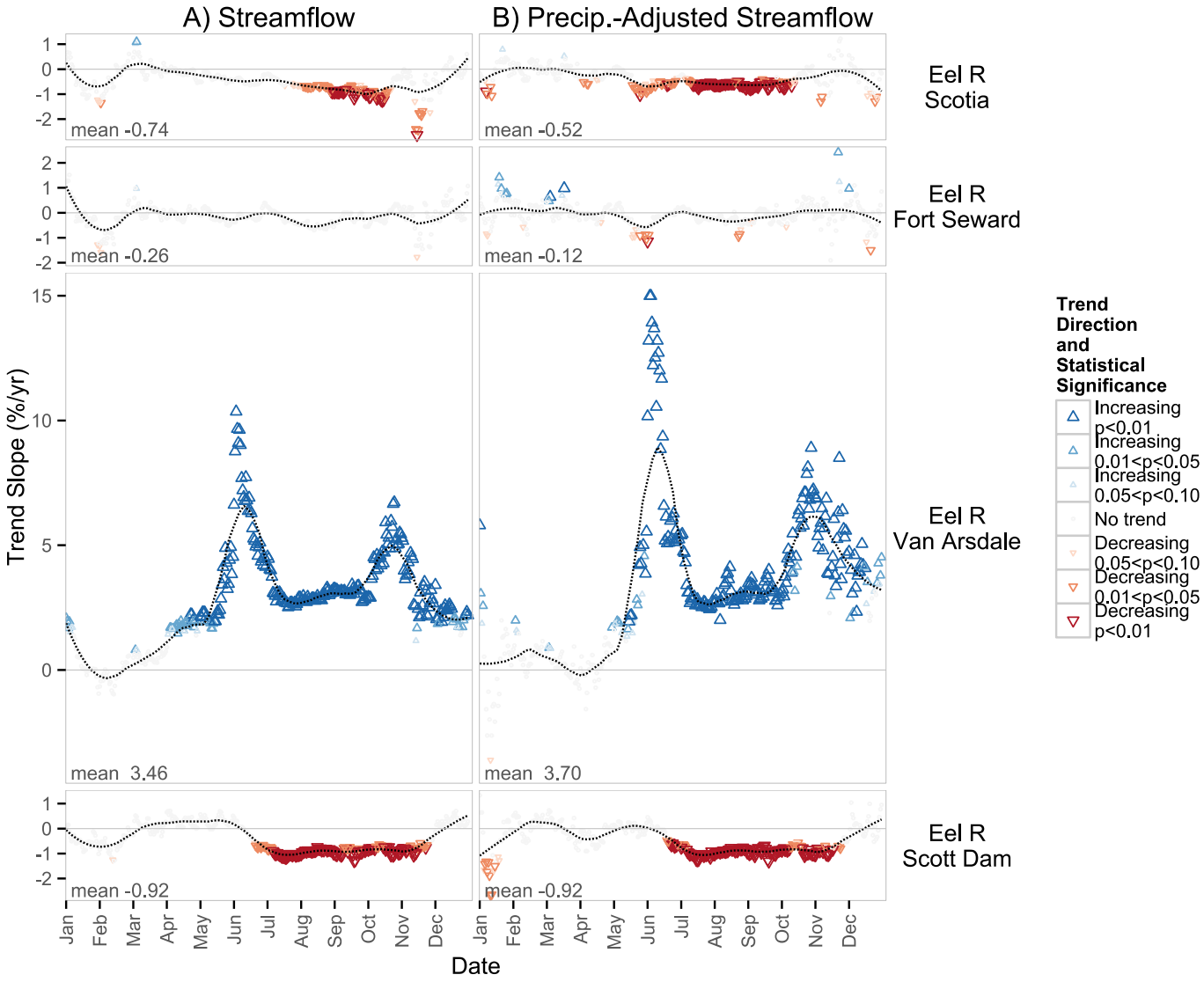

Figure 10. Summary of WY1953-2014 Mann-Kendall trend tests for each (365) day of the year for (A) streamflow and (B) precipitation-adjusted streamflow at mainstem Eel River sites. Symbols are color-coded by direction and statistical significance of the trend. Dashed lines are LOESS curves provided as visual aids to indicate the overall seasonal pattern. A horizontal line is placed at zero in each panel, so declining days are below the line and increasing days are above the line. Average (mean) of all July-October days is shown in lower-left corner of each panel. Y-axis scale is proportional in all panels (i.e., Van Arsdale panel is provided additional height but each Y-unit is same height as other panels in this figure). To preserve y-axis legibility, outlier values >15 were reduced to 15.

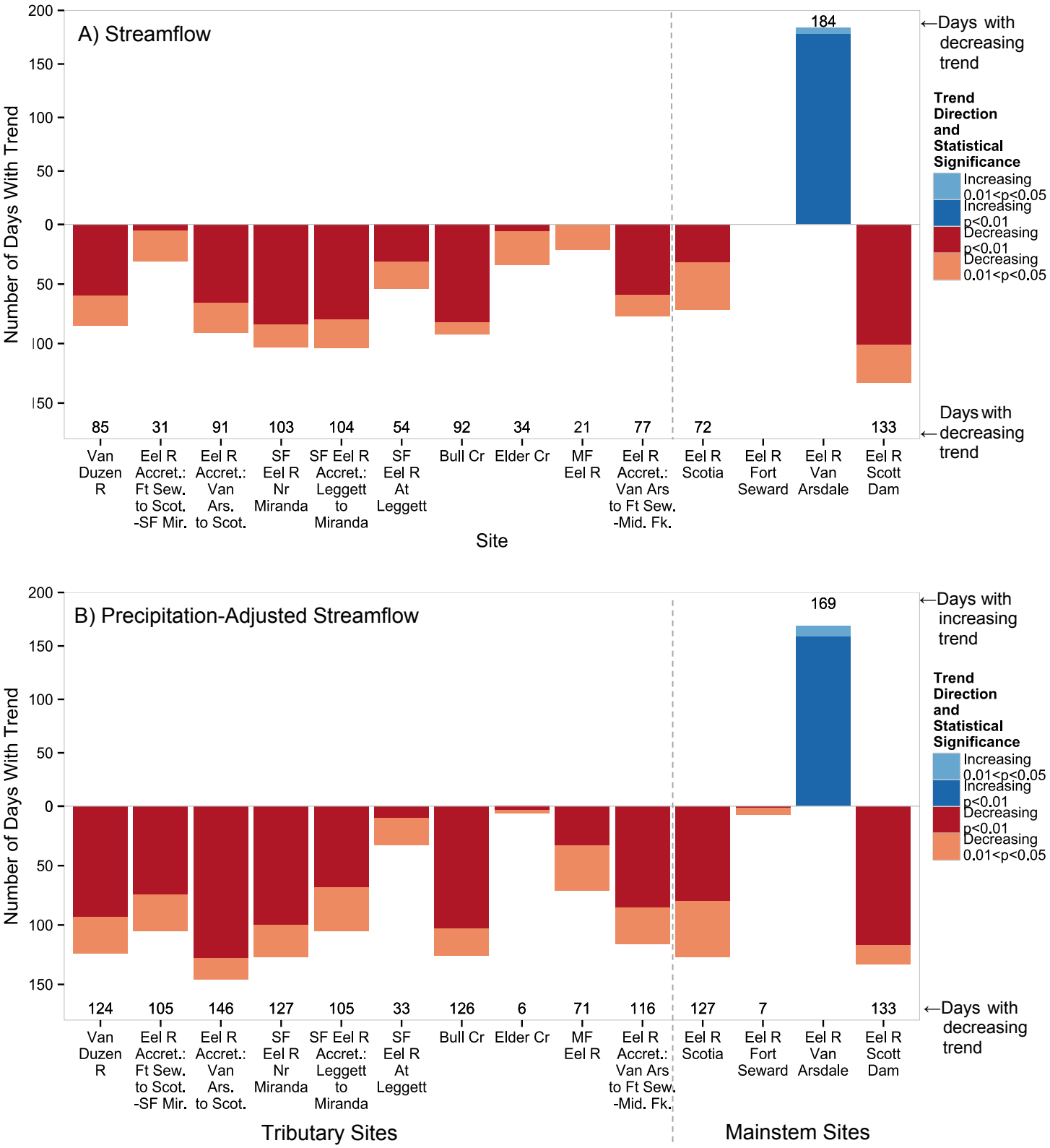

Figure 11. The number of days in May through October (184 possible days) with increasing or decreasing trends in (A) streamflow and (B) precipitation-adjusted streamflow at mainstem and tributary sites for WY1953-2014. Bars are stacked with colors indicating statistical significance and labels indicating the total number of days with an increasing or decreasing trend.

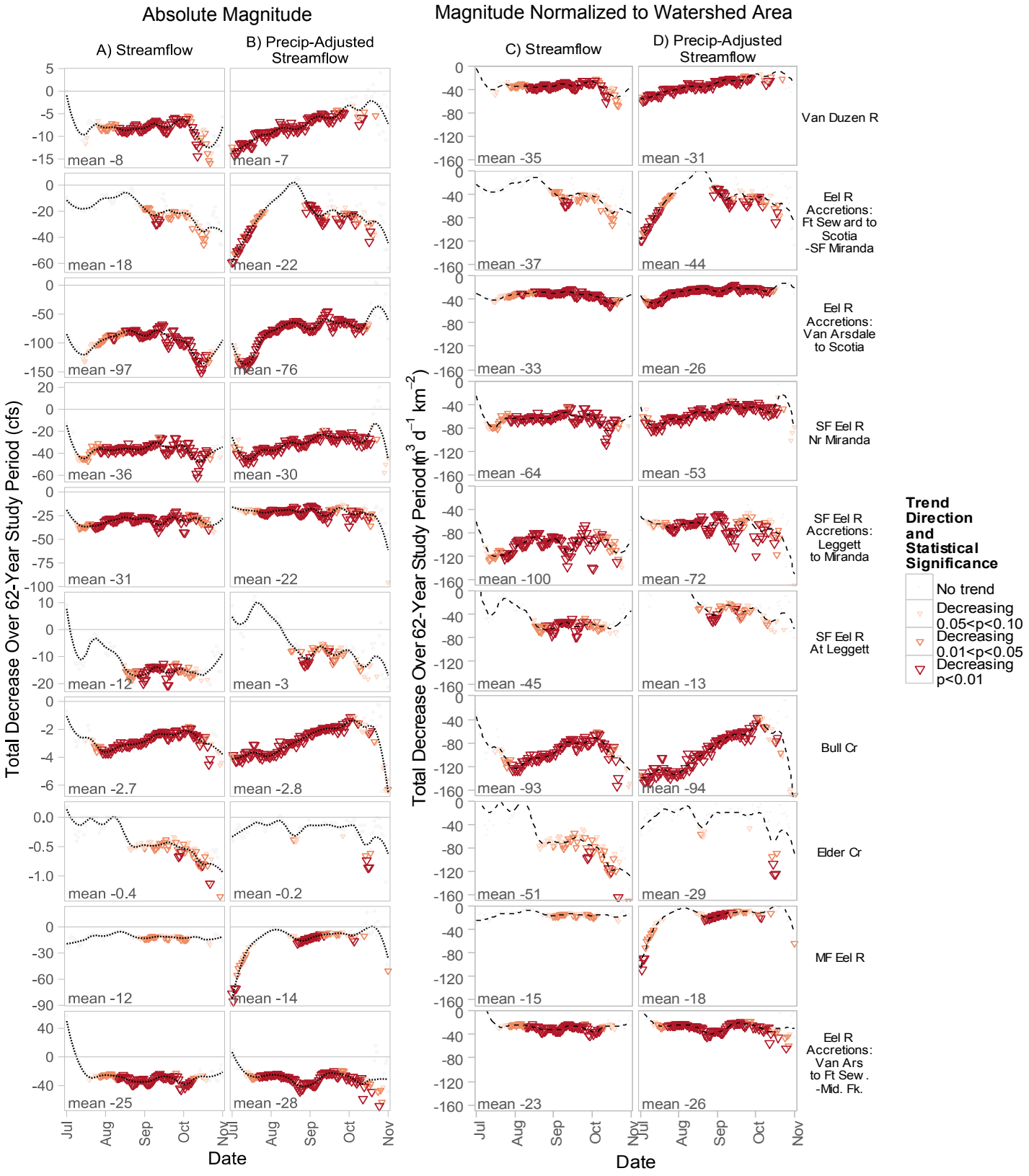

Figure 12. Total decrease over the 1953-2014 period (i.e., annual trend multiplied by 62) for each of the 123 days in July through October for (A) absolute magnitude of streamflow, (B) absolute magnitude of precipitation-adjusted streamflow , (C) streamflow normalized to watershed area, (D) precipitation-adjusted streamflow normalized to watershed area, for tributary sites. Symbols are color-coded by direction and statistical significance of the trend. Dashed lines are LOESS curves provided as visual aids to indicate the overall seasonal pattern. A horizontal line is placed at zero in each panel, so declining days are below the line and increasing days are above the line. Average (mean) of all July-October days is shown in lower-left corner of each panel. Y-axis scale is variable for panels in (A) and (B) but same in (C) and (D).

3.4 LONG-TERM TRENDS IN PRECIPITATION-ADJUSTED STREAMFLOW

At most tributary sites, there were a greater number of days with declining trends in precipitation-adjusted streamflow than there were days with decling trends in streamflow (Figure 11). This is likely because accounting for precipitation reduces the inter-annual variation that can obscure trends. There were exceptions with fewer days of declining precipitation-streamflow than streamflow, including Elder Creek and the South Fork Eel River at Leggett (Figure 11). The magnitude of declines in precipitation-adjusted streamflow was lower than the magnitude of streamflow declines (Figure 9). This indicates that precipitation patterns are contributing to streamflow declines, as annual precipitation was higher in the earlier part of the study period (see Figure 7). The much higher number of days with declining precipitation-adjusted streamflow as opposed to simple streamflow at the Middle Fork Eel may indicate poor quality data at one of the three stations (Potter Valley Powerhouse) used to calculate watershed precipitation (see 3.6 below), rather than a "real" condition.

At the two uppermost mainstem Eel River sites (below Scott and Van Arsdale dams), trends in precipitation-adjusted streamflow during summer are very similar to streamflow trends. This is partially because streamflows at those sites are only loosely related to precipitation in July through October, as noted above in section 0. Trends at Scotia (the most downstream of the three mainstem sites) were similar to those of the tributaries, with precipitation-adjusted streamflow having more days of decline, but with slightly lower magnitude, than streamflow.

3.5 POTENTIAL EXPLANATIONS FOR TRENDS IN PRECIPITATION-ADJUSTED STREAMFLOW

With the exception of precipitation, the methods used in this analysis do not allow individual quantitation of the factors contributing to streamflow declines. However, the long-term streamflow gages in the Eel River include a diverse range of watershed and climate conditions. Thus, we can hypothesize about causal mechanisms by carefully examining the trends in precipitation-adjusted streamflow that have occurred in watersheds with different conditions/histories. Potential factors include increased water diversions and/or increased evapotranspiration by vegetation and forests. Increased evapotranspiration could be due to either climate (i.e., air temperature, wind, humidity, or precipitation shifting from snow to rain) and/or structure and composition of vegetation.

Elder Creek is one of the most pristine watersheds within the Eel River Basin, with almost no diversions, roads, or history of timber harvest[18]. Elder Creek had declining trends in streamflow (Figure 11a) but showed very little change in precipitation-adjusted streamflow (Figure 11b). A previous analysis (Asarian and Walker *in press*) found similar results from other pristine watersheds within the region (i.e., Smith River, Salmon River, and tributaries to the Klamath River between Seiad Valley and Orleans). These results suggest that streamflow decreases at other sites are more likely the result of increased water withdrawals and/or changes in vegetation structure and composition than from climate factors other than precipitation.

[18] The only exceptions that I am aware of are: 1) one domestic diversion near the mouth of Elder Creek, 2) a trespass marijuana grow of tens of thousands of plants, including water diversions, was found/eradicated in recent years on U.S. Bureau of Land Management land in the headwaters of Elder Creek, 3) one road crosses the creek near its mouth and there are short lengths of ridgetop roads in the headwaters, 4) there are a few houses, a greenhouse, and a pond in the headwaters.

3.5.1 WATER DIVERSIONS

This study did not quantify water diversions, but the trends in precipitation-adjusted streamflow from this study (Figure 11b), as well as previous analyses (Asarian and Walker *in press*), suggest that diversions are an important factor influencing summer streamflow declines in the Eel River Basin. There are only two watersheds with long-term stream gages in the Eel River Basin that are not affected by diversions. The first is Elder Creek, which showed few declines in precipitation-adjusted streamflow. The second is Bull Creek, which is located entirely within a California State Park. Despite having no known diversions, Bull Creek showed large declines in precipitation-adjusted streamflow which are likely due to vegetation change, as discussed in section 0 below. Previous analyses within the region (Asarian and Walker *in press*) found that most streams without substantial diversions did not have declines in summer precipitation-adjusted streamflow, including Elder Creek, Smith River, Salmon River, and tributaries to the Klamath River between Seiad Valley and Orleans, Little River, South Fork Trinity River, the Trinity River above Trinity Lake, and accretions to the lower Trinity River. In contrast, most streams that had substantial diversions and were regulated by dams had declines in summer precipitation-adjusted streamflow.

Data regarding small-scale domestic and agricultural water diversions are relatively scarce within the Eel River Basin, in part due to the conflicted legal status of marijuana (*Cannabis sativa*), which is a major crop within the Basin. The State of California requires that anyone diverting water from a stream register that diversion with the State; however, compliance with that requirement is low and very few diversions within the Eel River Basin are registered (Bauer et al. 2015). The State has recently increased education and enforcement of water rights within the Basin, and increasing numbers of people are registering diversions.

Bauer et al. (2015) and Bauer (2015) estimated the water used at marijuana cultivation sites within five Northwest California watersheds, including three within the Eel River Basin, in units of liters per day (Table 2, second column). None of the watersheds analyzed by Bauer et al. (2015) or Bauer (2015) have long-term stream gages that are currently operating[19]; however, these water use estimates can be compared to streamflow trends observed at other gages within the Eel River Basin by normalizing them by watershed area (i.e., divide water use by watershed area) to estimate the water use per watershed area[20]. Area-normalized water use estimates range from approximately 1 to 10 $m^3\ d^{-1}\ km^{-2}$ (cubic meters of water per day per square kilometer of watershed area) (Table 2, far right column). In contrast, the total magnitude of the decline in precipitation-adjusted streamflows across the entire 62 year period 1953-2014 (i.e., annual trend multiplied magnitude multiplied by 62 years) during the months of July-October is in the range of 30-100 $m^3\ d^{-1}\ km^{-2}$ for most tributary sites (Figure 12d). This indicates that water diversions for marijuana cultivation likely explain only a relatively small fraction (i.e., roughly 1% to 33%) of the total declines. For example, the area-normalized marijuana water use estimates of 7 to 9 $m^3\ d^{-1}\ km^{-2}$ in two tributaries of the South Fork Eel River (Salmon and Redwood creeks) represent only 12 to 15% of the area-normalized total decline in precipitation-adjusted streamflow for the accretions to the South Fork Eel between the Leggett and Miranda gauges, which is approximately 60 $m^3\ d^{-1}\ km^{-2}$ (Figure 12). *These results do not mean that water diversions for marijuana cultivation do not have serious detrimental effects on streamflows and salmonids in many Eel River Basin streams. It just means that these diversions are only a partial explanation for declining*

[19] Outlet Creek was gaged from WY1957-1994.

[20] This per-area approach for comparing water use with streamflow takes into account the density (i.e., number per area) of cultivation sites within a watershed, the number of plants within each cultivation site, and the amount of water used by each plant. In contrast, the comparison of streamflow and water use presented by Carah et al. (2015) make the odd assumption that the entire Eel River watershed is completely

streamflows at basin scales. The effects of diversions are likely to be particularly acute during droughts when streamflows are already extremely low and streams are highly vulnerable to dewatering. Despite being responsible for only a portion of streamflow declines, recent increases in diversions are a key additional impact compounding with previous impacts. Furthermore, diversions are perhaps the only factor causing streamflow declines that could actually be substantively addressed in the near-term (i.e., water can be stored in tanks and ponds when it is abundant during winter and early spring, offsetting the need for summer diversions).

Table 2. Estimated water use at marijuana cultivation sites within five Northwest California watersheds. Mad River data adapted from Bauer (2015) and data for other watersheds adapted from Bauer et al. (2015).

Watershed	Marijuana water use estimated by CDFW ($L\ d^{-1}$)	Marijuana water use estimated by CDFW ($m^3\ d^{-1}$)	Watershed area (km^2)	Marijuana water use estimated by CDFW, normalized (i.e., divided) by watershed area ($m^3\ d^{-1}\ km^{-2}$)
Upper Redwood Creek	523,144	523	175.3	2.98
Salmon Creek	684,110	684	95.1	7.19
Redwood Creek South	618,620	619	64.7	9.56
Outlet Creek	724,016	724	417.0	1.74
Mad River	1,292,930	1,293	1257.0	1.03

3.5.2 VEGETATION/FOREST STRUCTURE/COMPOSITION

Annual water budgets indicate that approximately 25-50% of the precipitation that falls in the Eel River Basin (Asarian and Walker *in press*)[21] is evapotranspired by vegetation. Because evapotranspiration is such a large percent of the water budget, small changes in evapotranspiration have the potential for large effects on summer streamflows.

The Eel River Basin's forests have undergone substantial changes in the past century as a result of timber harvest, fire suppression, and other land use changes. Clear-cut harvests temporarily increase streamflow for several years immediately following harvest (Jones and Post 2004, Jones et al. 2009) but as young stands regenerate they can have high evapotranspiration rates in future decades (Moore et al. 2004, Jassal et al. 2009). Although logging began with European-American settlement in the mid-1800s, many areas were not harvested until they became readily accessible due to the advent of tractor logging following World War II (Power et al. 2015).

Fire suppression and lack of prescribed fire has dramatically altered the vegetation in the Eel River Basin, altering both stand density (i.e., trees per acre) and species composition. During the 20th century, reduced fire frequency has increased stand density in many forests in the western United States (Perry et al. 2011, McIntyre et al. 2015). Fire history studies near the headwaters of the mainstem and Middle Fork Eel River indicate fires have been far less frequent since 1850 (Skinner et al. 2009). Historical reconstruction of vegetation in the Nork Fork Eel River watershed indicates that between 1865 and 1996, fire suppression and a lack of Native American cultural burning resulted in the area of Douglas-fir (*Pseudotsuga menziesii*) forest increasing six-fold with a commensurate

[21] The online supporting information for Asarian and Walker (*in press*) lists the long-term average of annual runoff coefficient (annual streamflow divided by annual precipitation) for stream gages in the Eel River basin, which range from 0.45 to 0.77. Actual evapotranspiration (AET) can be calculated as annual precipitation minus annual runoff (Zhang et al. 2001).

decrease in oak (*Quercus*) woodlands (Keter and Busam 1997)(Figure 13). In addition, extensive research from areas outside the Eel River Basin, including nearby areas such as Redwood Creek (Fritschle 20008, Engber et al. 2011) and the Mattole River where 16,240 acres (37%) of prairie area (approximately 8% of the entire Mattole watershed) were lost between 1950 and 1998 (MRRP 2009), as well as in Oregon and Washington (Devine and Harrington 2007, Murphy 2008) indicate that without fire or mechanical intervention to clear invading conifers, oak woodlands/savannahs and prairies are diminishing except where soil conditions are unsuitable (e.g., too dry, shallow, or poorly drained) to support conifers (Keter and Busam 1997, Murphy 2008). The extent of encroachment of conifers into oak woodlands/savannahs and prairies has not been quantified across the entire Eel River or the larger region. McIntyre et al. (2015) compared plots from the 1920–1930s Vegetation Type Mapping project with plots from the US Forest Service's 2001-2010 Forest Inventory Analysis plots from across California and found that both oaks and Douglas-fir were increasing while pines (*Pinus*) decreased; however there were extremely few plots from the North Coast. The effect on streamflow of conifer encroachment into oak woodlands/savannahs have not been well-studied, but mechanical removal of encroaching Douglas-fir has been shown to decrease interception of precipitation and increased shallow soil moisture (Devine and Harrington 2007). Several North American studies indicate lower levels of rainfall interception in oak forests than conifer forests, likely due to oak's lower leaf surface area (Fenn and Bytnerowicz 1997, Silva and Rodríguez 2001, Devine and Harrington 2007).

Research from other fire-suppressed areas of California (albeit at higher elevations where snow is more prevalent than in the Eel River basin) suggests that re-introduction of fire can alter vegetation enough to increase streamflow. For example, preliminary results from the snowmelt-dominated Illilouette Creek in Yosemite National Park indicate that following 40 years of letting lightning fires burn, forest heterogeneity has increased (i.e., a mix of open areas and varying levels of density), water yields (i.e., streamflow per unit precipitation) are increasing, and wetland vegetation is replacing former dry-adapted vegetation (Boisrame et al. 2015, Stephens and Collins 2015). Of all streamflow sites evaluated by Asarian and Walker (*in press*), the Salmon River had the highest percent areas burned by wildfire and was the only site unregulated by dams that had an increasing precipitation-adjusted streamflow for July, August, and September. The Salmon River was also the only gage where Sawaske and Freyberg (2014) found a decreasing trend in the rate of baseflow recession.

Bull Creek (tributary to South Fork Eel River) provides an interesting case study to assess the effects of vegetation change on streamflow. The stream gage is located in the middle of the watershed. The area upstream (west and south) of the gage was almost entirely clear-cut in the 1940s and 1950s, prior to installation of the gage in October 1960 and protection within a State Park, while the downstream ungaged portion of the watershed remains almost entirely covered in old-growth redwoods (Stillwater Sciences 1999). Tractor logging and road building set the stage for catastrophic landslides and erosion that occurred following the 1955 and 1964 floods. With no mechanical thinning or substantial fires[22], the forest upstream of the gage has since regrown vigorously in the previously harvest areas as well as encroached slightly into prairies (Figure 14). Despite having no substantial water diversions, Bull Creek had the largest number of days with declining precipitation-adjusted streamflow (Figure 11b), and nearly the greatest percent (Figure 9b) and area-normalized (Figure 12b) magnitude of declines in precipitation-adjusted streamflow. Bull Creek probably had the largest change in vegetation of any long-term streamflow site within the Eel River Basin.

[22] The 2003 Canoe fire did burn within Humboldt Redwoods State Park in the adjacent Canoe Creek watershed, but only about a very small area (approximately 0.6 km^2 in the headwaters of Preacher Gulch) of the gaged portion of the Bull Creek watershed was affected.

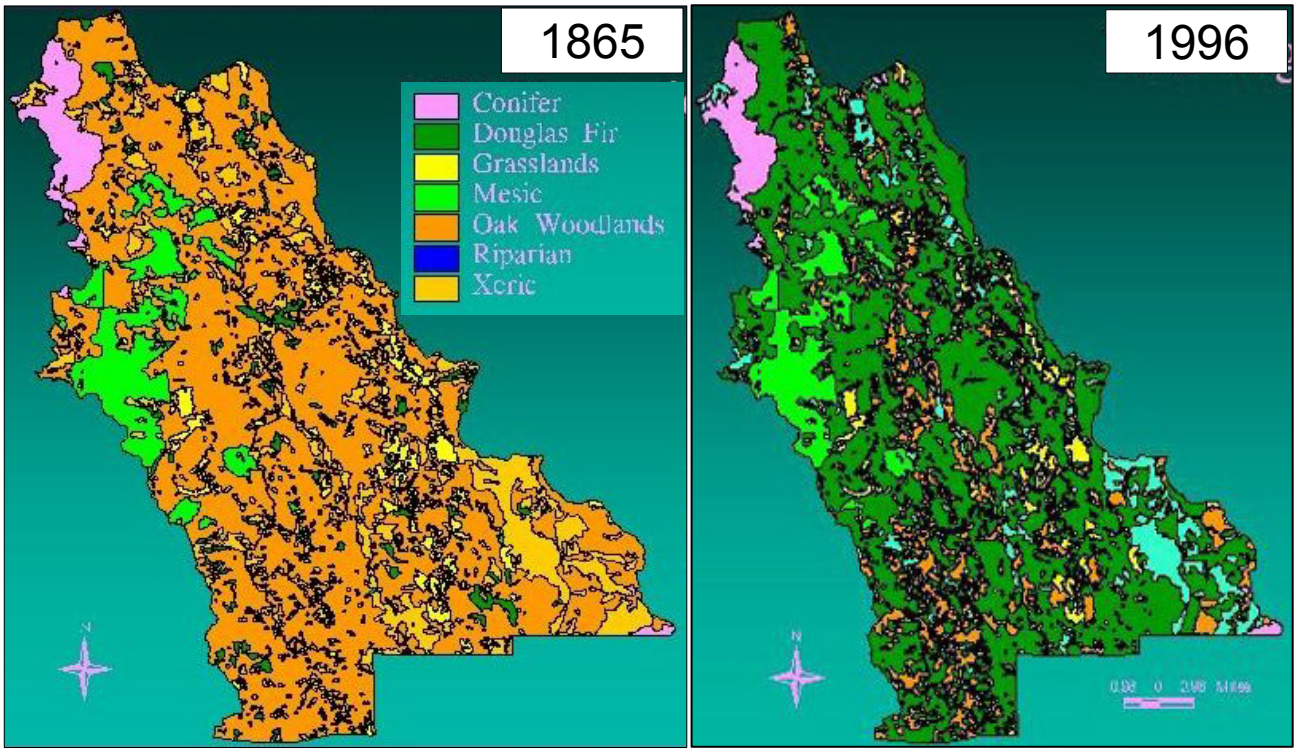

Figure 13. Comparison of vegetation types in the northern half (primarily federally-owned) of the North Fork Eel River watershed in 1865 and 1996, based on a combination of 1985-1989 field surveys[23] and GIS modeling. The southern half of the watershed is private land and was not included in the surveys or this map. Figure adapted from Keter and Busam (1997).

[23] Excerpt from Keter and Busam (1997): "It is obvious, even to the casual observer, that the oak woodlands and the Douglas-fir within the basin have undergone profound changes in distribution since 1865. These changes are relatively easy to quantify in the field. Within the even-aged stands of Douglas-fir that have overgrown the oaks, one can invariably find several old-growth Douglas-fir. These trees have large lower radiating branches, evidence that they grew in a more open environment with little intra-species competition. After cessation of burning, these trees became the seed source for today's even-aged stands. The oaks provided shade that conserved the moisture content of the top layer of soils, allowing the Douglas-fir seedlings to become established. When the Douglas fir grew above the oaks and shaded them out, the oaks began to die. It should also be noted that within many of the young Douglas-fir stands there are a few old-growth ponderosa pine. These trees are not shade tolerant and cannot become established under a dense canopy. They provide additional evidence that a particular area was more open prior to 1865."

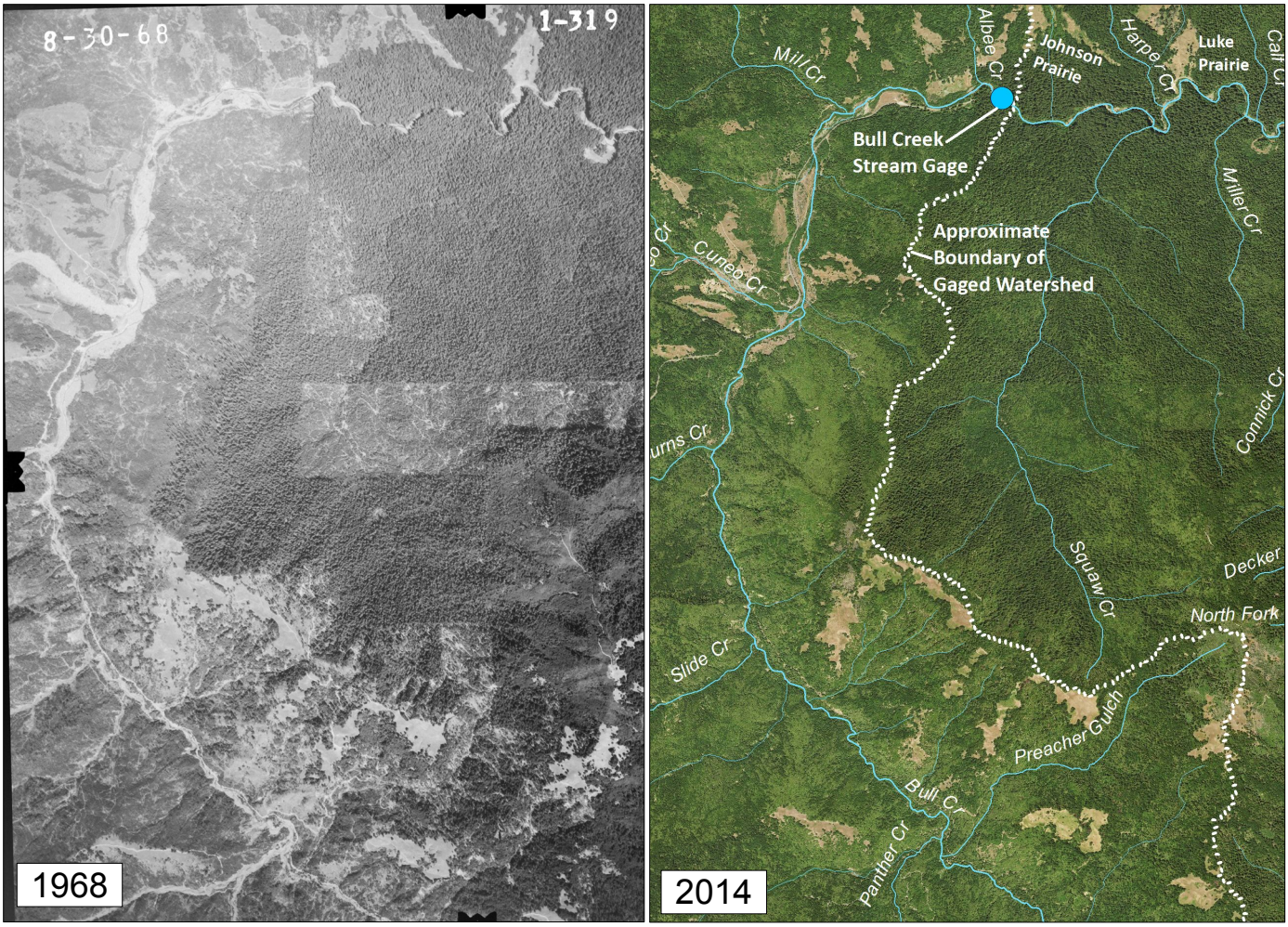

Figure 14. Comparison of aerial photos showing the majority of the Bull Creek watershed in 1968 (from USGS EROS data center: http://earthexplorer.usgs.gov/metadata/4660/AR1VBZX00010319/, note it is not orthorectified and is rotated slightly from true north) and 2014 (from U.S. Department of Agriculture's National Agriculture Inventory Program [NAIP]).Bull Creek flows clockwise from lower middle of image to upper-right. Image from 1968 shows extensive damage from tractor logging, road-building, and subsequent 1955 and 1964 floods. Bare areas in the 1968 photo are a combination of highly aggraded channels (particularly near the mouth of Cuneo Creek in upper-left corner of the images), recently cleared forest, and ridgetop/hillside prairies. The 2014 photo shows substantial forest regeneration and stream channel narrowing as well as some encroachment of trees into prairies (e.g., areas north of Cuneo Creek, Johnson Prairie east of Albee Creek, and Luke Prairie east of Harper Creek).

3.5.3 OTHER CLIMATE VARIABLES BESIDES PRECIPITATION

Two other important climate variables that appear to be changing and could affect streamflow are air temperature and coastal fog. Cordero et al. (2011) found increasing air temperatures for the period 1918-2006 in the two regions (North Coast and North Central) of California that overlap with the Eel River Basin, with accelerated warming since 1970 and minimum temperatures increasing faster than maximum temperatures. The warming trend has continued, with 2014 being the warmest on record in California (AghaKouchak et al. 2014). Increased air temperatures increase potential evapotranspiration (PET), which can deplete soil moisture and result in reduced streamflow (Thorne et al. 2015). For example, models of Pacific Northwest streams by Vano et al. (2015) predicted streamflow decreases of 31%, 21%, and 7% for July, August, and September, respectively, for each 1°C of annual warming. Reduced streamflows are likely to further exacerbate increases in stream temperature that are expected to result from warming air temperatures (Mayer 2012).

Coastal fog also declined along the California Coast during the 20th century (Johnstone and Dawson 2010). Long-term direct measurement of the inland extension of coastal fog are lacking, but cores extracted from old growth redwood trees near the floodplain along lower Bull Creek indicates that tree growth there has been higher since 1970 than any time in the past few hundred years, which was attributed to increased light resulting from reduced fog (Sillett et al. 2013, Carroll et al. 2014). Of all watersheds with long-term stream gages in the Eel River Basin, Bull Creek is the one most likely to be directly affected by fog[24]. Thus, decreased fog could be contributing to the observed decreases in precipitation-adjusted streamflow.

3.6 SENSITIVITY ANALYSIS HOW CHOICE OF PRECIPITATION STATIONS AFFECTS LONG-TERM TRENDS

Long-term trends in API, streamflow, and precipitation-adjusted streamflow were evaluated separately for each individual precipitation station in addition to the combined mean of the precipitation stations. Results are contained in Appendix E and Appendix F. The use of the Standish Hickey and Upper Mattole precipitation stations appeared to result in a much lower number of days with declining precipitation-adjusted streamflow than other precipitation stations (Appendix E). For these sites, the ratio of site precipitation to mean of all primary sites' precipitation has increased in recent years (precisely coinciding with when these stations ceased operating), indicating that regressions used to estimating missing data likely over-estimated precipitation values (Figure A2 in Appendix A). In contrast, the use of Fort Bragg and Potter Valley Powerhouse precipitation stations generally resulted in a much higher number of days with declining precipitation-adjusted streamflow. The number of days per years with precipitation data at the Fort Bragg and Potter Valley Powerhouse sites was relatively high throughout the entire 1953-2014 period (Figure A2 in Appendix A), indicating that this difference is likely to some other unknown cause rather than to regression error[25]. The site most affected by the potentially erroneous Potter Valley Powerhouse precipitation data is the Middle Fork Eel River (see Appendix E).

[24] Others gages are located further inland, or are larger watersheds which also encompass inland areas.

[25] Regressions are only used to fill gaps (i.e., missing data). Because there were few days with missing data at Fort Bragg and Potter Valley, and therefore few days where regressions were used to estimate data, the data are unlikely to be affected by errors/uncertainties in the values estimated by regression. Fort Bragg and Potter Valley are located at the southern edge of our study area, so we could not easily compare data from those stations with stations further south to see if the apparently odd patterns (i.e., not matching the rest of our study area) at those two stations would match patterns at stations further south (i.e., be part of a larger coherent geographic pattern).

4 REFERENCES CITED

AghaKouchak, A., L. Cheng, O. Mazdiyasni, and A. Farahmand, 2014. Global Warming and Changes in Risk of Concurrent Climate Extremes: Insights from the 2014 California Drought. Geophysical Research Letters 41:2014GL062308. doi: 10.1002/2014GL062308.

Asarian, J.E. 2015. Assessment of altered hydrologic function, dams, and diversions within the Southern Oregon/Northern California Coast evolutionarily significant unit of coho salmon, version 2. Prepared for NOAA Fisheries, Arcata, CA. 73 p. + appendices. https://archive.org/details/soncc_hydrologic_report_20151002_revised

Asarian, J.E. and J. Walker. *in press*. Long-Term Trends in Streamflow and Precipitation in Southwest Oregon and Northwest California. *Journal of the American Water Resources Association*.

Bauer, S., J. Olson, A. Cockrill, M. van Hattem, L. Miller, M. Tauzer, and G. Leppig, 2015. Impacts of Surface Water Diversions for Marijuana Cultivation on Aquatic Habitat in Four Northwestern California Watersheds. PLoS ONE 10:e0120016. doi: 10.1371/journal.pone.0120016.

Bauer, S. 2015. Marijuana Cultivation in the Mad River Watershed. Presentation to the Humboldt Bay Municipal Water District. California Department of Fish and Wildlife, Eureka, CA.

Boisrame, G.F.S., M. Naranjo, S. Stephens, S.E. Thompson, and A. Wong, 2014. Seeing the Forest Without the Trees: Long-Term Influence of Wildfire on the Ecohydrology of a Mountain Watershed. AGU Fall Meeting Abstracts 54:05. http://adsabs.harvard.edu/abs/2014AGUFM.H54D..05B

Carah, J.K., J.K. Howard, S.E. Thompson, A.G.S. Gianotti, S.D. Bauer, S.M. Carlson, D.N. Dralle, M.W. Gabriel, L.L. Hulette, B.J. Johnson, C.A. Knight, S.J. Kupferberg, S.L. Martin, R.L. Naylor, and M.E. Power, 2015. High Time for Conservation: Adding the Environment to the Debate on Marijuana Liberalization. BioScience:biv083. doi: 10.1093/biosci/biv083.

Chang, H., I.-W. Jung, M. Steele, and M. Gannett. 2012. Spatial Patterns of March and September Streamflow Trends in Pacific Northwest Streams, 1958–2008. Geographical Analysis 44:177–201. doi: 10.1111/j.1538-4632.2012.00847.x.

Clark, G.M., 2010. Changes in Patterns of Streamflow From Unregulated Watersheds in Idaho, Western Wyoming, and Northern Nevada. Journal of the American Water Resources Association (JAWRA) 46:486–497. doi: 10.1111/j.1752-1688.2009.00416.x.

Cordero, E.C., W. Kessomkiat, J. Abatzoglou, and S.A. Mauget, 2011. The Identification of Distinct Patterns in California Temperature Trends. Climatic Change 108:357–382. doi: 10.1007/s10584-011-0023-y.

Devine, W.D. and C.A. Harrington. 2007. Release of Oregon White Oak from Overtopping Douglas-Fir: Effects on Soil Water and Microclimate. Northwest Science 81:112–124. doi: 10.3955/0029-344X-81.2.112.

Edmund, H., S. Chamberlain, and K. Ram. 2014. rnoaa: NOAA Climate Data from R. R package version 0.3.3. http://cran.r-project.org/web/packages/rnoaa

Engber, E.A., J.M. Varner III, L.A. Arguello, and N.G. Sugihara, 2011. The Effects of Conifer Encroachment and Overstory Structure on Fuels and Fire in an Oak Woodland Landscape. Fire Ecology 7:32–50. doi: 10.4996/fireecology.0702032.

Falcone, J.A. 2011. GAGES-II: Geospatial Attributes of Gages for Evaluating Streamflow. U.S. Geological Survey, Reston, VA. http://water.usgs.gov/GIS/metadata/usgswrd/XML/gagesII_Sept2011.xml#stdorder

Fenn, M.E. and A. Bytnerowicz. 1997. Summer Throughfall and Winter Deposition in the San Bernardino Mountains in Southern California. Atmospheric Environment 31:673–683.

Fritschle, J.A., 2008. Reconstructing Historic Ecotones Using the Public Land Survey: The Lost Prairies of Redwood National Park. Annals of the Association of American Geographers 98:24–39. doi: 10.1080/00045600701734018.

Helsel, D.R. and R.M. Hirsch, 2002. Statistical Methods in Water Resources. Techniques of Water Resources Investigations, Book 4, Chapter A3. U.S. Geological Survey, 522p. http://pubs.er.usgs.gov/publication/twri04A3

Jassal R.S., T.A. Black, D.L. Spittlehouse, C. Brümmer, and Z. Nesic. 2009. Evapotranspiration and water use efficiency in different-aged Pacific Northwest Douglas-fir stands. Agricultural and Forest Meteorology 149:1168–1178.

Jassby, A.D. and J.E. Cloern. 2012. wq: Some tools for exploring water quality monitoring data. R package version 0.3-8. http://cran.r-project.org/web/packages/wq

Johnstone, J.A. and T.E. Dawson, 2010. Climatic Context and Ecological Implications of Summer Fog Decline in the Coast Redwood Region. Proceedings of the National Academy of Sciences 107:4533–4538. doi: 10.1073/pnas.0915062107.

Jones, J.A. and D.A. Post, 2004. Seasonal and Successional Streamflow Response to Forest Cutting and Regrowth in the Northwest and Eastern United States. Water Resources Research 40:W05203. doi: 10.1029/2003WR002952.

Jones, J.A., G.L. Achterman, L.A. Augustine, I.F. Creed, P.F. Ffolliott, L. MacDonald, and B.C. Wemple, 2009. Hydrologic Effects of a Changing Forested Landscape-Challenges for the Hydrological Sciences. Hydrological Processes 23:2699–2704. doi: 10.1002/hyp.7404.

Keter, T.S. and H. Busam, 1997. Growing the Forest Backwards Virtual Prehistory on the North Fork of the Eel River. Paper Presented to the Society for California Archaeology, March 27, 1997, Rohnert Park, California. http://solararch.org/Papers/SCA1997GISvegmappingintheNorthFork.pdf

Kim, J.-S. and S. Jain, 2010. High-Resolution Streamflow Trend Analysis Applicable to Annual Decision Calendars: A Western United States Case Study. Climatic Change 102:699–707. doi: 10.1007/s10584-010-9933-3.

Klein, R.D. 2012. Hydrologic Assessment of Low Flows in the Mattole River Basin, 2004-2011. Prepared for Sanctuary Forest Inc. Mattole Flow Program, February 2012. 22 p.

Lins, H.F., 2012. USGS Hydro-Climatic Data Network 2009 (HCDN-2009). United States Geological Survey. http://pubs.usgs.gov/fs/2012/3047/. Accessed 14 Aug 2014.

Livneh, B., E.A. Rosenberg, C. Lin, B. Nijssen, V. Mishra, K.M. Andreadis, E.P. Maurer, and D.P. Lettenmaier, 2013. A Long-Term Hydrologically Based Dataset of Land Surface Fluxes and States for the Conterminous United States: Update and Extensions. Journal of Climate 26:9384–9392. doi: 10.1175/JCLI-D-12-00508.1.

Livneh, B., E.A. Rosenberg, C. Lin, B. Nijssen, V. Mishra, K.M. Andreadis, E.P. Maurer, and D.P. Lettenmaier, 2014. Corrigendum. Journal of Climate 27:477–486. doi: 10.1175/JCLI-D-13-00697.1.

Mattole River and Range Partnership (MRRP). 2009. Mattole Integrated Coastal Watershed Management Plan Foresight 2020. Mattole River and Range Partnership (Mattole Restoration Council, Mattole Salmon Group, and Sanctuary Forest). http://www.mattole.org/wp-content/uploads/2014/08/WatershedPlan_Final_w_Cover.pdf.

Mayer, T.D., 2012. Controls of Summer Stream Temperature in the Pacific Northwest. Journal of Hydrology 475:323–335. doi: 10.1016/j.jhydrol.2012.10.012.

Mayer, T.D. and S.W. Naman, 2011. Streamflow Response to Climate as Influenced by Geology and Elevation. Journal of the American Water Resources Association (JAWRA) 47:724–738. doi: 10.1111/j.1752-1688.2011.00537.x.

McIntyre, P.J., J.H. Thorne, C.R. Dolanc, A.L. Flint, L.E. Flint, M. Kelly, and D.D. Ackerly, 2015. Twentieth-Century Shifts in Forest Structure in California: Denser Forests, Smaller Trees, and Increased Dominance of Oaks. Proceedings of the National Academy of Sciences:201410186. doi: 10.1073/pnas.1410186112.

Menne, M. J. , C.N. Williams, Jr., and R.S. Vose. 2015. United States Historical Climatology Network (USHCN) Version 2.5 Serial Monthly Dataset. Carbon Dioxide Information Analysis Center, Oak Ridge National Laboratory, Oak Ridge, Tennessee. http://cdiac.ornl.gov/epubs/ndp/ushcn/ushcn.html

Moore, G.W., B.J. Bond, J.A. Jones, N. Phillips, and F.C. Meinzer, 2004. Structural and Compositional Controls on Transpiration in 40- and 450-Year-Old Riparian Forests in Western Oregon, USA. Tree Physiology 24:481–491. doi: 10.1093/treephys/24.5.481.

Murphy, M.S., 2008. Edaphic Controls Over Succession In Former Oak Savanna, Willamette Valley, Oregon. Thesis, University of Oregon. http://scholarsbank.uoregon.edu/xmlui/handle/1794/7887. Accessed 2 Sep 2015

National Marine Fisheries Service (NMFS). 2002. Endangered Species Act Section 7 Consultation, Biological Opinion for the Proposed License Amendment for the Potter Valley Project. Federal Energy Regulatory Commission Project Number 77-110. National Marine Fisheries Service, Southwest Region, Long Beach, CA. 135p. http://elibrary.ferc.gov/idmws/file_list.asp?accession_num=20021202-0257

National Marine Fisheries Service (NMFS). 2014. Final Recovery Plan for the Southern Oregon/Northern California Coast Evolutionarily Significant Unit of Coho Salmon (Oncorhynchus kisutch). National Marine Fisheries Service. Arcata, CA. http://www.nmfs.noaa.gov/pr/recovery/plans/cohosalmon_soncc.pdf

Perry, D.A., P.F. Hessburg, C.N. Skinner, T.A. Spies, S.L. Stephens, A.H. Taylor, J.F. Franklin, B. McComb, and G. Riegel. 2011. The Ecology of Mixed Severity Fire Regimes in Washington, Oregon, and Northern California. Forest Ecology and Management 262:703–717.

Poff, L.N., 1996. A Hydrogeography of Unregulated Streams in the United States and an Examination of Scale-Dependence in Some Hydrological Descriptors. Freshwater Biology 36:71-79.

Power, M.E., K. Bouma-Gregson, P. Higgins, and S.M. Carlson, 2015. The Thirsty Eel: Summer and Winter Flow Thresholds That Tilt the Eel River of Northwestern California from Salmon-Supporting to Cyanobacterially Degraded States. Copeia 2015:200–211. doi: 10.1643/CE-14-086.

R Core Team, 2012. R: A language and environment for statistical computing. R Foundation for Statistical Computing, Vienna, Austria. ISBN 3-900051-07-0. http://www.R-project.org.

Rantz, S.E., 1964. Surface-Water Hydrology of Coastal Basins of Northern California. Surface-water hydrology of California coastal basins between San Francisco Bay and Eel River. Geological Survey Water-Supply Paper 1758. Prepared in cooperation with the California Department of Water Resources, Sacramento, California.

Rantz, S. E., and T. H. Thompson. 1967. Surface-water hydrology of California coastal basins between San Francisco Bay and Eel River. Geological Survey Water-Supply Paper 1851. Prepared in cooperation with the California Department of Water Resources, Sacramento, California.

Reid, L. and J. Lewis, 2011. Evaluating Cumulative Effects of Logging and Potential Climate Change on Dry-Season Flow in a Coast Redwood Forest. The Fourth Interagency Conference on Research in the Watersheds, 26-30 September 2011, Fairbanks, AK. 6p. http://www.treesearch.fs.fed.us/pubs/38977

Sahara, A.E., D.A. Sarr, R.W. Van Kirk, and E.S. Jules, 2015. Quantifying Habitat Loss: Assessing Tree Encroachment into a Serpentine Savanna Using Dendroecology and Remote Sensing. Forest Ecology and Management 340:9–21. doi: 10.1016/j.foreco.2014.12.019.

Sawaske, S.R. and D.L. Freyberg, 2014. An Analysis of Trends in Baseflow Recession and Low-Flows in Rain-Dominated Coastal Streams of the Pacific Coast. Journal of Hydrology 59:599–610. doi: 10.1016/j.jhydrol.2014.07.046.

Silva, I.C. and H.G. Rodríguez, 2001. Interception Loss, Throughfall and Stemflow Chemistry in Pine and Oak Forests in Northeastern Mexico. Tree Physiology 21:1009–1013. doi: 10.1093/treephys/21.12-13.1009.

Skinner, C.N., C.S. Abbott, D.L. Fry, S.L. Stephens, A.H. Taylor, and V. Trouet, 2009. Human and Climatic Influences on Fire Occurrence in California's North Coast Range, USA. Fire Ecology 5:76–99. doi: 10.4996/fireecology.0503076.

Stephens, S. and B. Collins. 2015. Variability in Forest Structure across a Central Sierra Nevada Landscape from 1911 Inventory Data. Variability in Forest Structure across a Central Sierra Nevada Landscape from 1911 Inventory Data. Presentation.

https://acconsensus.files.wordpress.com/2015/03/stephens-scott-1911-forests-presented-2-18-15.pdf.

Stillwater Sciences. 1999. South Fork Eel TMDL: Sediment Source Analysis, Final Report. Prepared for Tetra Tech, Inc. by Stillwater Sciences, Berkeley, California. http://www.ibrarian.net/navon/paper/SOUTH_FORK_EEL_TMDL__SEDIMENT_SOURCE_ANALYSIS_Fin.pdf?paperid=15131729

Templ, M., A. Alfons, A. Kowarik, and B. Prantner, 2013. VIM: Visualization and Imputation of Missing Values. http://cran.r-project.org/web/packages/VIM/index.html.

Thorne, J.H., R.M. Boynton, L.E. Flint, and A.L. Flint. 2015. The Magnitude and Spatial Patterns of Historical and Future Hydrologic Change in California's Watersheds. http://www.esajournals.org/doi/10.1890/ES14-00300.1. Accessed 16 May 2015.

van Buuren, S and K Groothuis-Oudshoorn. 2011. mice: Multivariate Imputation by Chained Equations in R. Journal of Statistical Software, 45(3), 1-67. URL http://www.jstatsoft.org/v45/i03/.

Vano, J.A., B. Nijssen, and D.P. Lettenmaier. 2015. Seasonal Hydrologic Responses to Climate Change in the Pacific Northwest. Water Resources Research 51:1959–1976. doi: 10.1002/2014WR015909.

Yoshiyama, R.M. and P.B. Moyle, 2010. Historical Review of Eel River Anadromous Salmonids, with Emphasis on Chinook Salmon, Coho Salmon and Steelhead. Prepared for CalTrout by the University of California, Davis. https://watershed.ucdavis.edu/pdf/Yoshiyama-Moyle_Eel%20River%20Final%20Report%202010.pdf.

Yue, S., P. Pilon, and G. Cavadias, 2002. Power of the Mann–Kendall and Spearman's Rho Tests for Detecting Monotonic Trends in Hydrological Series. Journal of Hydrology 259:254–271. doi: 10.1016/S0022-1694(01)00594-7.

Zhang, L., W.R. Dawes, and G.R. Walker, 2001. Response of Mean Annual Evapotranspiration to Vegetation Changes at Catchment Scale. Water Resources Research 37:701–708. doi: 10.1029/2000WR900325.

5 ACKNOWLEDGMENTS

Jeff Walker provided invaluable assistance by developing R code, including implementing the API-flow model and Mann-Kendall trend tests. Scott Greacen of Friends of the Eel River and Bryan McFadin of the North Coast Regional Water Quality Control Board reviewed a draft of this report and provided helpful comments.

APPENDIX A: ADDITIONAL INFORMATION ON PRECIPITATION DATA SOURCES

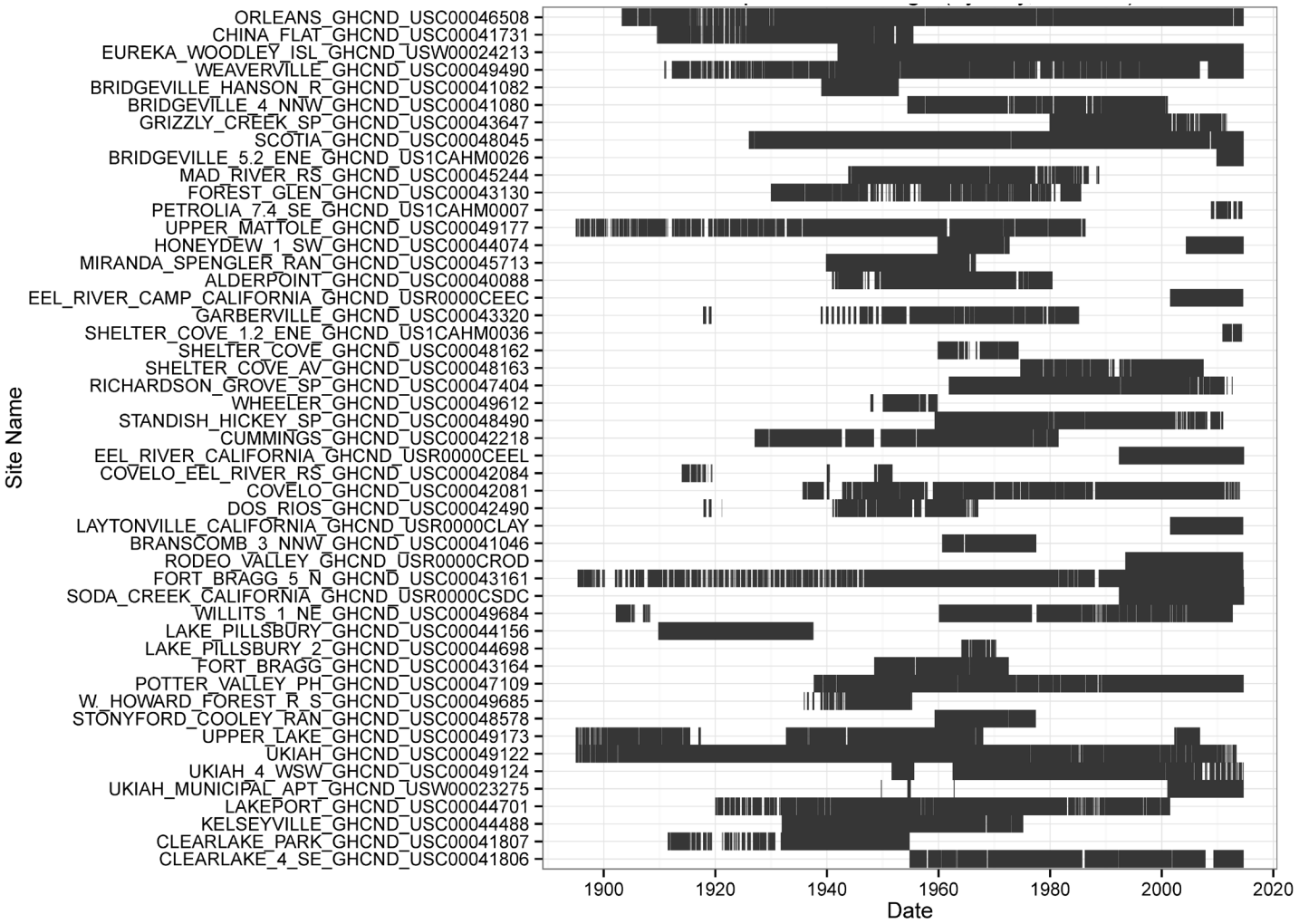

Figure A1. Period of record for selected precipitation stations in the Eel River Basin and adjacent areas from the Global Historical Climatology Network (GHCN) database, compiled by the National Oceanic and Atmospheric Administration (NOAA) National Centers for Environmental Information (NCEI).

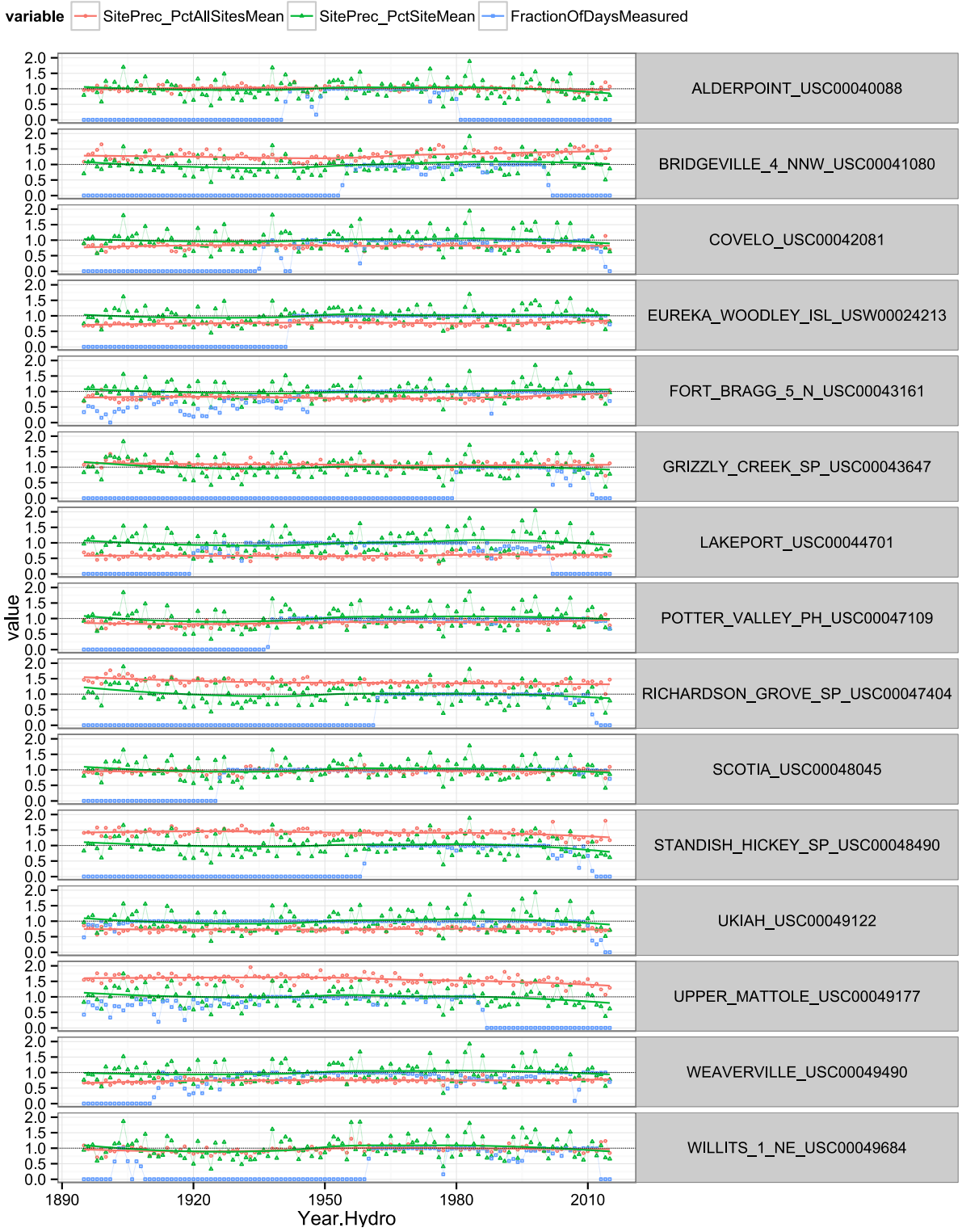

Figure A2. Time series of precipitation data from 1895-2015 for each primary precipitation station including values estimated based on nearby stations, showing for each year: ratio of site precipitation to site's long-term precipitation (SitePrec_PctSiteMean), ratio of site precipitation to mean of all sites' precipitation in year (SitePrec_PctAllSitesMean), and % of days in year with measured (i.e., not estimated) precipitation data.

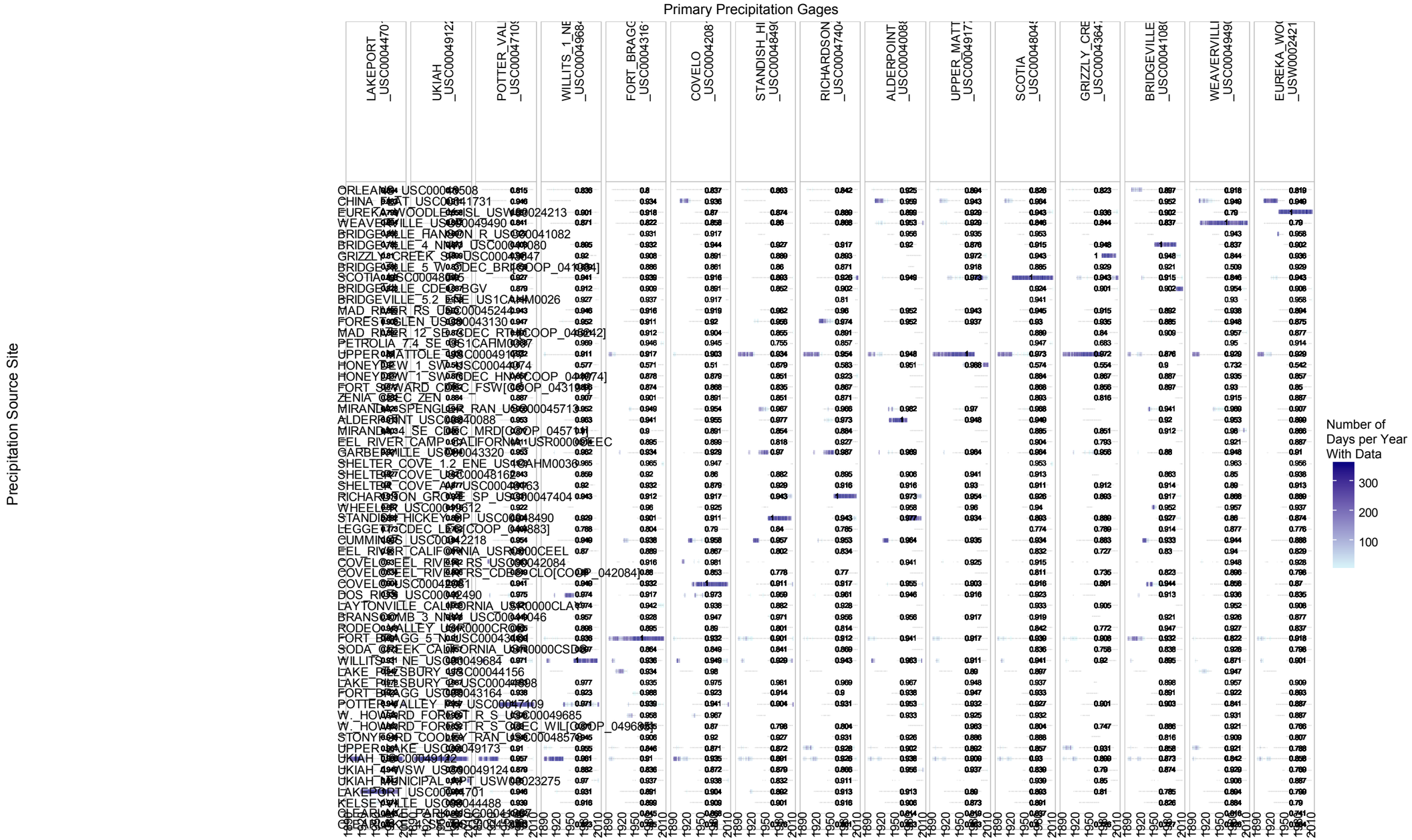

Figure A2. Matrix showing which precipitation gages (rows) were used to fills gaps in records for primary precipitation gages (columns) for each year. The shading of the tall blue vertical bars (see legend) indicates the number of days in each year that were used to assemble the dataset for the primary precipitation gage. Short grey bars indicate which years had precipitation data available. Number overlaid on each gage combination indicates the r^2 value of the regression between the monthly total precipitation of the two gages.

APPENDIX B: ADDITIONAL INFORMATION ON API MODEL USED TO CALCULATE PRECIPITATION-ADJUSTED STREAMFLOW

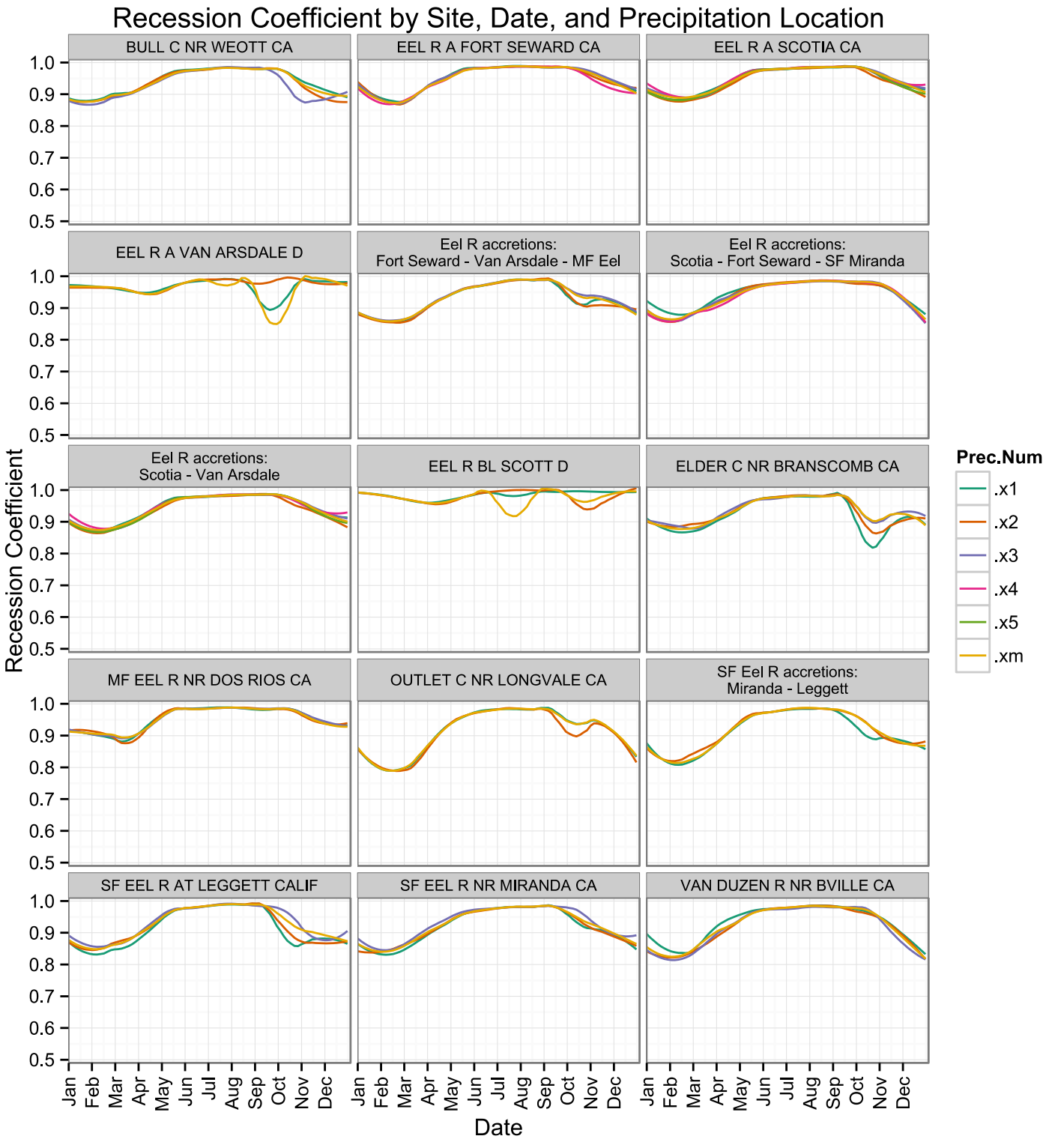

Figure B1. Recession coefficient at each streamflow site, calculated using different precipitation stations for each day of the 365 days of the year. Each station is in its own panel, with a label at the top of panel. Precipitation stations are labelled .x1, .x2, .x3, .x4, and .x5 while the mean precipitation calculated from all stations is labelled as .xm.

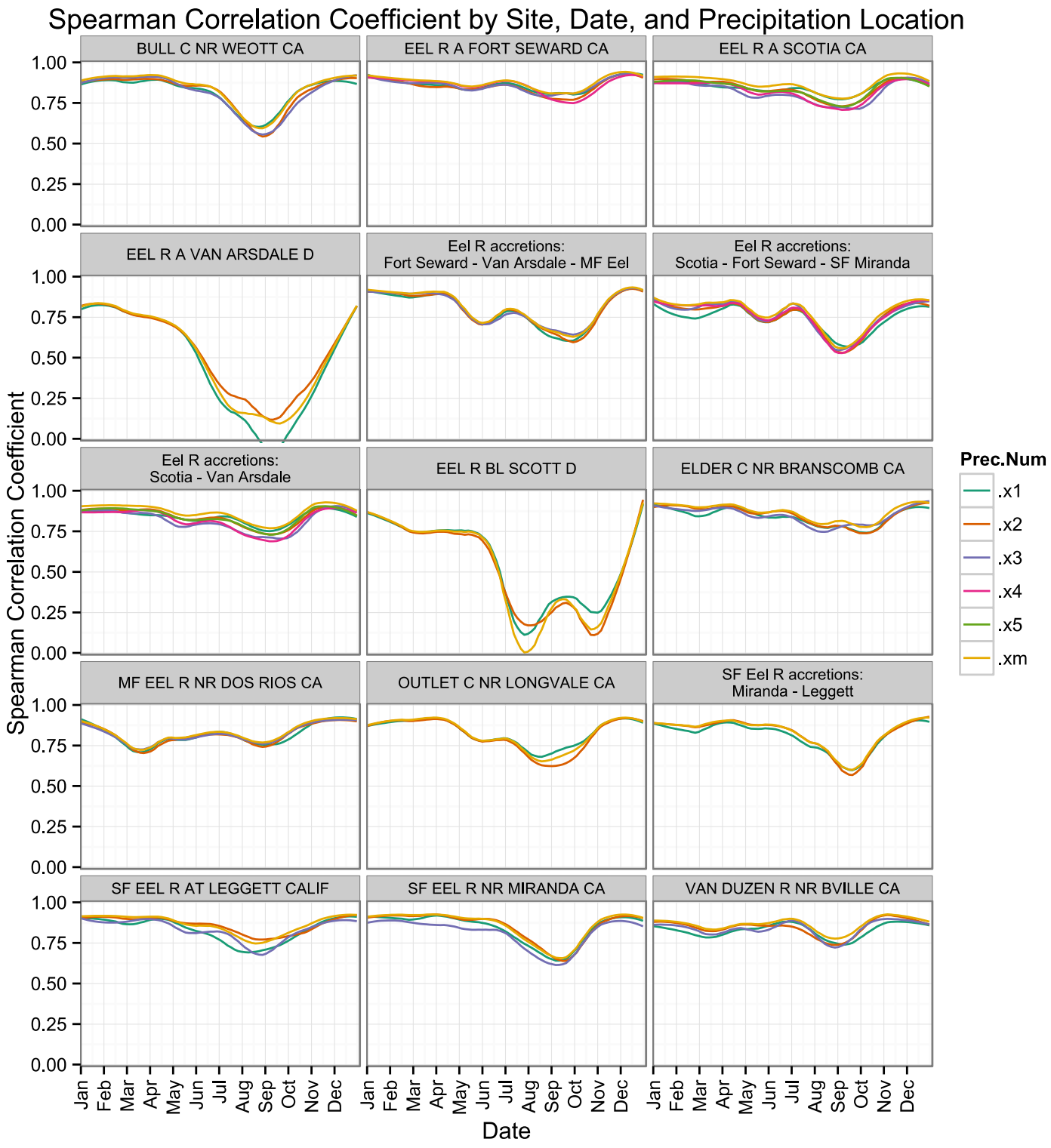

Figure B2. Correlation between streamflow and Antecedent Precipitation Index (API) at each streamflow site, calculated using different precipitation stations for each day of the 365 days of the year. Each station is in its own panel, with a label at the top of panel. Precipitation stations are labelled .x1, .x2, .x3, .x4, and .x5 while the mean precipitation calculated from all stations is labelled as .xm.

APPENDIX C: ADDITIONAL SUMMARIES OF STREAMFLOW TRENDS

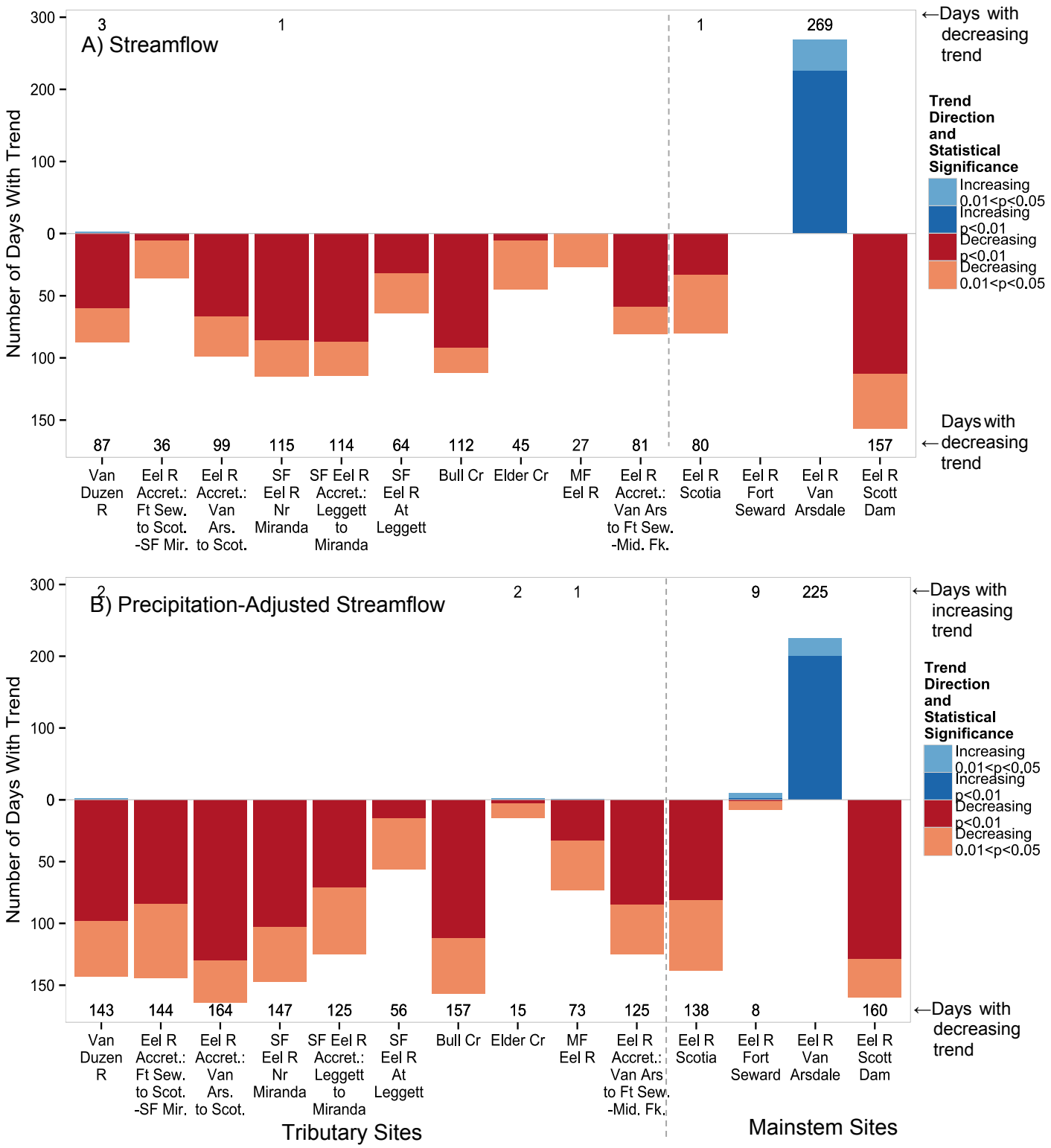

Figure C1. The number of days in entire year (365 possible days) with increasing or decreasing trends in (A) streamflow and (B) precipitation-adjusted streamflow at mainstem and tributary sites for WY1953-2014. Bars are stacked with colors indicating statistical significance and labels indicating the total number of days with an increasing or decreasing trend.

APPENDIX D: ANNUAL TIME SERIES OF SEPTEMBER 1ST STREAMFLOW AND PRECIPITATION-ADJUSTED STREAMFLOW, 1953-2014 AND 1910-2014

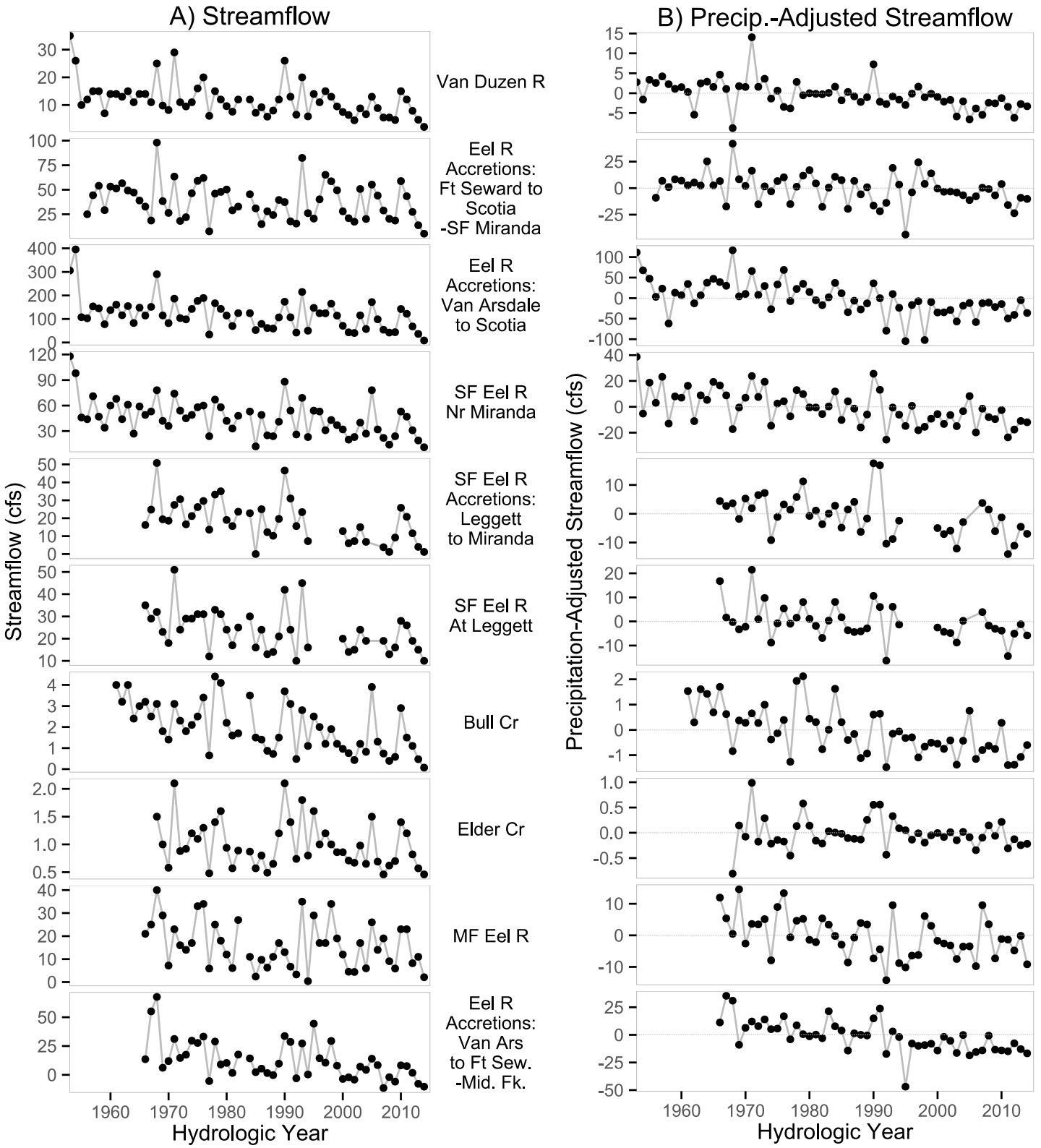

Figure D1. Time series of September 1st (A) streamflow and (B) precipitation-adjusted streamflow at tributary sites for hydrologic years 1953-2014. September 1st streamflows were extremely high in hydrologic year 1983 so are excluded from (A) to preserve legibility of y-axis.

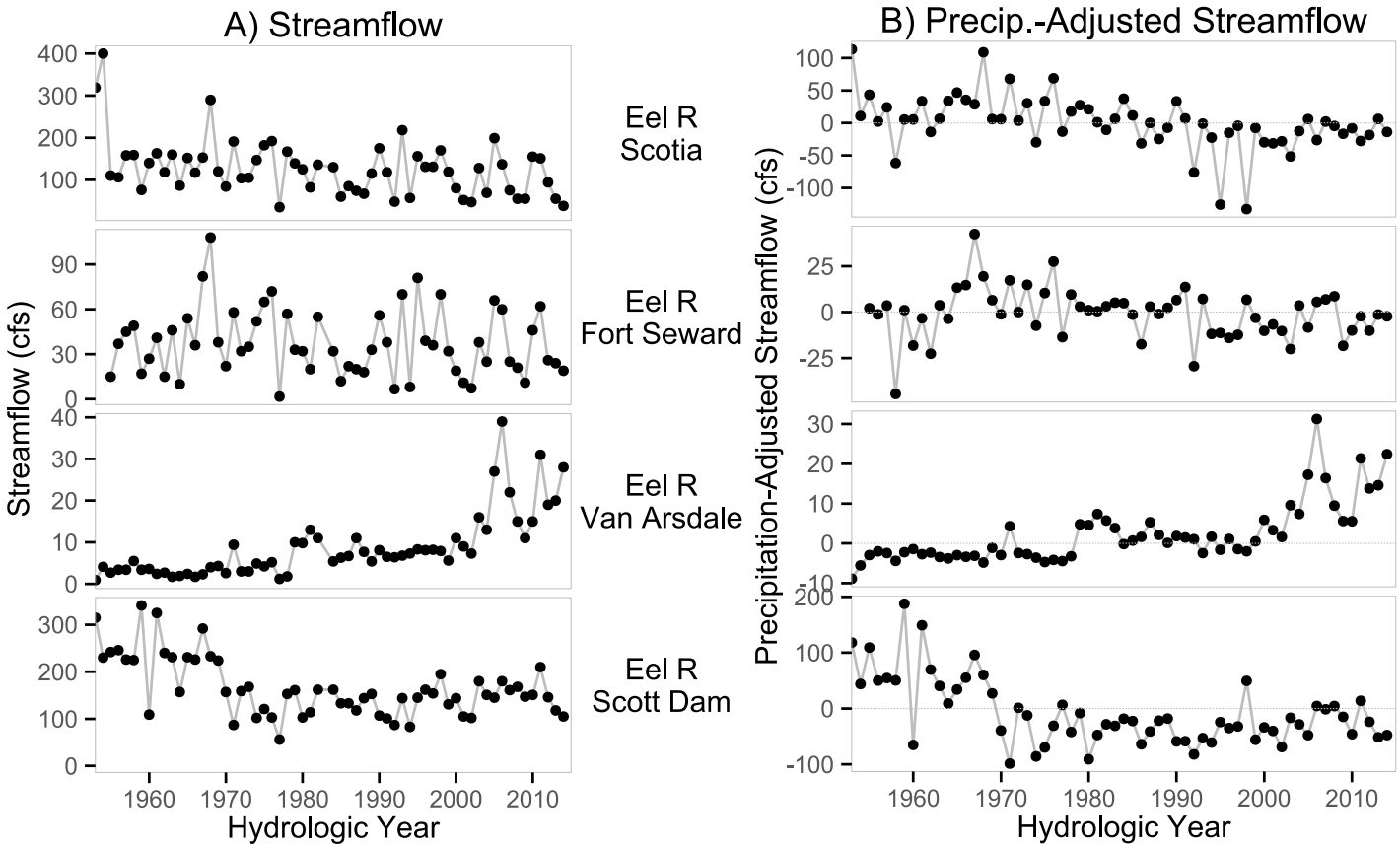

Figure D2. Time series of September 1st (A) streamflow and (B) precipitation-adjusted streamflow at mainstem sites for hydrologic years 1953-2014. Streamflows were extremely high in hydrologic year 1983 so are excluded from (A) to preserve legibility of y-axis.

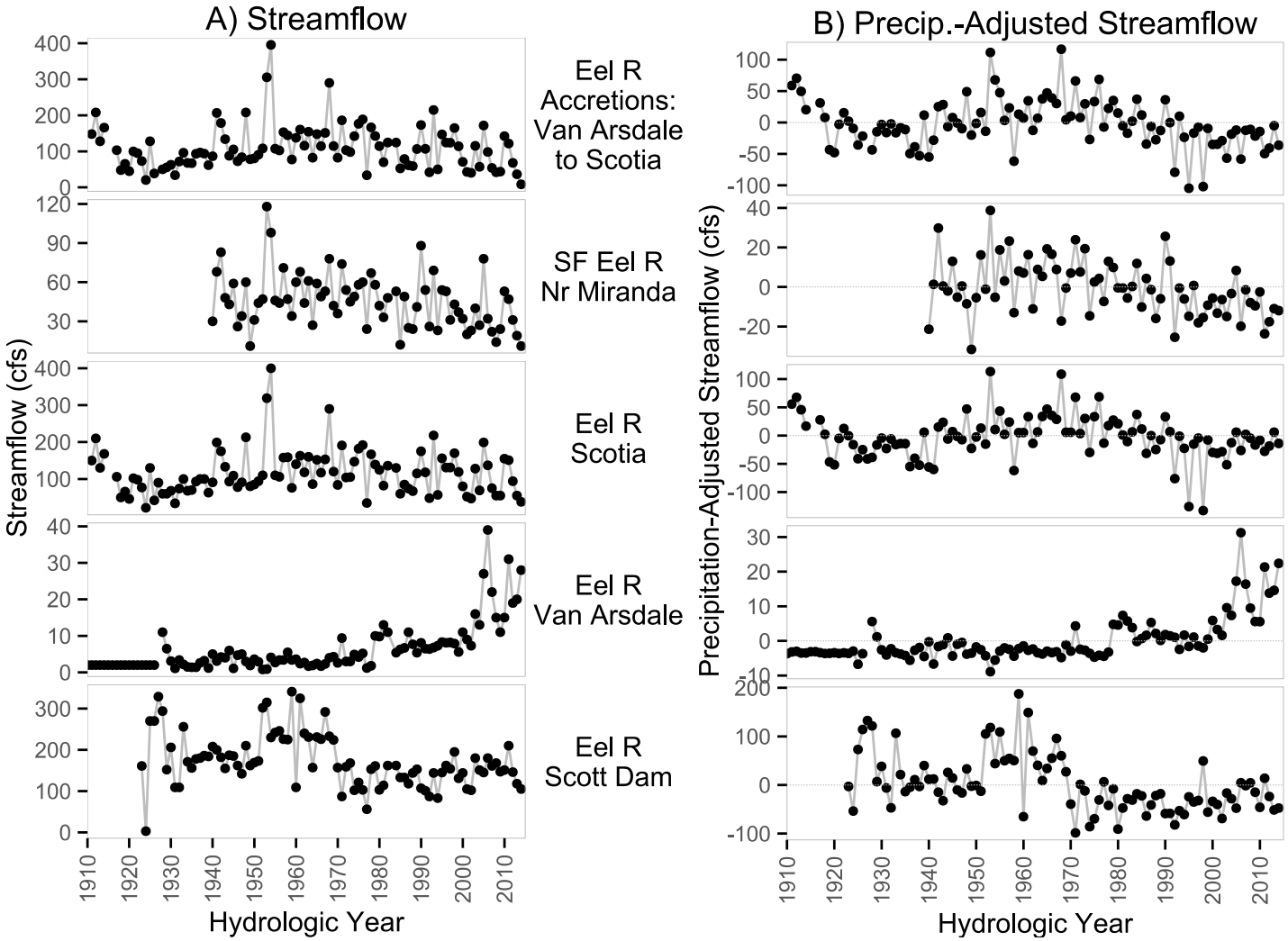

Figure D3. Time series of September 1 (A) streamflow and (B) precipitation-adjusted streamflow for hydrologic years 1910-2014 at the tributary and mainstem sites with the longest gaging records. September 1 streamflows were extremely high in 1983 so are excluded from (A) to preserve legibility of y-axis.

APPENDIX E: SENSITIVITY OF 1953-2014 TREND TO CHOICE OF PRECIPITATION STATIONS

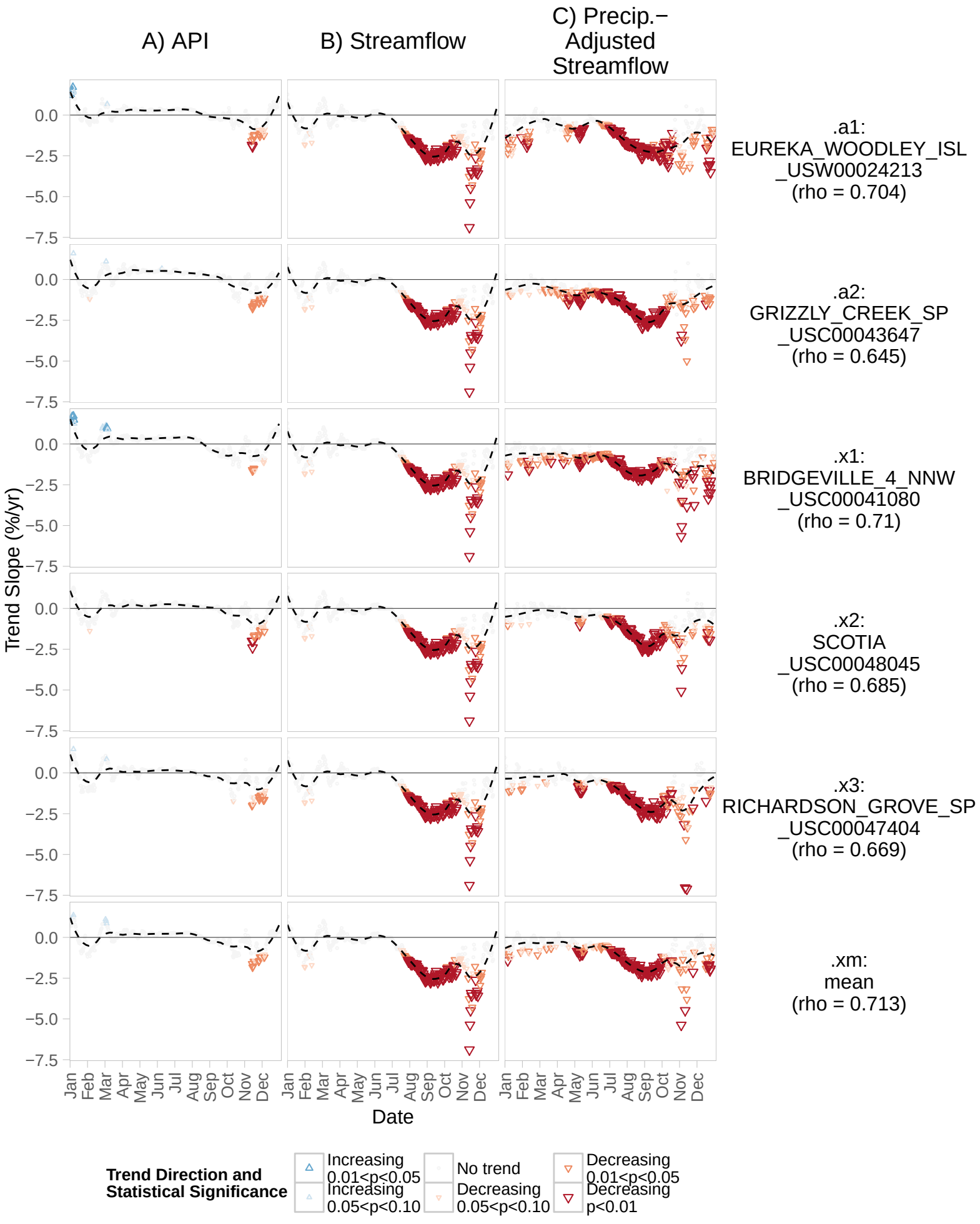
Bull Cr:
Trends for WY1953−2012
A) API
B) Streamflow
C) Precip.−
Adjusted
Streamflow
Trend Slope (%/yr)
0.0
−2.5
−5.0
−7.5
Jan
Feb
Mar
Apr
May
Jun
Jul
Aug
Sep
Oct
Nov
Dec
Date
.a1:
EUREKA_WOODLEY_ISL
_USW00024213
(rho = 0.704)
.a2:
GRIZZLY_CREEK_SP
_USC00043647
(rho = 0.645)
.x1:
BRIDGEVILLE_4_NNW
_USC00041080
(rho = 0.71)
.x2:
SCOTIA
_USC00048045
(rho = 0.685)
.x3:
RICHARDSON_GROVE_SP
_USC00047404
(rho = 0.669)
.xm:
mean
(rho = 0.713)
Trend Direction and
Statistical Significance
Increasing
0.01<p<0.05
Increasing
0.05<p<0.10
No trend
Decreasing
0.05<p<0.10
Decreasing
0.01<p<0.05
Decreasing
p<0.01

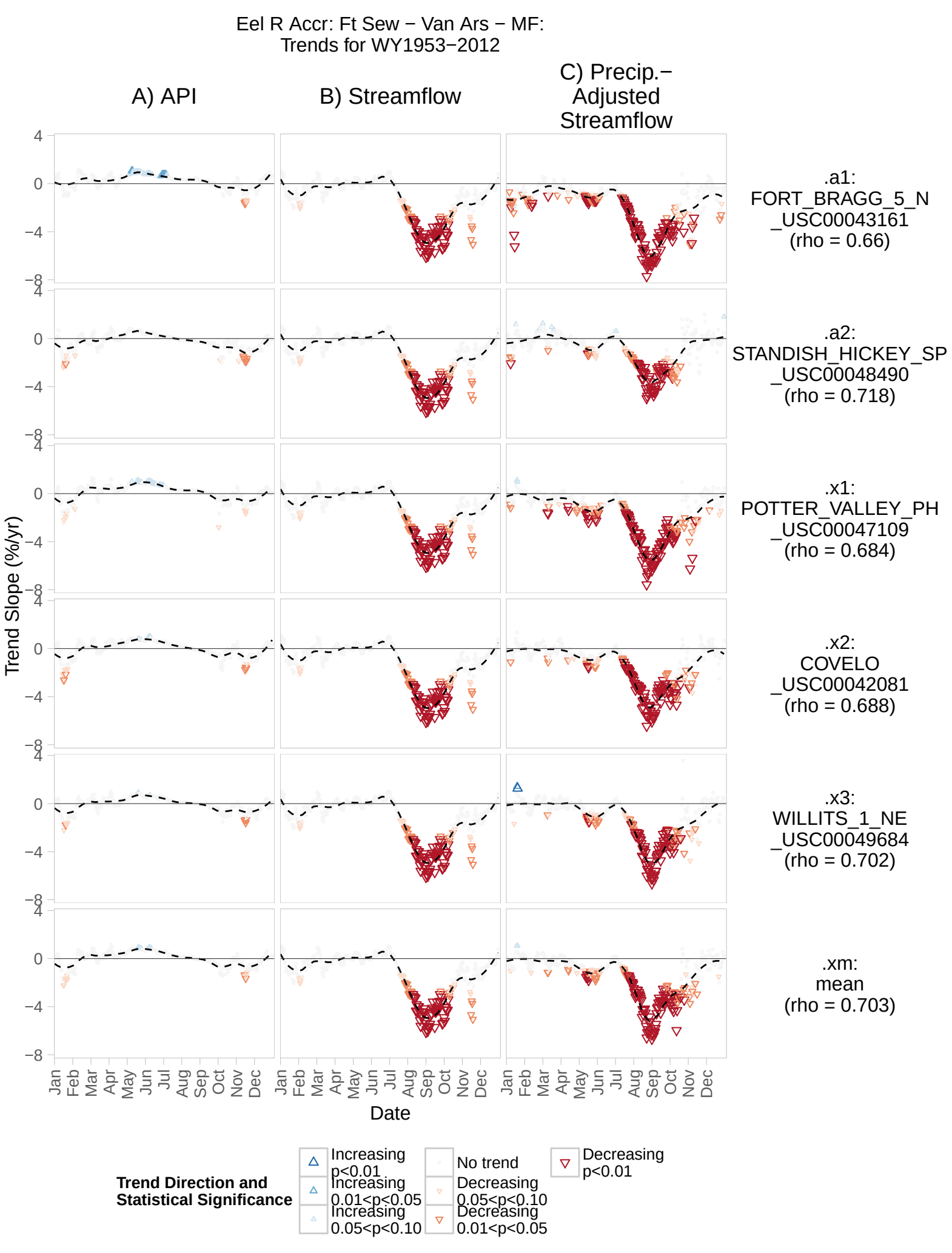
Eel R Accr: Ft Sew − Van Ars − MF:
Trends for WY1953−2012
A) API
B) Streamflow
C) Precip.−
Adjusted
Streamflow
.a1:
FORT_BRAGG_5_N
_USC00043161
(rho = 0.66)
.a2:
STANDISH_HICKEY_SP
_USC00048490
(rho = 0.718)
.x1:
POTTER_VALLEY_PH
_USC00047109
(rho = 0.684)
.x2:
COVELO
_USC00042081
(rho = 0.688)
.x3:
WILLITS_1_NE
_USC00049684
(rho = 0.702)
.xm:
mean
(rho = 0.703)
Trend Slope (%/yr)
4
0
−4
−8
Jan
Feb
Mar
Apr
May
Jun
Jul
Aug
Sep
Oct
Nov
Dec
Date
Trend Direction and
Statistical Significance
Increasing
p<0.01
Increasing
0.01<p<0.05
Increasing
0.05<p<0.10
No trend
Decreasing
0.05<p<0.10
Decreasing
0.01<p<0.05
Decreasing
p<0.01

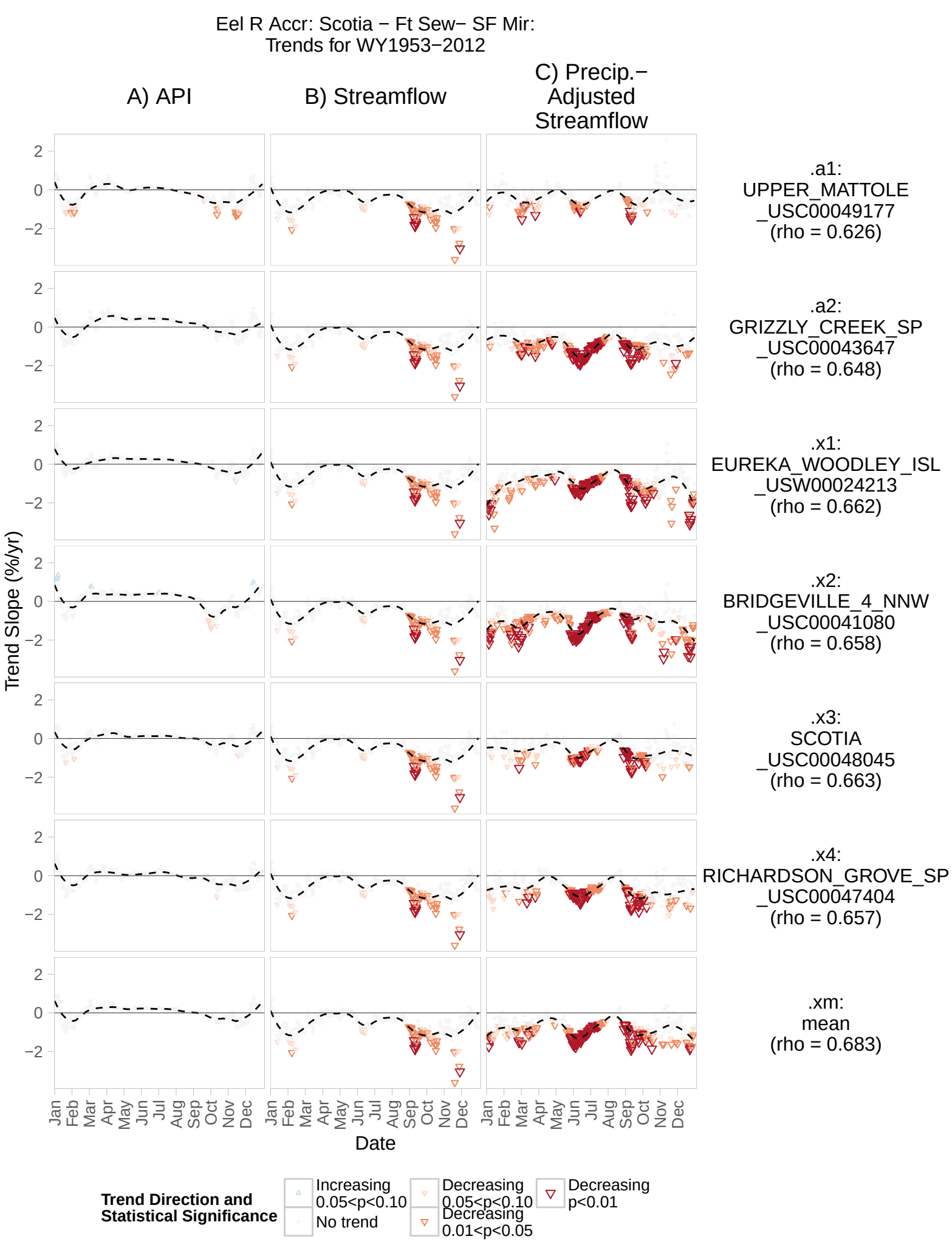
Eel R Accr: Scotia − Ft Sew− SF Mir:
Trends for WY1953−2012
A) API
B) Streamflow
C) Precip.−
Adjusted
Streamflow
.a1:
UPPER_MATTOLE
_USC00049177
(rho = 0.626)
.a2:
GRIZZLY_CREEK_SP
_USC00043647
(rho = 0.648)
.x1:
EUREKA_WOODLEY_ISL
_USW00024213
(rho = 0.662)
.x2:
BRIDGEVILLE_4_NNW
_USC00041080
(rho = 0.658)
.x3:
SCOTIA
_USC00048045
(rho = 0.663)
.x4:
RICHARDSON_GROVE_SP
_USC00047404
(rho = 0.657)
.xm:
mean
(rho = 0.683)
Trend Slope (%/yr)
2
0
−2
Jan
Feb
Mar
Apr
May
Jun
Jul
Aug
Sep
Oct
Nov
Dec
Date
Trend Direction and
Statistical Significance
Increasing
0.05<p<0.10
No trend
Decreasing
0.05<p<0.10
Decreasing
0.01<p<0.05
Decreasing
p<0.01

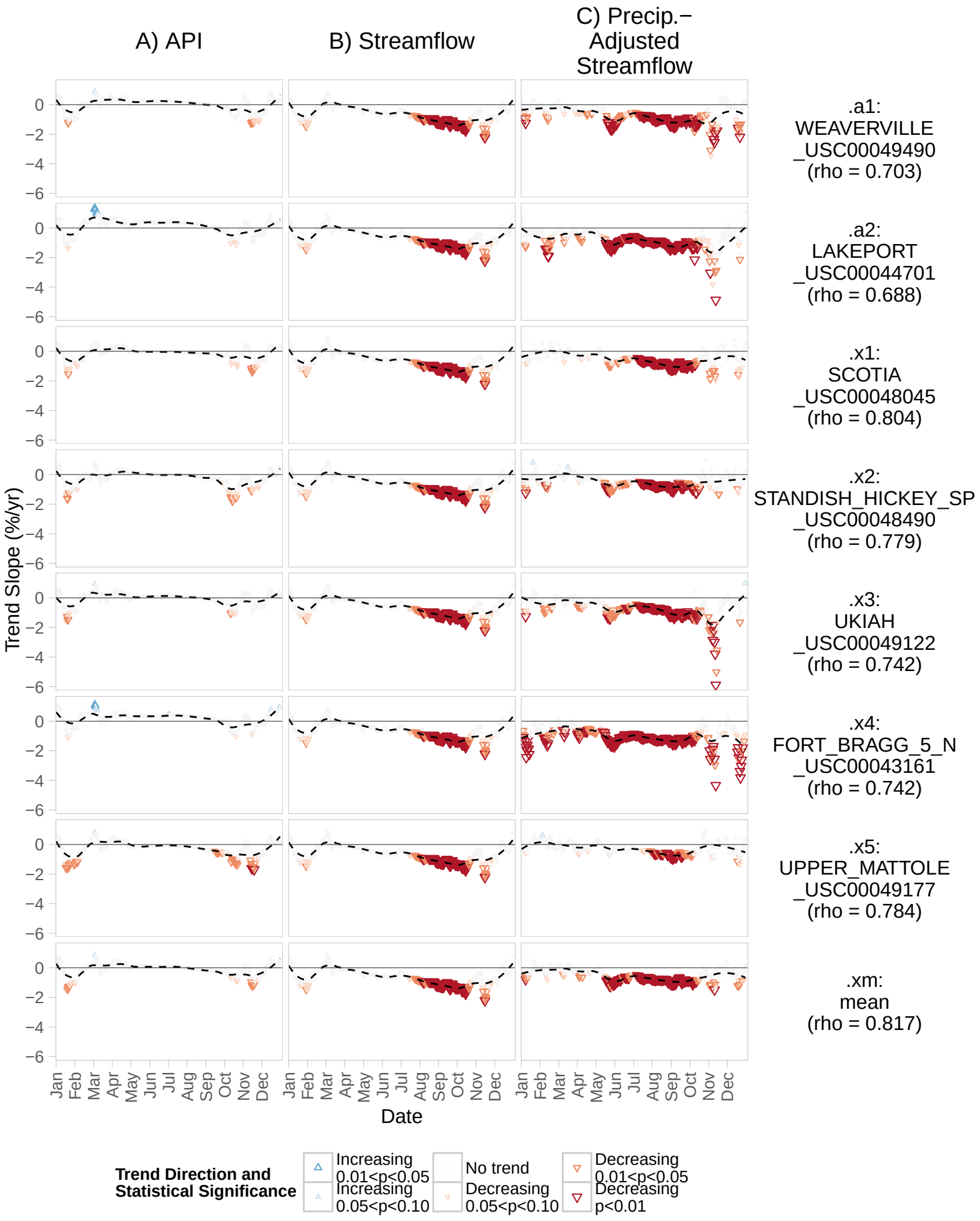
Eel R Accr: Scotia − Van Ars:
Trends for WY1953−2012
A) API
B) Streamflow
C) Precip.−
Adjusted
Streamflow
.a1:
WEAVERVILLE
_USC00049490
(rho = 0.703)
.a2:
LAKEPORT
_USC00044701
(rho = 0.688)
.x1:
SCOTIA
_USC00048045
(rho = 0.804)
.x2:
STANDISH_HICKEY_SP
_USC00048490
(rho = 0.779)
.x3:
UKIAH
_USC00049122
(rho = 0.742)
.x4:
FORT_BRAGG_5_N
_USC00043161
(rho = 0.742)
.x5:
UPPER_MATTOLE
_USC00049177
(rho = 0.784)
.xm:
mean
(rho = 0.817)
Trend Slope (%/yr)
0
−2
−4
−6
Jan
Feb
Mar
Apr
May
Jun
Jul
Aug
Sep
Oct
Nov
Dec
Date
Trend Direction and
Statistical Significance
Increasing
0.01<p<0.05
Increasing
0.05<p<0.10
No trend
Decreasing
0.05<p<0.10
Decreasing
0.01<p<0.05
Decreasing
p<0.01

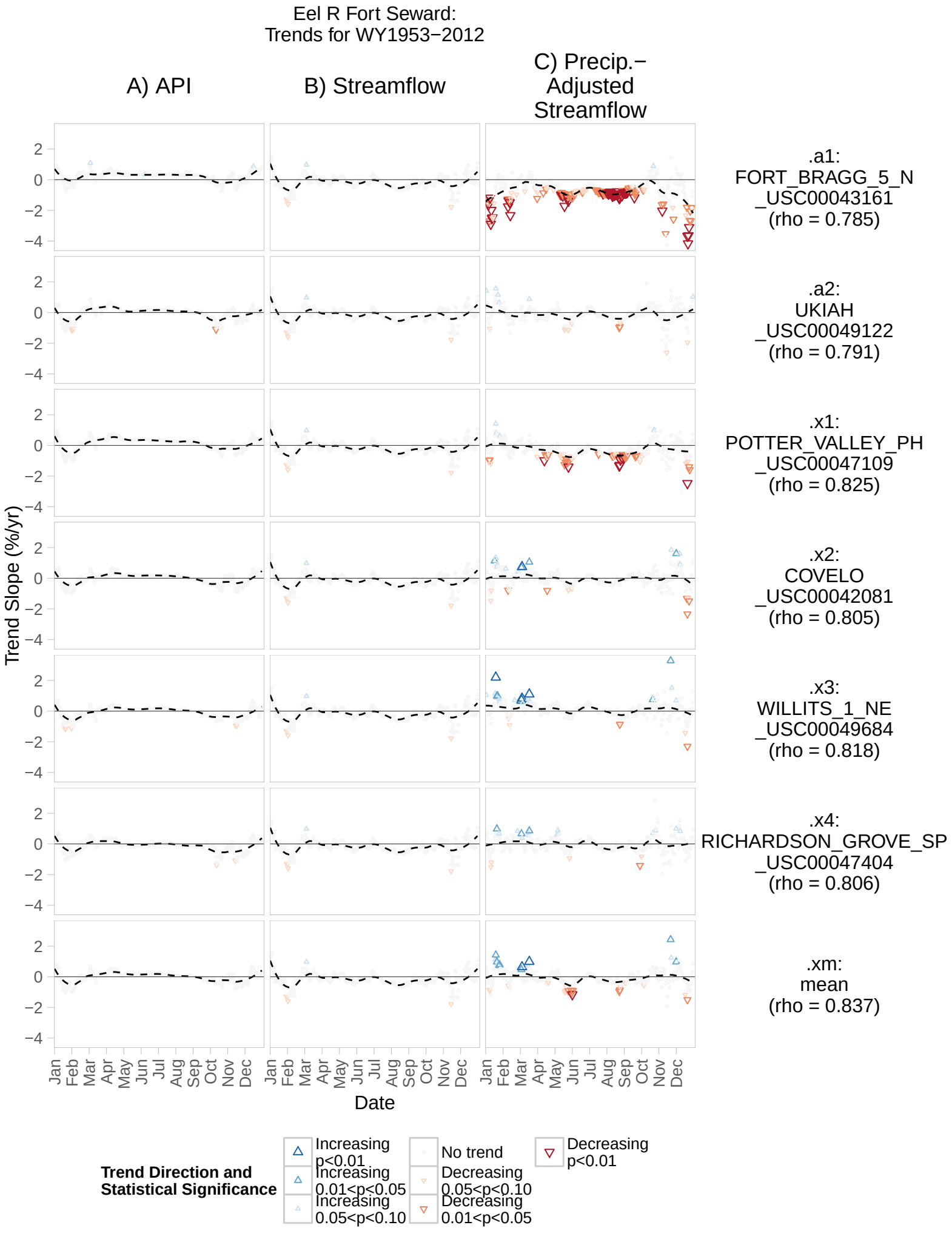
Eel R Fort Seward:
Trends for WY1953−2012
A) API
B) Streamflow
C) Precip.−
Adjusted
Streamflow
.a1:
FORT_BRAGG_5_N
_USC00043161
(rho = 0.785)
.a2:
UKIAH
_USC00049122
(rho = 0.791)
.x1:
POTTER_VALLEY_PH
_USC00047109
(rho = 0.825)
.x2:
COVELO
_USC00042081
(rho = 0.805)
.x3:
WILLITS_1_NE
_USC00049684
(rho = 0.818)
.x4:
RICHARDSON_GROVE_SP
_USC00047404
(rho = 0.806)
.xm:
mean
(rho = 0.837)
Trend Slope (%/yr)
2
0
−2
−4
Jan
Feb
Mar
Apr
May
Jun
Jul
Aug
Sep
Oct
Nov
Dec
Date
Trend Direction and
Statistical Significance
Increasing
p<0.01
Increasing
0.01<p<0.05
Increasing
0.05<p<0.10
No trend
Decreasing
0.05<p<0.10
Decreasing
0.01<p<0.05
Decreasing
p<0.01

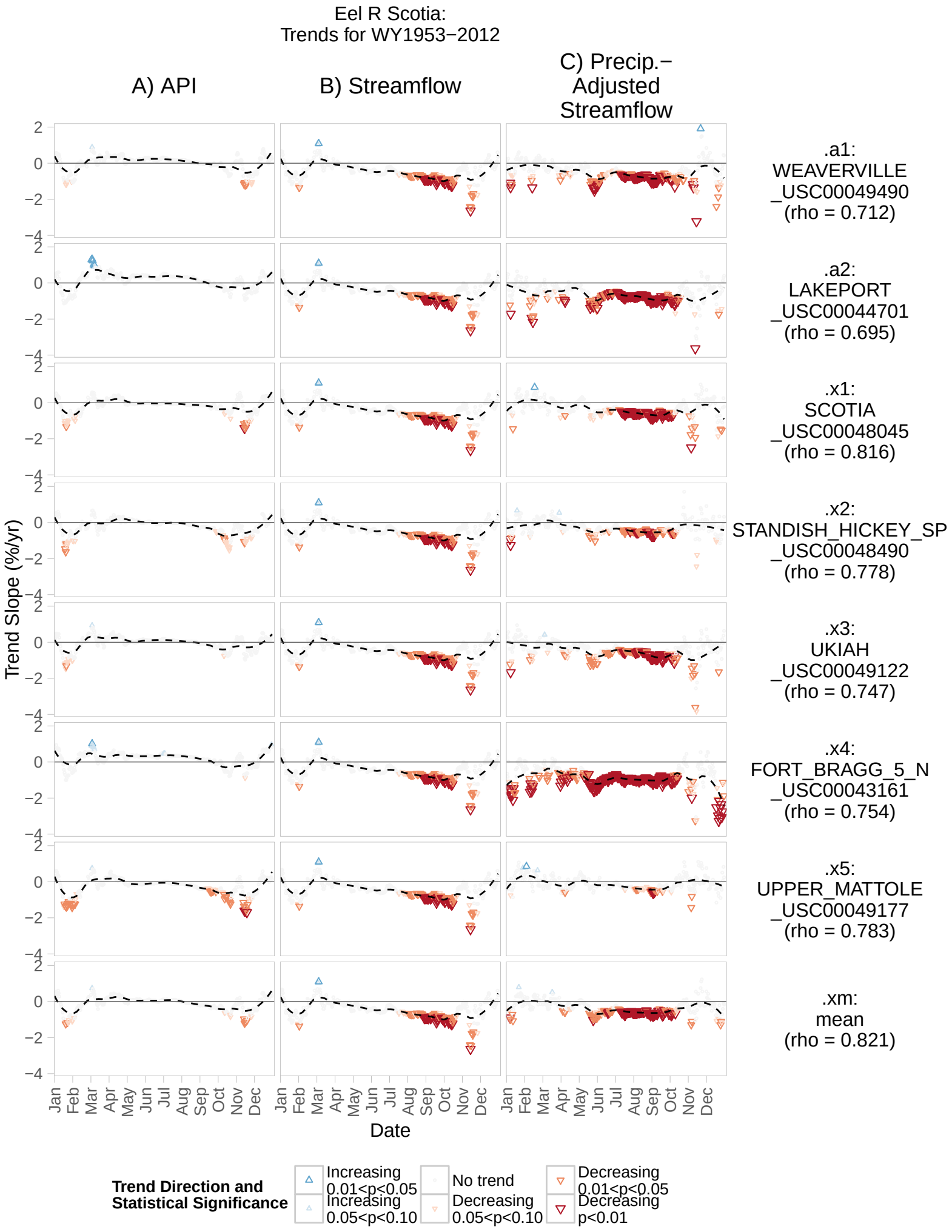
Eel R Scotia:
Trends for WY1953−2012
A) API
B) Streamflow
C) Precip.−
Adjusted
Streamflow
.a1:
WEAVERVILLE
_USC00049490
(rho = 0.712)
.a2:
LAKEPORT
_USC00044701
(rho = 0.695)
.x1:
SCOTIA
_USC00048045
(rho = 0.816)
.x2:
STANDISH_HICKEY_SP
_USC00048490
(rho = 0.778)
.x3:
UKIAH
_USC00049122
(rho = 0.747)
.x4:
FORT_BRAGG_5_N
_USC00043161
(rho = 0.754)
.x5:
UPPER_MATTOLE
_USC00049177
(rho = 0.783)
.xm:
mean
(rho = 0.821)
Trend Slope (%/yr)
2
0
−2
−4
Jan
Feb
Mar
Apr
May
Jun
Jul
Aug
Sep
Oct
Nov
Dec
Date
Trend Direction and
Statistical Significance
Increasing
0.01<p<0.05
Increasing
0.05<p<0.10
No trend
Decreasing
0.05<p<0.10
Decreasing
0.01<p<0.05
Decreasing
p<0.01

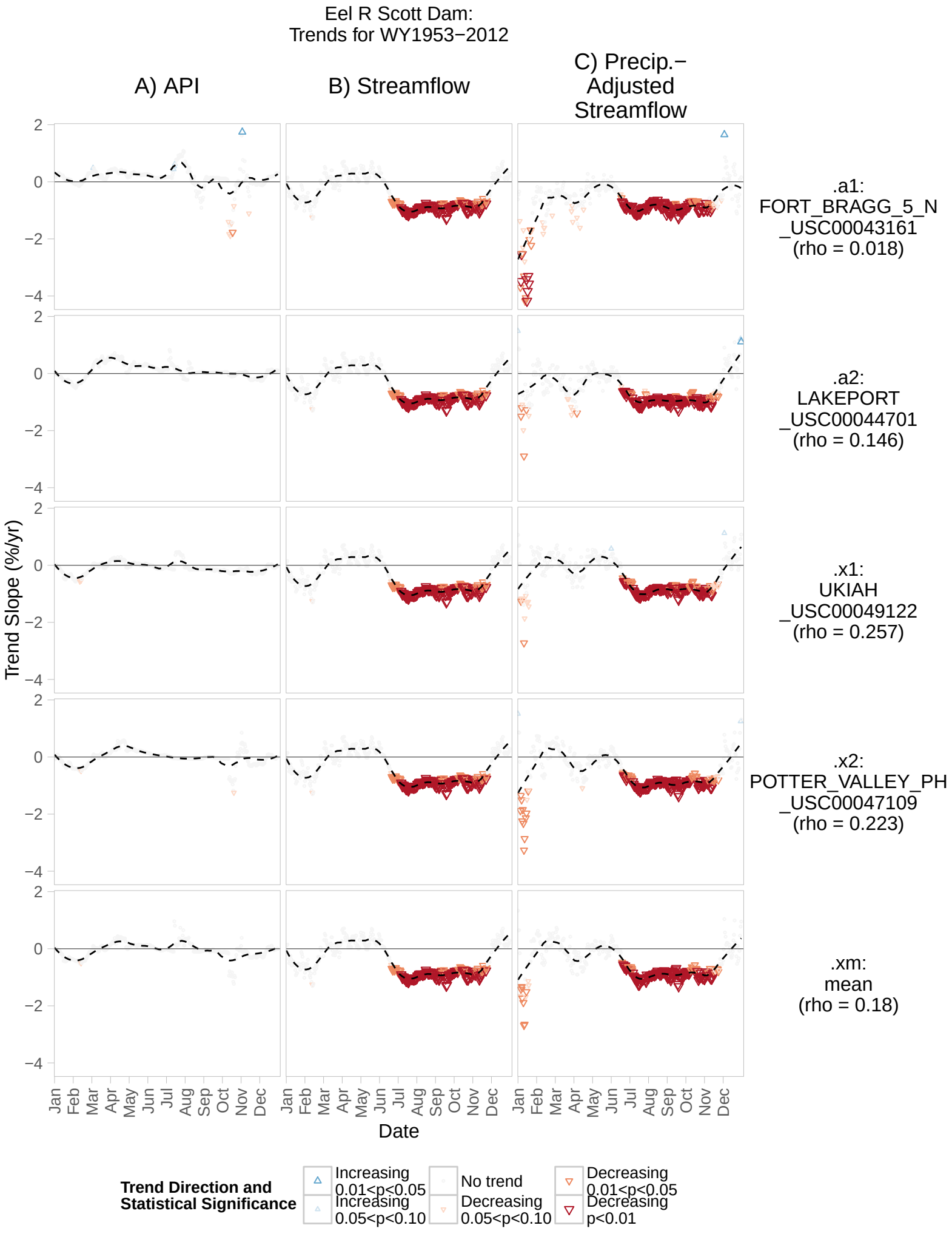
Eel R Scott Dam:
Trends for WY1953−2012
A) API
B) Streamflow
C) Precip.−
Adjusted
Streamflow
.a1:
FORT_BRAGG_5_N
_USC00043161
(rho = 0.018)
.a2:
LAKEPORT
_USC00044701
(rho = 0.146)
.x1:
UKIAH
_USC00049122
(rho = 0.257)
.x2:
POTTER_VALLEY_PH
_USC00047109
(rho = 0.223)
.xm:
mean
(rho = 0.18)
Trend Slope (%/yr)
2
0
−2
−4
Jan
Feb
Mar
Apr
May
Jun
Jul
Aug
Sep
Oct
Nov
Dec
Date
Trend Direction and
Statistical Significance
Increasing
0.01<p<0.05
Increasing
0.05<p<0.10
No trend
Decreasing
0.05<p<0.10
Decreasing
0.01<p<0.05
Decreasing
p<0.01

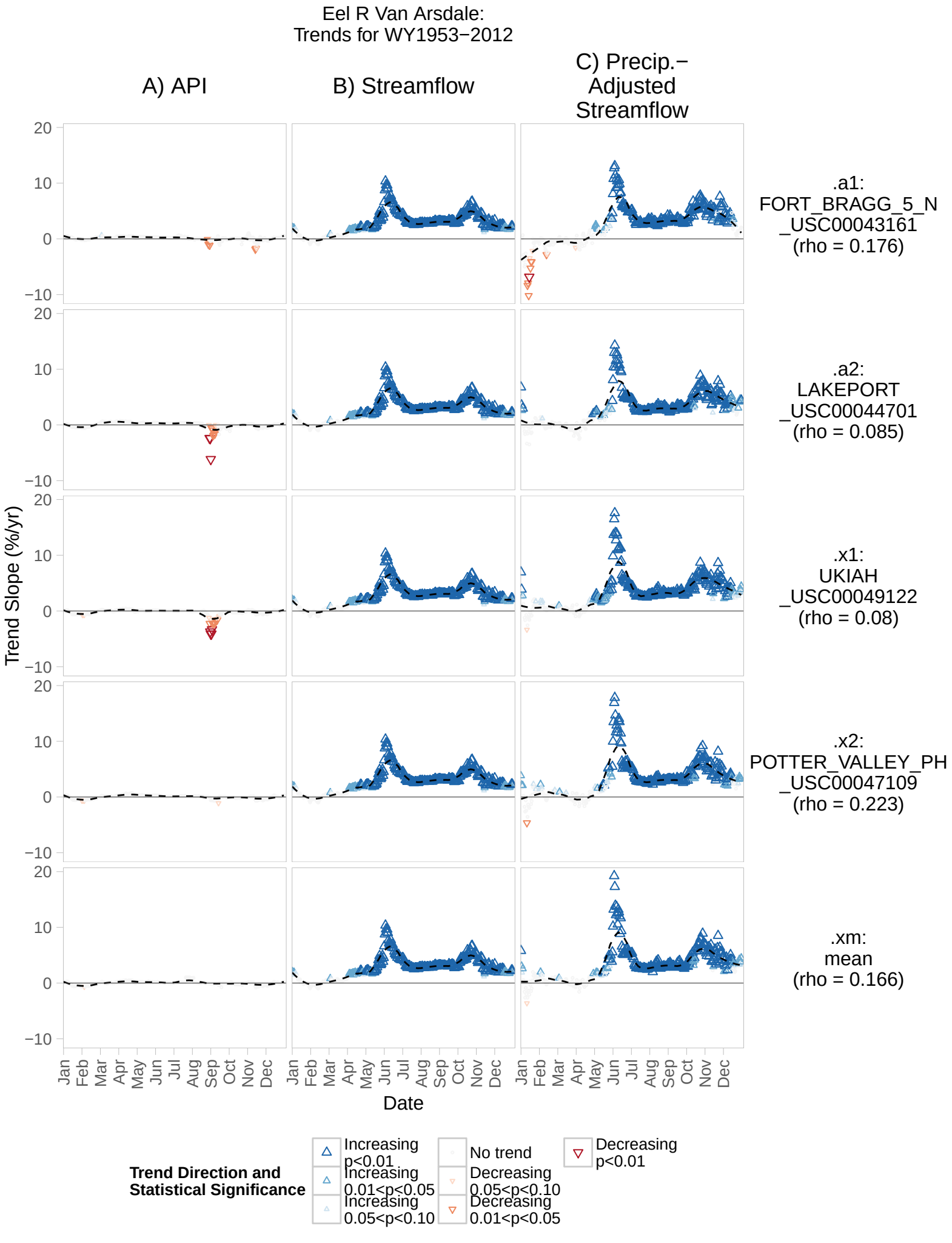
Eel R Van Arsdale:
Trends for WY1953−2012
A) API
B) Streamflow
C) Precip.−
Adjusted
Streamflow
.a1:
FORT_BRAGG_5_N
_USC00043161
(rho = 0.176)
.a2:
LAKEPORT
_USC00044701
(rho = 0.085)
.x1:
UKIAH
_USC00049122
(rho = 0.08)
.x2:
POTTER_VALLEY_PH
_USC00047109
(rho = 0.223)
.xm:
mean
(rho = 0.166)
Trend Slope (%/yr)
20
10
0
−10
Jan
Feb
Mar
Apr
May
Jun
Jul
Aug
Sep
Oct
Nov
Dec
Date
Trend Direction and
Statistical Significance
Increasing
p<0.01
Increasing
0.01<p<0.05
Increasing
0.05<p<0.10
No trend
Decreasing
0.05<p<0.10
Decreasing
0.01<p<0.05
Decreasing
p<0.01

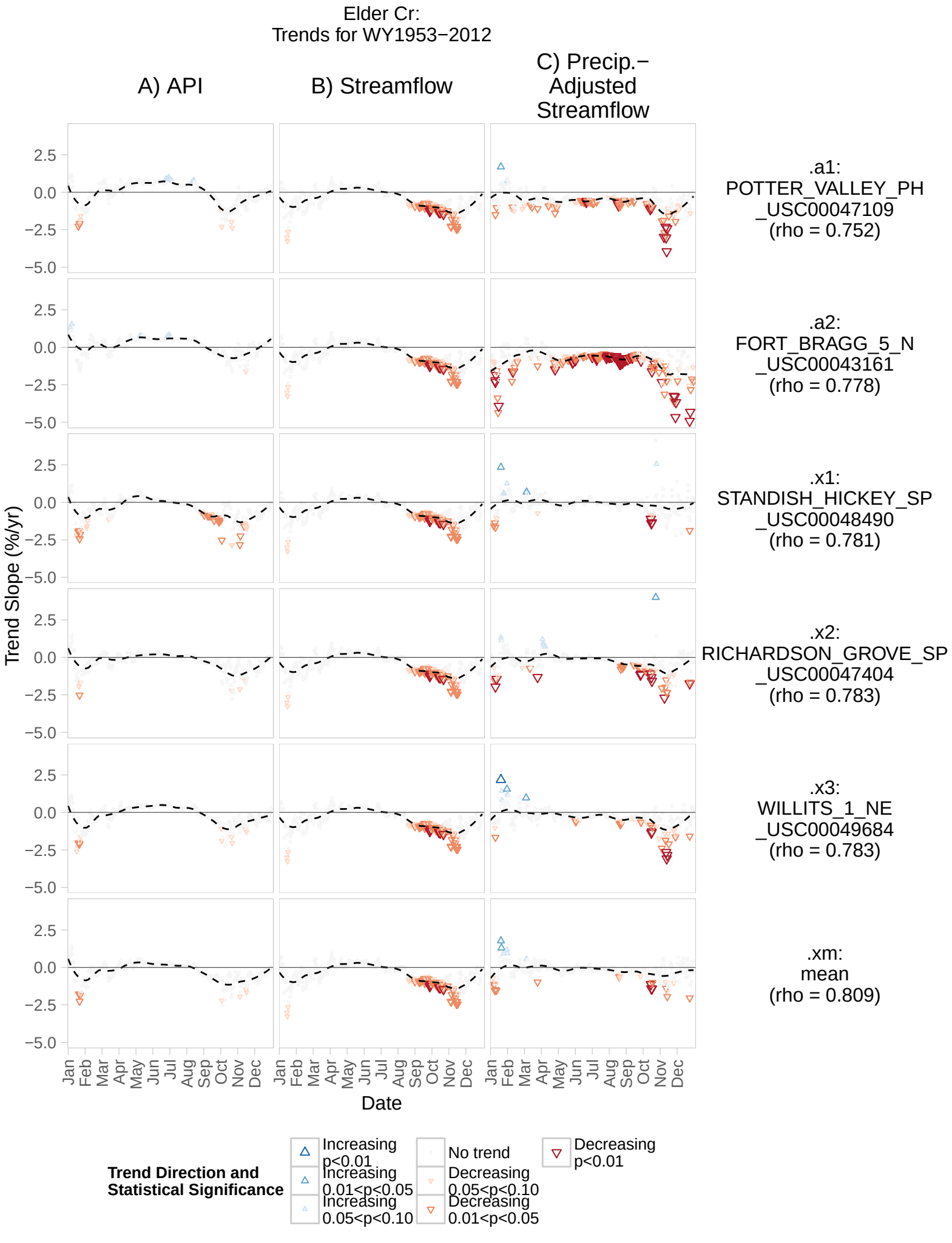
Elder Cr:
Trends for WY1953−2012
A) API
B) Streamflow
C) Precip.−
Adjusted
Streamflow
.a1:
POTTER_VALLEY_PH
_USC00047109
(rho = 0.752)
.a2:
FORT_BRAGG_5_N
_USC00043161
(rho = 0.778)
.x1:
STANDISH_HICKEY_SP
_USC00048490
(rho = 0.781)
.x2:
RICHARDSON_GROVE_SP
_USC00047404
(rho = 0.783)
.x3:
WILLITS_1_NE
_USC00049684
(rho = 0.783)
.xm:
mean
(rho = 0.809)
Trend Slope (%/yr)
2.5
0.0
−2.5
−5.0
Jan
Feb
Mar
Apr
May
Jun
Jul
Aug
Sep
Oct
Nov
Dec
Date
Trend Direction and
Statistical Significance
Increasing
p<0.01
Increasing
0.01<p<0.05
Increasing
0.05<p<0.10
No trend
Decreasing
0.05<p<0.10
Decreasing
0.01<p<0.05
Decreasing
p<0.01

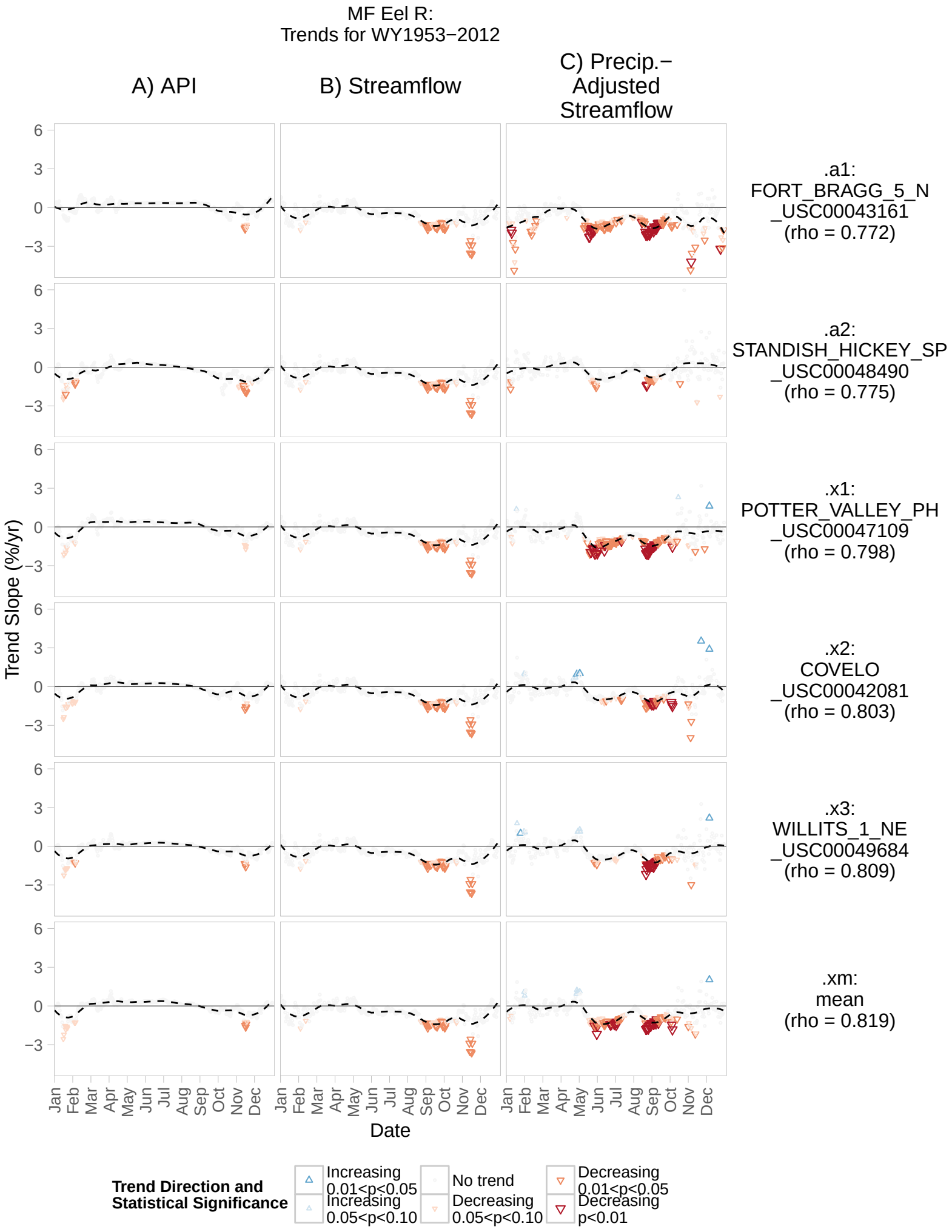
MF Eel R:
Trends for WY1953−2012
A) API
B) Streamflow
C) Precip.−
Adjusted
Streamflow
.a1:
FORT_BRAGG_5_N
_USC00043161
(rho = 0.772)
.a2:
STANDISH_HICKEY_SP
_USC00048490
(rho = 0.775)
.x1:
POTTER_VALLEY_PH
_USC00047109
(rho = 0.798)
.x2:
COVELO
_USC00042081
(rho = 0.803)
.x3:
WILLITS_1_NE
_USC00049684
(rho = 0.809)
.xm:
mean
(rho = 0.819)
Trend Slope (%/yr)
6
3
0
−3
Jan
Feb
Mar
Apr
May
Jun
Jul
Aug
Sep
Oct
Nov
Dec
Date
Trend Direction and
Statistical Significance
Increasing
0.01<p<0.05
Increasing
0.05<p<0.10
No trend
Decreasing
0.05<p<0.10
Decreasing
0.01<p<0.05
Decreasing
p<0.01

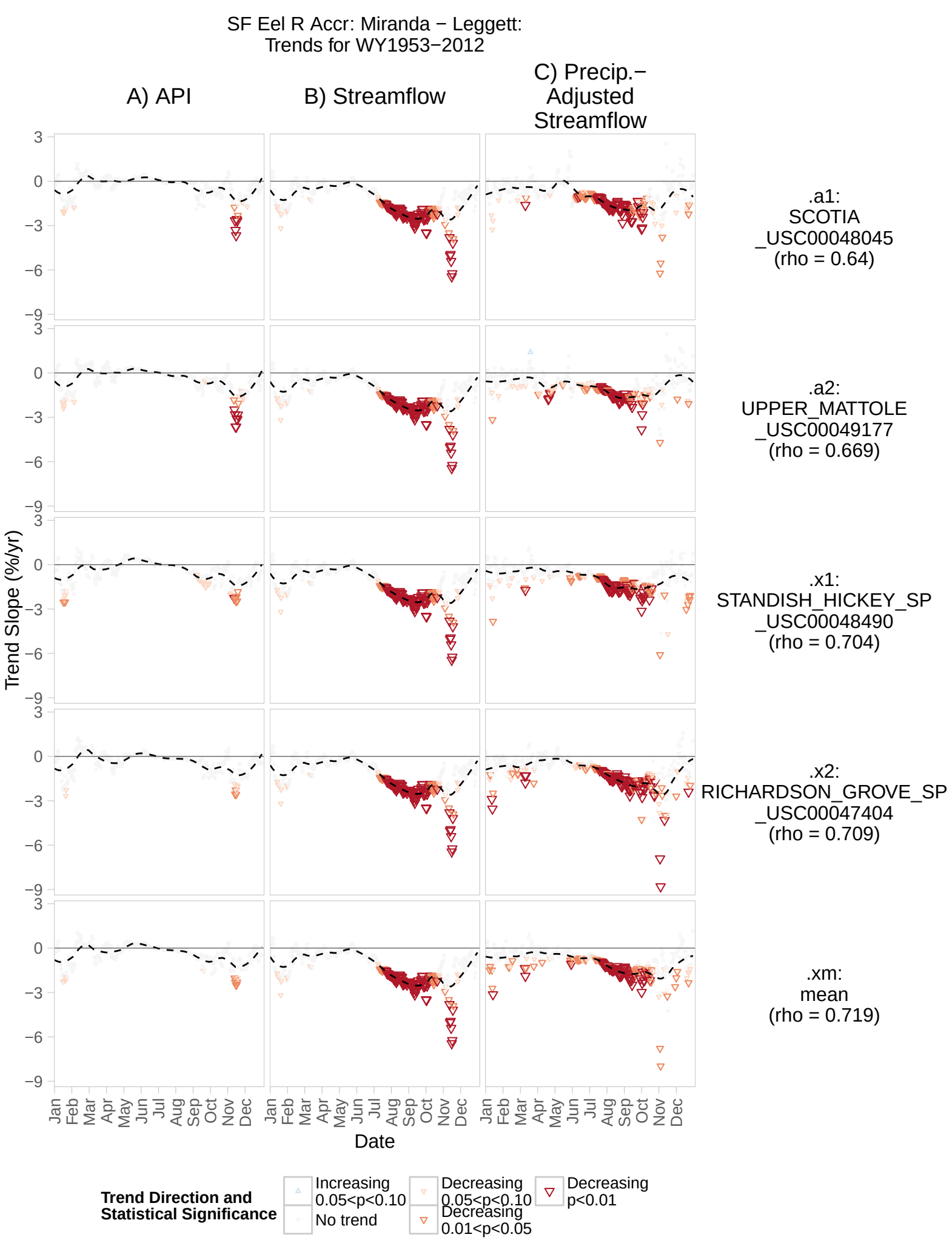
SF Eel R Accr: Miranda − Leggett:
Trends for WY1953−2012
A) API
B) Streamflow
C) Precip.−
Adjusted
Streamflow
.a1:
SCOTIA
_USC00048045
(rho = 0.64)
.a2:
UPPER_MATTOLE
_USC00049177
(rho = 0.669)
.x1:
STANDISH_HICKEY_SP
_USC00048490
(rho = 0.704)
.x2:
RICHARDSON_GROVE_SP
_USC00047404
(rho = 0.709)
.xm:
mean
(rho = 0.719)
Trend Slope (%/yr)
3
0
−3
−6
−9
Jan
Feb
Mar
Apr
May
Jun
Jul
Aug
Sep
Oct
Nov
Dec
Date
Trend Direction and
Statistical Significance
Increasing
0.05<p<0.10
No trend
Decreasing
0.05<p<0.10
Decreasing
0.01<p<0.05
Decreasing
p<0.01

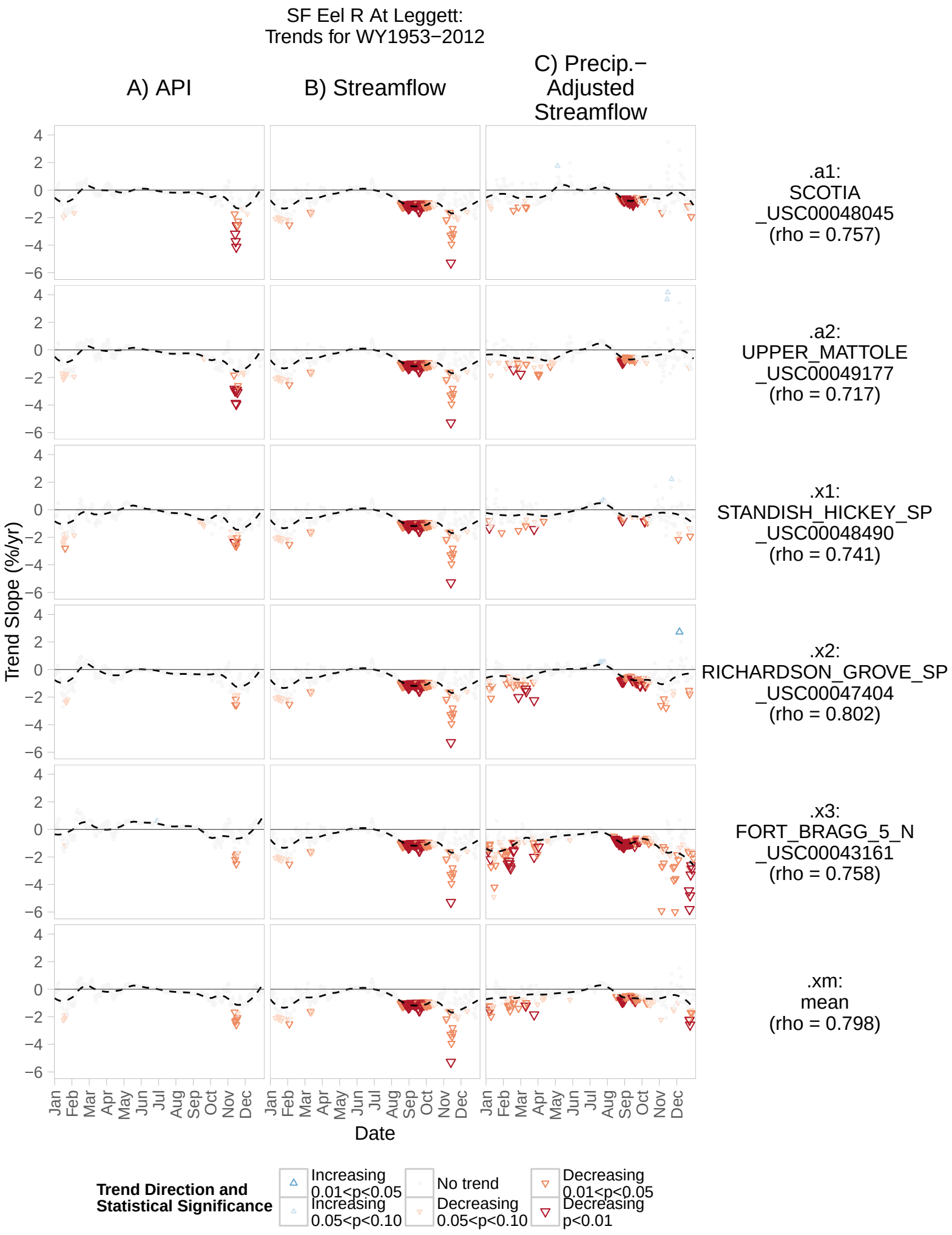
SF Eel R At Leggett:
Trends for WY1953−2012
A) API
B) Streamflow
C) Precip.−
Adjusted
Streamflow
.a1:
SCOTIA
_USC00048045
(rho = 0.757)
.a2:
UPPER_MATTOLE
_USC00049177
(rho = 0.717)
.x1:
STANDISH_HICKEY_SP
_USC00048490
(rho = 0.741)
.x2:
RICHARDSON_GROVE_SP
_USC00047404
(rho = 0.802)
.x3:
FORT_BRAGG_5_N
_USC00043161
(rho = 0.758)
.xm:
mean
(rho = 0.798)
Trend Slope (%/yr)
4
2
0
−2
−4
−6
Jan
Feb
Mar
Apr
May
Jun
Jul
Aug
Sep
Oct
Nov
Dec
Date
Trend Direction and
Statistical Significance
Increasing
0.01<p<0.05
Increasing
0.05<p<0.10
No trend
Decreasing
0.05<p<0.10
Decreasing
0.01<p<0.05
Decreasing
p<0.01

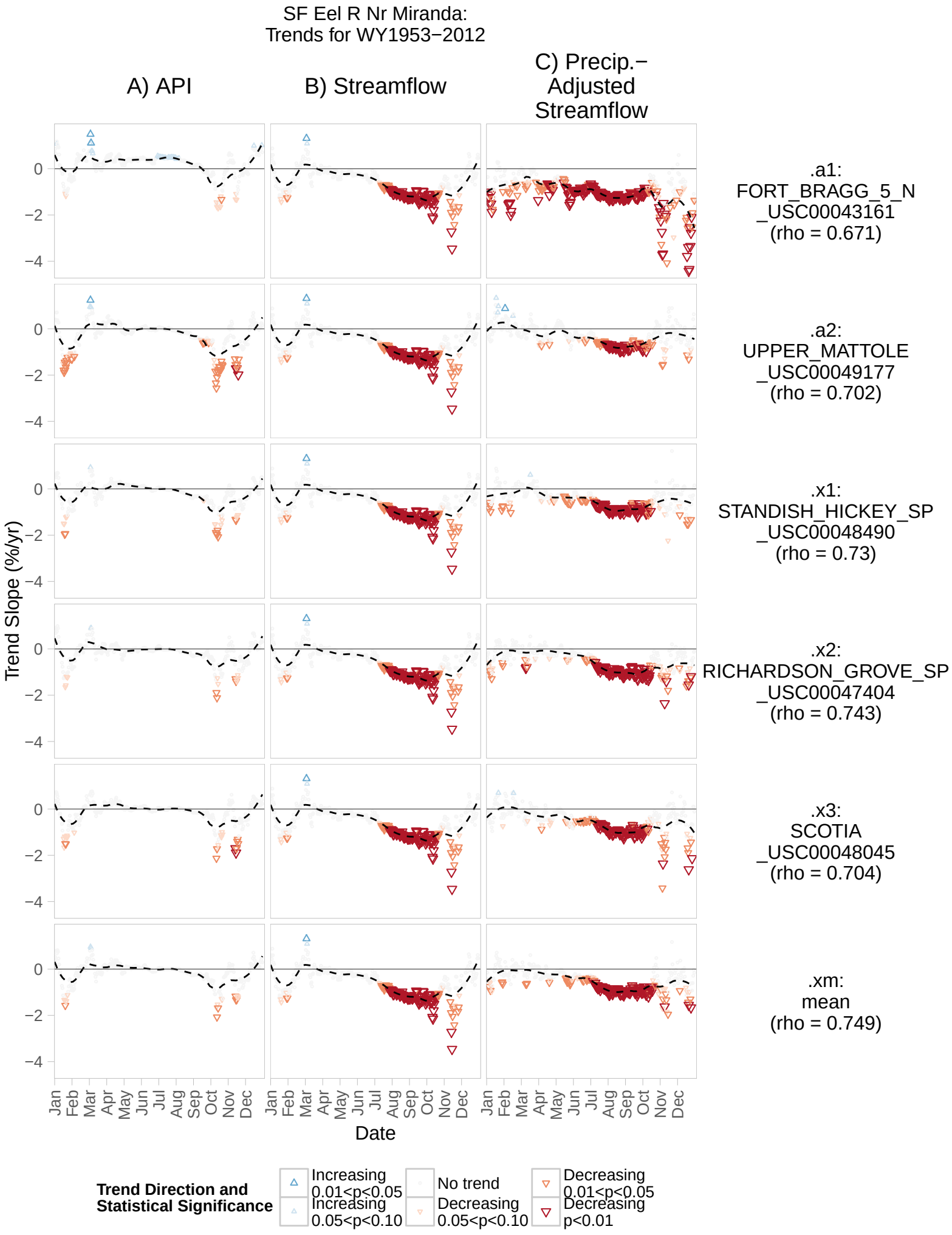
SF Eel R Nr Miranda:
Trends for WY1953−2012
A) API
B) Streamflow
C) Precip.−
Adjusted
Streamflow
.a1:
FORT_BRAGG_5_N
_USC00043161
(rho = 0.671)
.a2:
UPPER_MATTOLE
_USC00049177
(rho = 0.702)
.x1:
STANDISH_HICKEY_SP
_USC00048490
(rho = 0.73)
.x2:
RICHARDSON_GROVE_SP
_USC00047404
(rho = 0.743)
.x3:
SCOTIA
_USC00048045
(rho = 0.704)
.xm:
mean
(rho = 0.749)
Trend Slope (%/yr)
0
−2
−4
Jan
Feb
Mar
Apr
May
Jun
Jul
Aug
Sep
Oct
Nov
Dec
Date
Trend Direction and
Statistical Significance
Increasing
0.01<p<0.05
Increasing
0.05<p<0.10
No trend
Decreasing
0.05<p<0.10
Decreasing
0.01<p<0.05
Decreasing
p<0.01

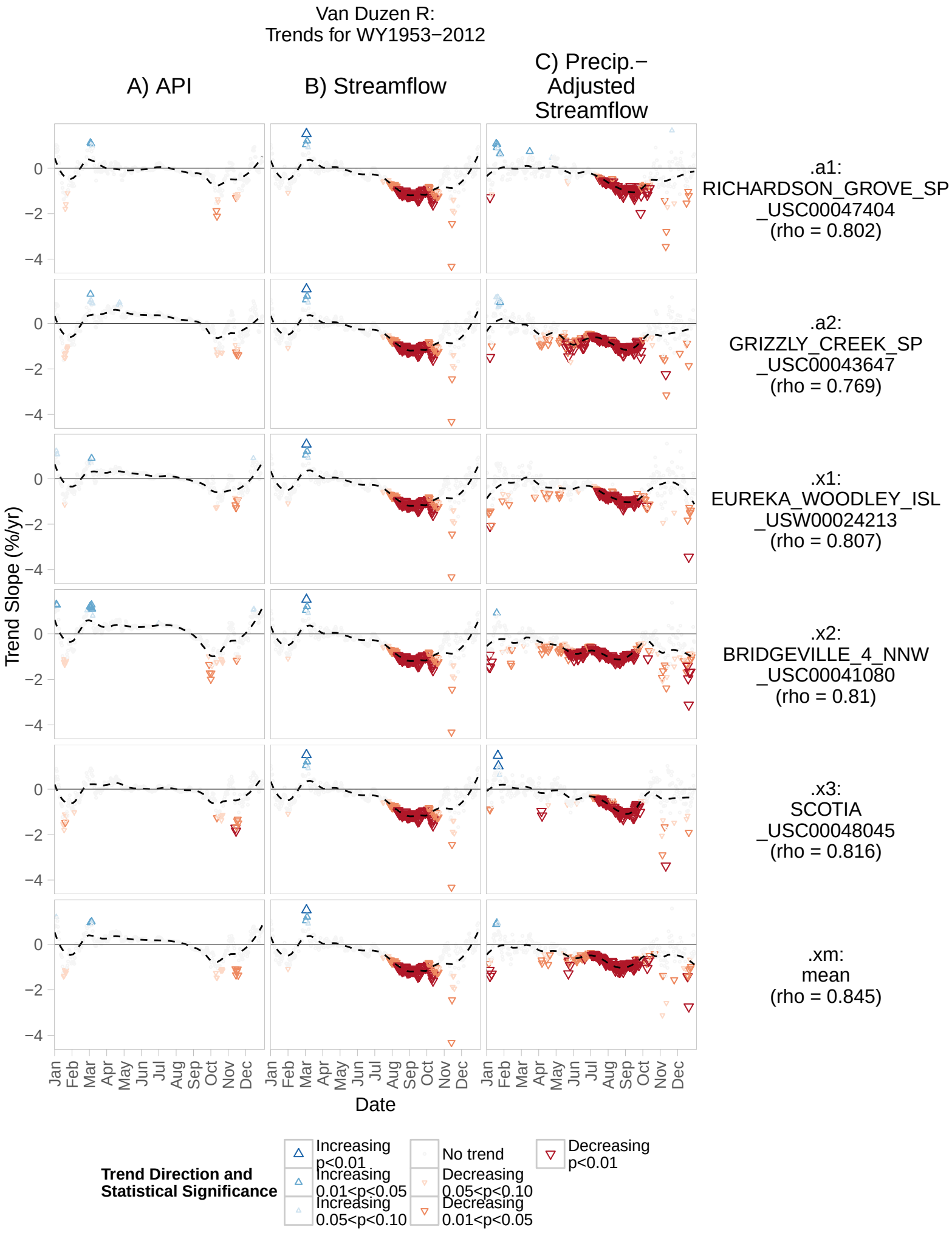
Van Duzen R:
Trends for WY1953−2012
A) API
B) Streamflow
C) Precip.−
Adjusted
Streamflow
.a1:
RICHARDSON_GROVE_SP
_USC00047404
(rho = 0.802)
.a2:
GRIZZLY_CREEK_SP
_USC00043647
(rho = 0.769)
.x1:
EUREKA_WOODLEY_ISL
_USW00024213
(rho = 0.807)
.x2:
BRIDGEVILLE_4_NNW
_USC00041080
(rho = 0.81)
.x3:
SCOTIA
_USC00048045
(rho = 0.816)
.xm:
mean
(rho = 0.845)
Trend Slope (%/yr)
0
−2
−4
Jan
Feb
Mar
Apr
May
Jun
Jul
Aug
Sep
Oct
Nov
Dec
Date
Trend Direction and
Statistical Significance
Increasing
p<0.01
Increasing
0.01<p<0.05
Increasing
0.05<p<0.10
No trend
Decreasing
0.05<p<0.10
Decreasing
0.01<p<0.05
Decreasing
p<0.01

APPENDIX F: SENSITIVITY OF PERIOD OF RECORD TRENDS TO CHOICE OF PRECIPITATION STATIONS

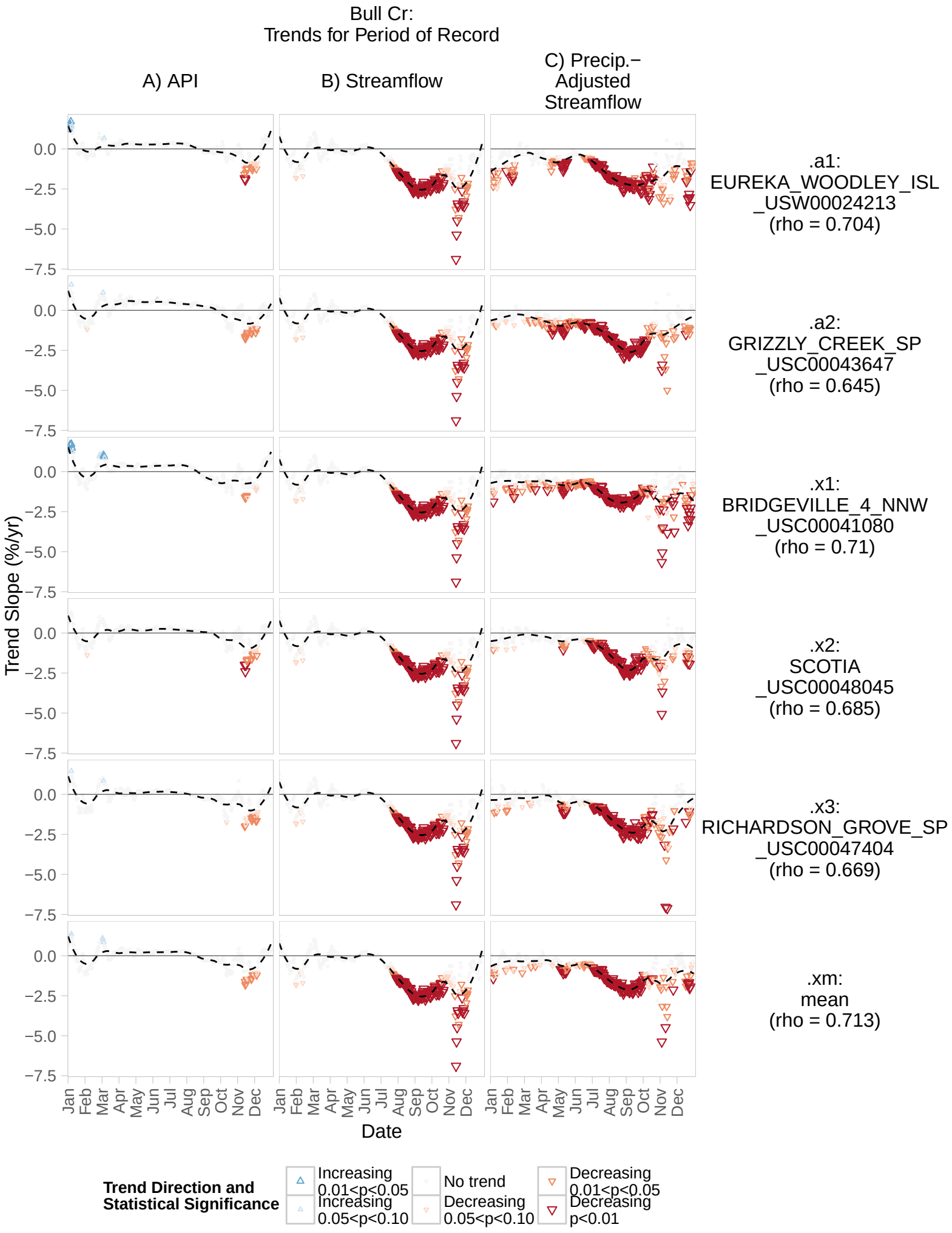
Bull Cr:
Trends for Period of Record
A) API
B) Streamflow
C) Precip.−
Adjusted
Streamflow
Trend Slope (%/yr)
0.0
−2.5
−5.0
−7.5
Jan
Feb
Mar
Apr
May
Jun
Jul
Aug
Sep
Oct
Nov
Dec
Date
.a1:
EUREKA_WOODLEY_ISL
_USW00024213
(rho = 0.704)
.a2:
GRIZZLY_CREEK_SP
_USC00043647
(rho = 0.645)
.x1:
BRIDGEVILLE_4_NNW
_USC00041080
(rho = 0.71)
.x2:
SCOTIA
_USC00048045
(rho = 0.685)
.x3:
RICHARDSON_GROVE_SP
_USC00047404
(rho = 0.669)
.xm:
mean
(rho = 0.713)
Trend Direction and
Statistical Significance
Increasing
0.01<p<0.05
Increasing
0.05<p<0.10
No trend
Decreasing
0.05<p<0.10
Decreasing
0.01<p<0.05
Decreasing
p<0.01

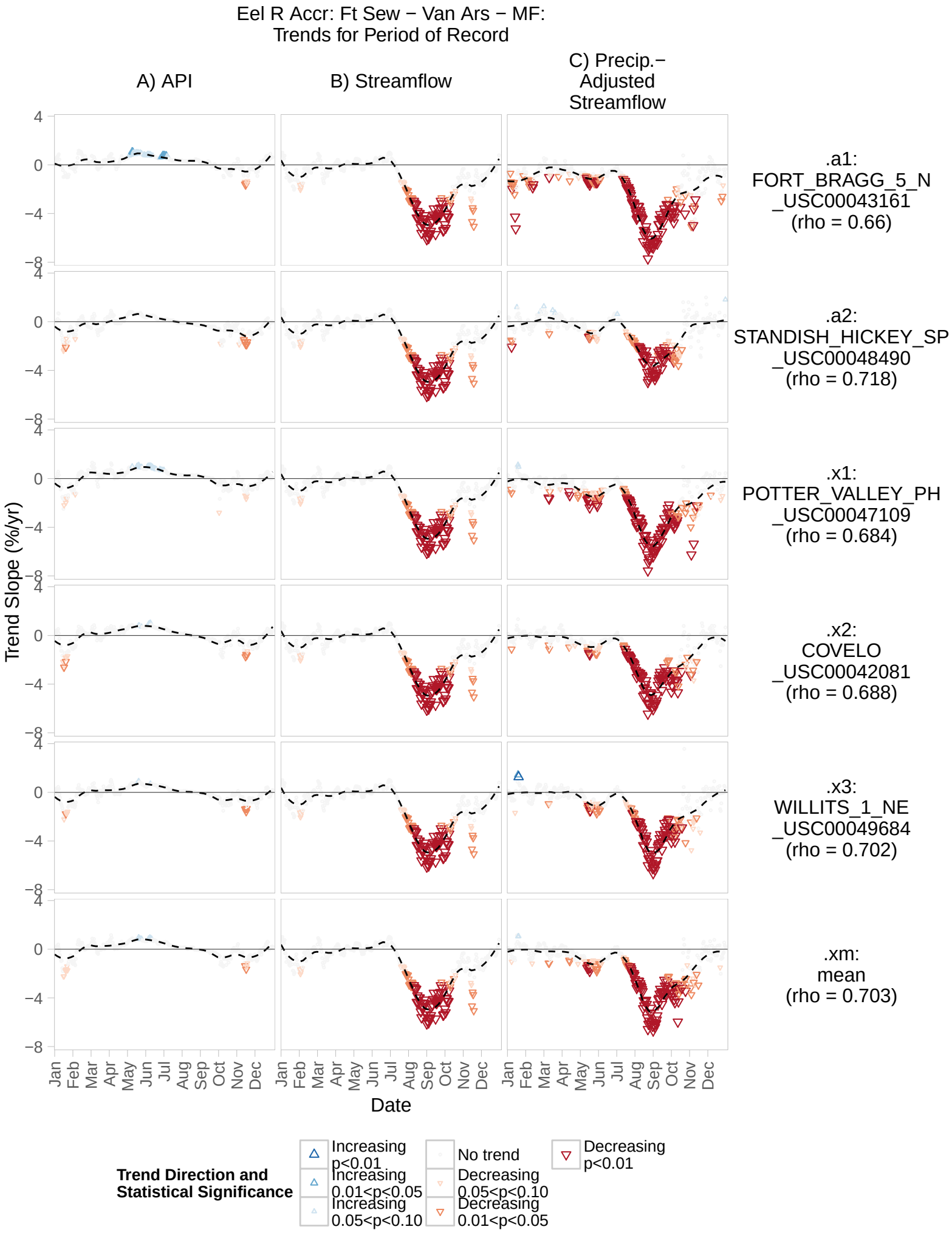
Eel R Accr: Ft Sew − Van Ars − MF:
Trends for Period of Record
A) API
B) Streamflow
C) Precip.−
Adjusted
Streamflow
.a1:
FORT_BRAGG_5_N
_USC00043161
(rho = 0.66)
.a2:
STANDISH_HICKEY_SP
_USC00048490
(rho = 0.718)
.x1:
POTTER_VALLEY_PH
_USC00047109
(rho = 0.684)
.x2:
COVELO
_USC00042081
(rho = 0.688)
.x3:
WILLITS_1_NE
_USC00049684
(rho = 0.702)
.xm:
mean
(rho = 0.703)
Trend Slope (%/yr)
4
0
−4
−8
Jan
Feb
Mar
Apr
May
Jun
Jul
Aug
Sep
Oct
Nov
Dec
Date
Trend Direction and
Statistical Significance
Increasing
p<0.01
Increasing
0.01<p<0.05
Increasing
0.05<p<0.10
No trend
Decreasing
0.05<p<0.10
Decreasing
0.01<p<0.05
Decreasing
p<0.01

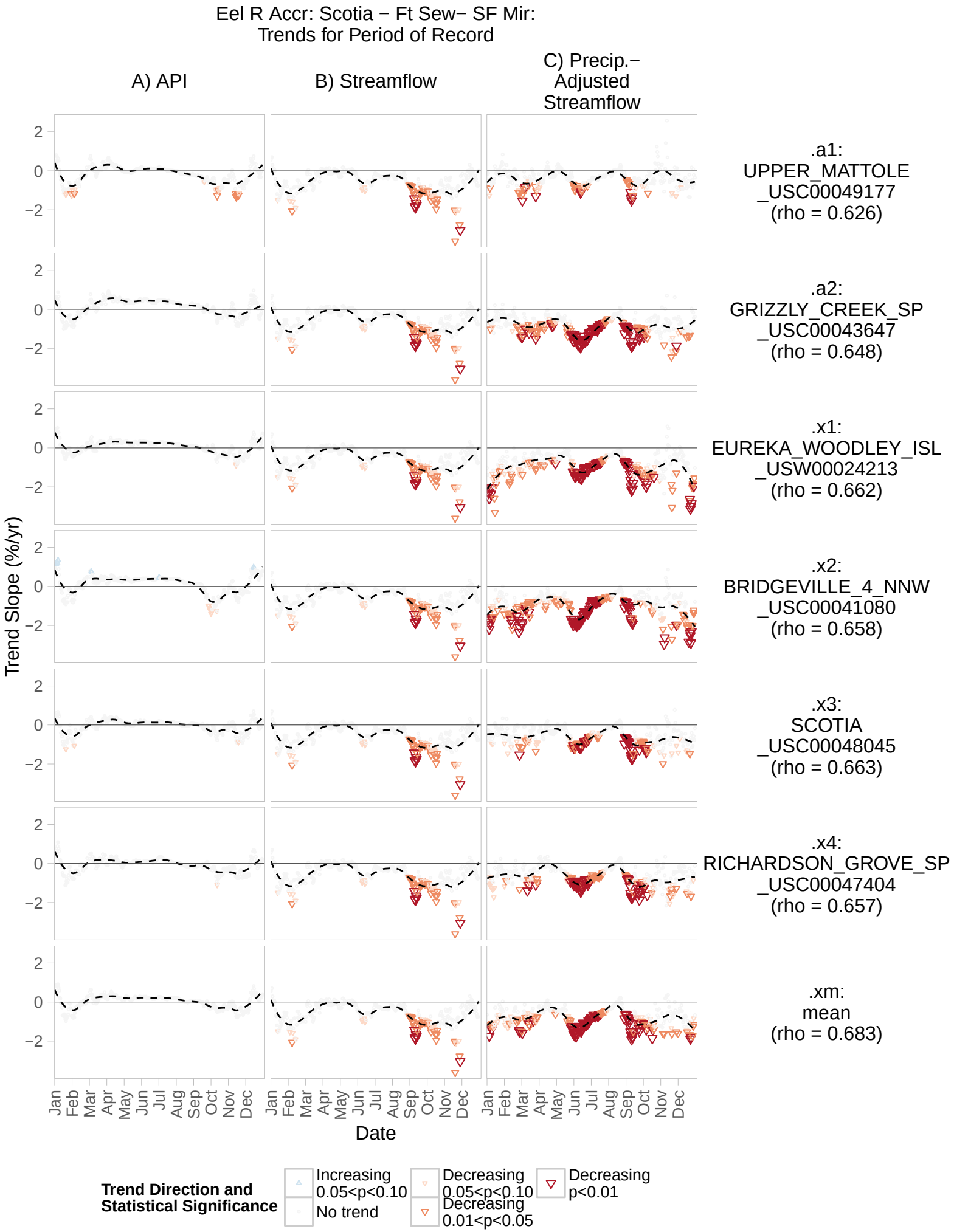
Eel R Accr: Scotia − Ft Sew− SF Mir:
Trends for Period of Record
A) API
B) Streamflow
C) Precip.−
Adjusted
Streamflow
.a1:
UPPER_MATTOLE
_USC00049177
(rho = 0.626)
.a2:
GRIZZLY_CREEK_SP
_USC00043647
(rho = 0.648)
.x1:
EUREKA_WOODLEY_ISL
_USW00024213
(rho = 0.662)
.x2:
BRIDGEVILLE_4_NNW
_USC00041080
(rho = 0.658)
.x3:
SCOTIA
_USC00048045
(rho = 0.663)
.x4:
RICHARDSON_GROVE_SP
_USC00047404
(rho = 0.657)
.xm:
mean
(rho = 0.683)
Trend Slope (%/yr)
2
0
−2
Jan
Feb
Mar
Apr
May
Jun
Jul
Aug
Sep
Oct
Nov
Dec
Date
Trend Direction and
Statistical Significance
Increasing
0.05<p<0.10
No trend
Decreasing
0.05<p<0.10
Decreasing
0.01<p<0.05
Decreasing
p<0.01

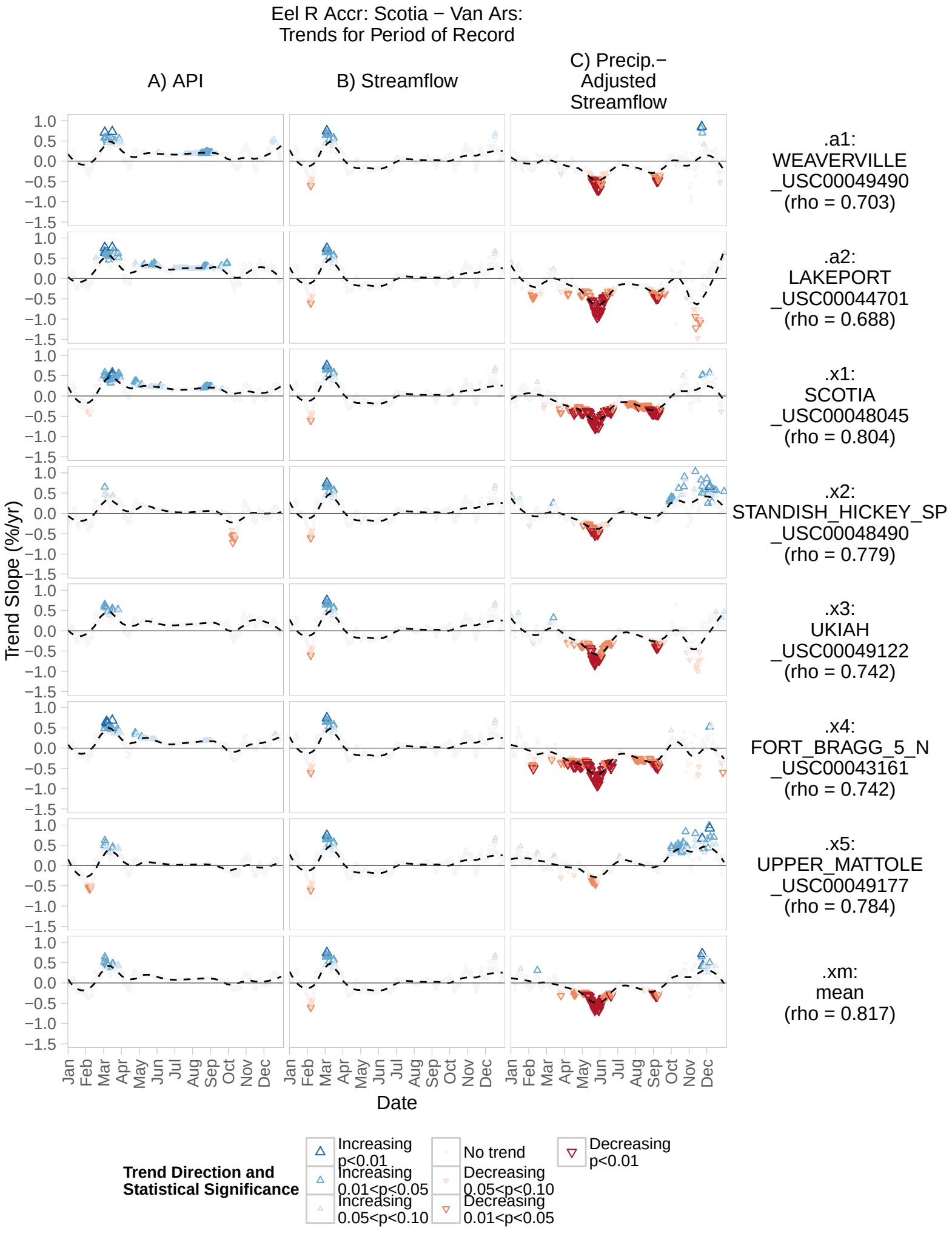
Eel R Accr: Scotia − Van Ars:
Trends for Period of Record
A) API
B) Streamflow
C) Precip.−
Adjusted
Streamflow
.a1:
WEAVERVILLE
_USC00049490
(rho = 0.703)
.a2:
LAKEPORT
_USC00044701
(rho = 0.688)
.x1:
SCOTIA
_USC00048045
(rho = 0.804)
.x2:
STANDISH_HICKEY_SP
_USC00048490
(rho = 0.779)
.x3:
UKIAH
_USC00049122
(rho = 0.742)
.x4:
FORT_BRAGG_5_N
_USC00043161
(rho = 0.742)
.x5:
UPPER_MATTOLE
_USC00049177
(rho = 0.784)
.xm:
mean
(rho = 0.817)
Trend Slope (%/yr)
1.0
0.5
0.0
−0.5
−1.0
−1.5
Jan
Feb
Mar
Apr
May
Jun
Jul
Aug
Sep
Oct
Nov
Dec
Date
Trend Direction and
Statistical Significance
Increasing
p<0.01
Increasing
0.01<p<0.05
Increasing
0.05<p<0.10
No trend
Decreasing
0.05<p<0.10
Decreasing
0.01<p<0.05
Decreasing
p<0.01

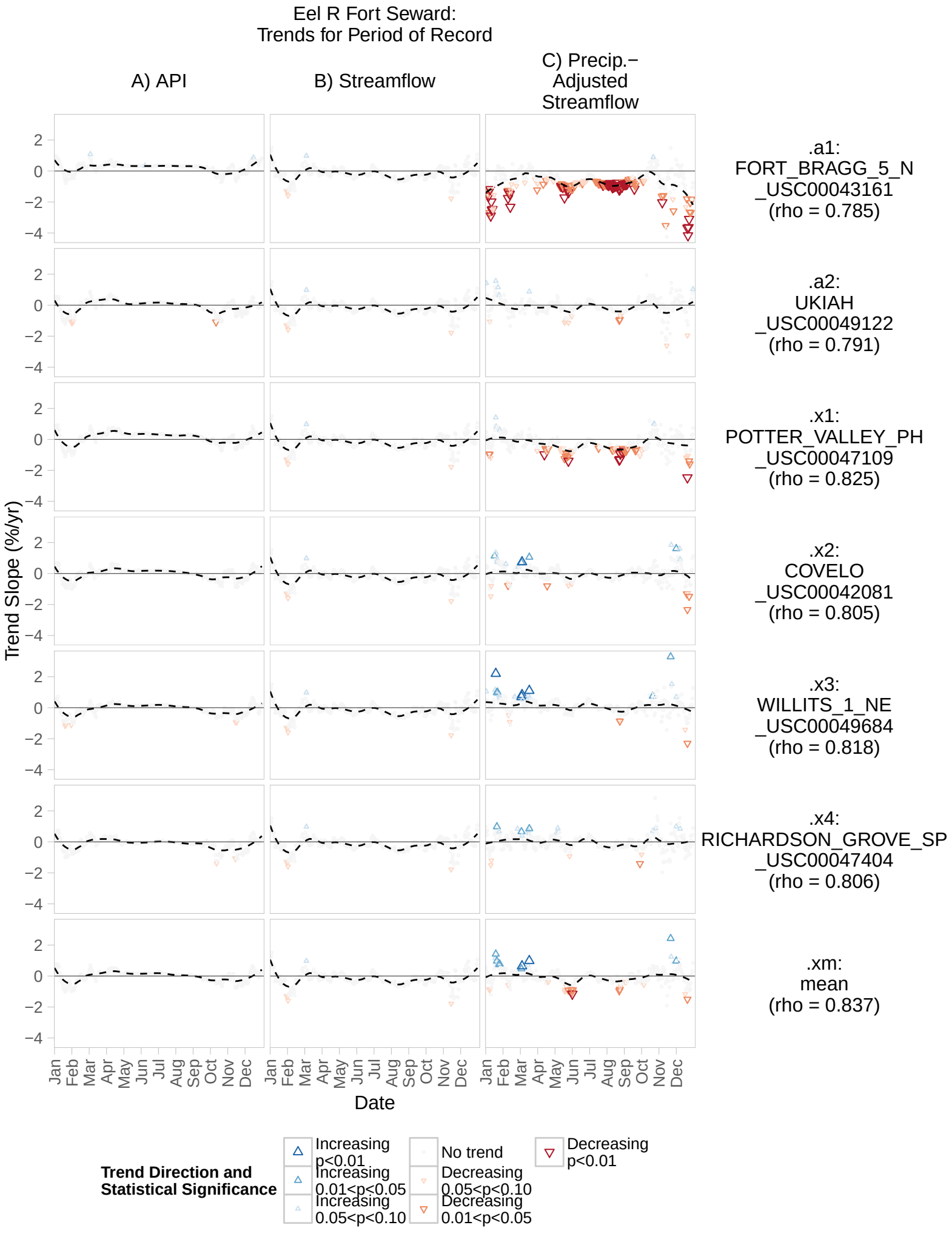
Eel R Fort Seward:
Trends for Period of Record
A) API
B) Streamflow
C) Precip.−
Adjusted
Streamflow
.a1:
FORT_BRAGG_5_N
_USC00043161
(rho = 0.785)
.a2:
UKIAH
_USC00049122
(rho = 0.791)
.x1:
POTTER_VALLEY_PH
_USC00047109
(rho = 0.825)
.x2:
COVELO
_USC00042081
(rho = 0.805)
.x3:
WILLITS_1_NE
_USC00049684
(rho = 0.818)
.x4:
RICHARDSON_GROVE_SP
_USC00047404
(rho = 0.806)
.xm:
mean
(rho = 0.837)
Trend Slope (%/yr)
2
0
−2
−4
Jan
Feb
Mar
Apr
May
Jun
Jul
Aug
Sep
Oct
Nov
Dec
Date
Trend Direction and
Statistical Significance
Increasing
p<0.01
Increasing
0.01<p<0.05
Increasing
0.05<p<0.10
No trend
Decreasing
0.05<p<0.10
Decreasing
0.01<p<0.05
Decreasing
p<0.01


Eel R Scotia:
Trends for Period of Record
A) API
B) Streamflow
C) Precip.−
Adjusted
Streamflow
.a1:
WEAVERVILLE
_USC00049490
(rho = 0.712)
.a2:
LAKEPORT
_USC00044701
(rho = 0.695)
.x1:
SCOTIA
_USC00048045
(rho = 0.816)
.x2:
STANDISH_HICKEY_SP
_USC00048490
(rho = 0.778)
.x3:
UKIAH
_USC00049122
(rho = 0.747)
.x4:
FORT_BRAGG_5_N
_USC00043161
(rho = 0.754)
.x5:
UPPER_MATTOLE
_USC00049177
(rho = 0.783)
.xm:
mean
(rho = 0.821)
Trend Slope (%/yr)
1
0
−1
Jan
Feb
Mar
Apr
May
Jun
Jul
Aug
Sep
Oct
Nov
Dec
Date
Trend Direction and
Statistical Significance
Increasing
p<0.01
Increasing
0.01<p<0.05
Increasing
0.05<p<0.10
No trend
Decreasing
0.05<p<0.10
Decreasing
0.01<p<0.05
Decreasing
p<0.01

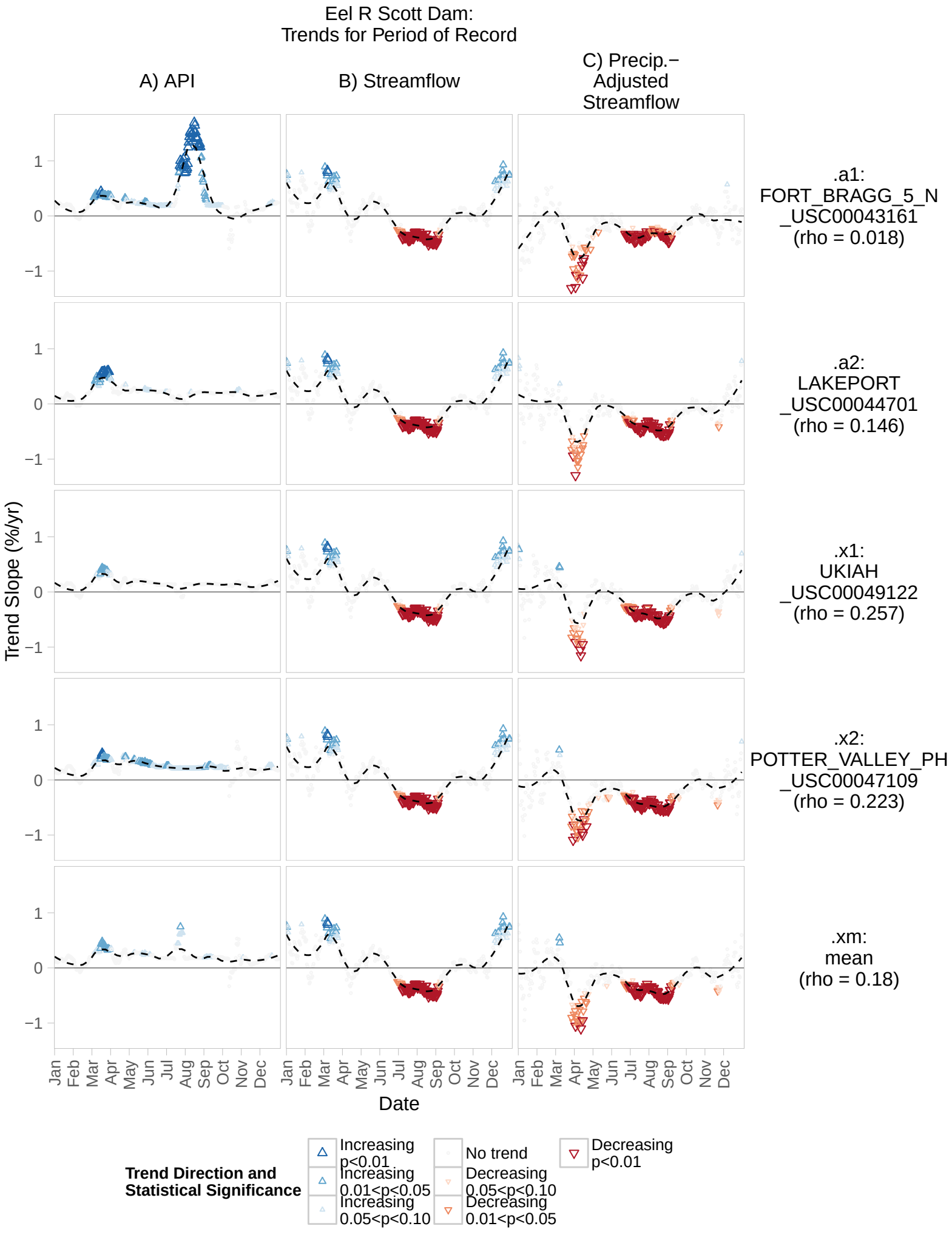
Eel R Scott Dam:
Trends for Period of Record
A) API
B) Streamflow
C) Precip.−
Adjusted
Streamflow
.a1:
FORT_BRAGG_5_N
_USC00043161
(rho = 0.018)
.a2:
LAKEPORT
_USC00044701
(rho = 0.146)
.x1:
UKIAH
_USC00049122
(rho = 0.257)
.x2:
POTTER_VALLEY_PH
_USC00047109
(rho = 0.223)
.xm:
mean
(rho = 0.18)
Trend Slope (%/yr)
1
0
−1
Jan
Feb
Mar
Apr
May
Jun
Jul
Aug
Sep
Oct
Nov
Dec
Date
Trend Direction and
Statistical Significance
Increasing
p<0.01
Increasing
0.01<p<0.05
Increasing
0.05<p<0.10
No trend
Decreasing
0.05<p<0.10
Decreasing
0.01<p<0.05
Decreasing
p<0.01

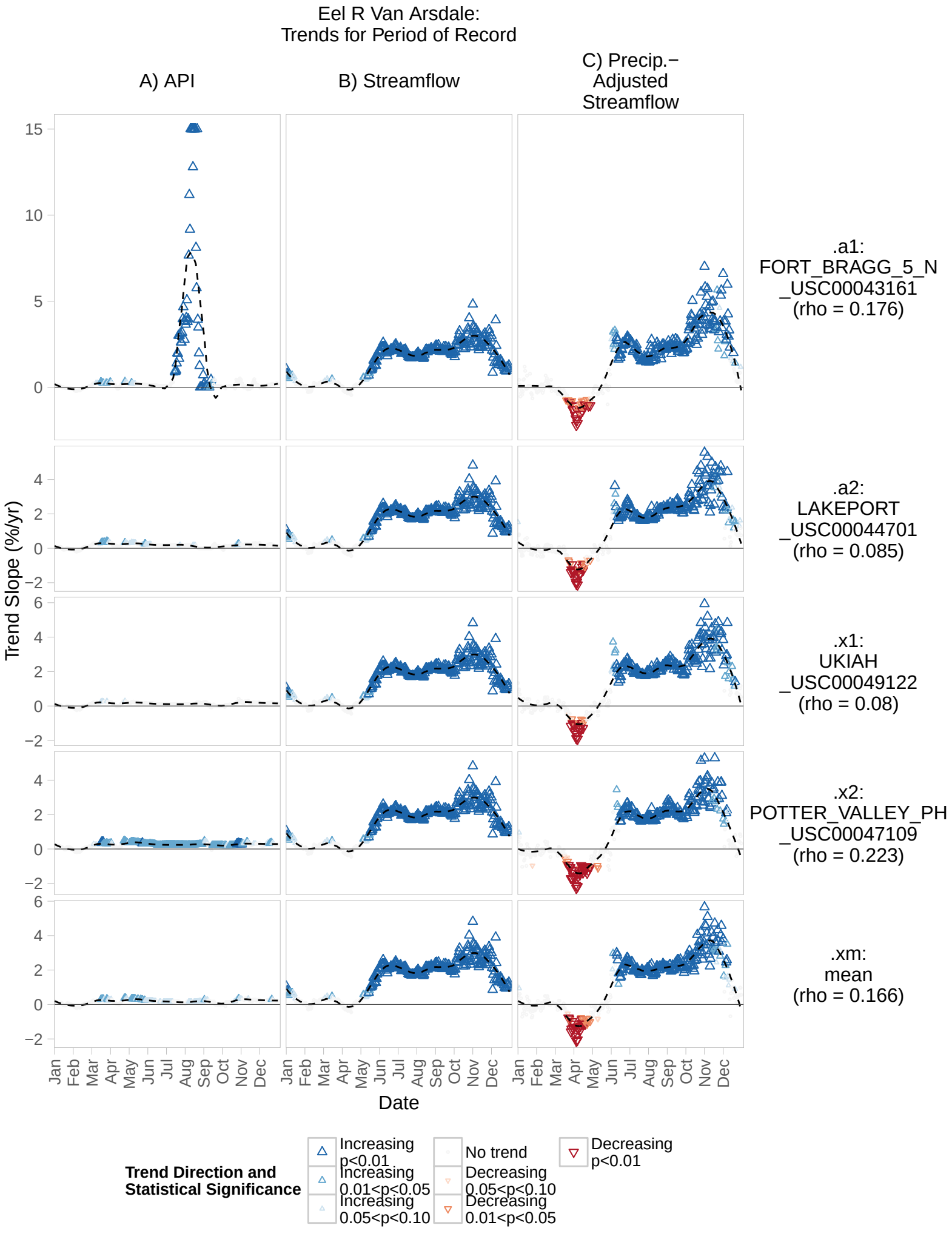
Eel R Van Arsdale:
Trends for Period of Record
A) API
B) Streamflow
C) Precip.−
Adjusted
Streamflow
.a1:
FORT_BRAGG_5_N
_USC00043161
(rho = 0.176)
.a2:
LAKEPORT
_USC00044701
(rho = 0.085)
.x1:
UKIAH
_USC00049122
(rho = 0.08)
.x2:
POTTER_VALLEY_PH
_USC00047109
(rho = 0.223)
.xm:
mean
(rho = 0.166)
Trend Slope (%/yr)
Date
Jan
Feb
Mar
Apr
May
Jun
Jul
Aug
Sep
Oct
Nov
Dec
Trend Direction and
Statistical Significance
Increasing
p<0.01
Increasing
0.01<p<0.05
Increasing
0.05<p<0.10
No trend
Decreasing
0.05<p<0.10
Decreasing
0.01<p<0.05
Decreasing
p<0.01

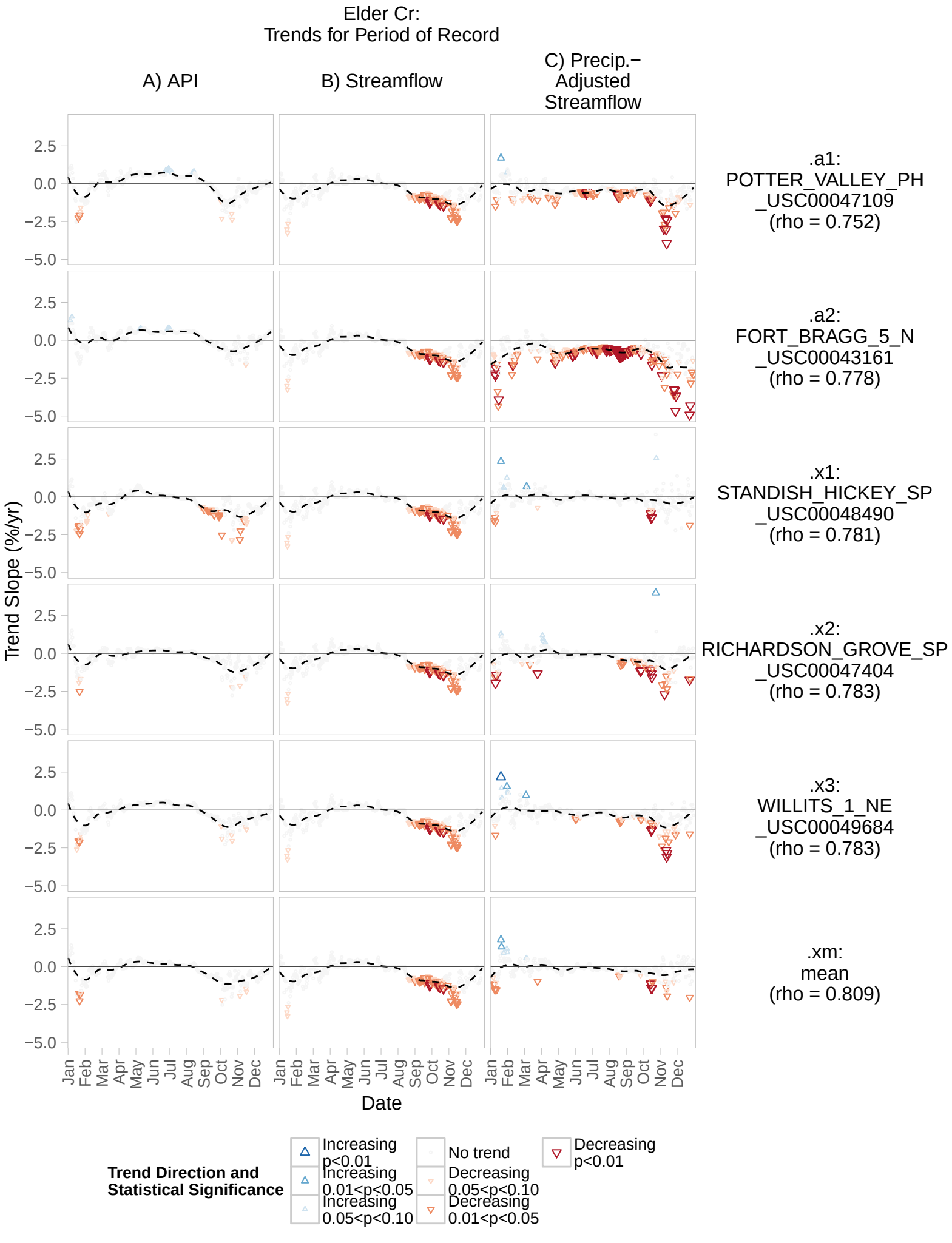
Elder Cr:
Trends for Period of Record
A) API
B) Streamflow
C) Precip.−
Adjusted
Streamflow
.a1:
POTTER_VALLEY_PH
_USC00047109
(rho = 0.752)
.a2:
FORT_BRAGG_5_N
_USC00043161
(rho = 0.778)
.x1:
STANDISH_HICKEY_SP
_USC00048490
(rho = 0.781)
.x2:
RICHARDSON_GROVE_SP
_USC00047404
(rho = 0.783)
.x3:
WILLITS_1_NE
_USC00049684
(rho = 0.783)
.xm:
mean
(rho = 0.809)
Trend Slope (%/yr)
2.5
0.0
−2.5
−5.0
Jan
Feb
Mar
Apr
May
Jun
Jul
Aug
Sep
Oct
Nov
Dec
Date
Trend Direction and
Statistical Significance
Increasing
p<0.01
Increasing
0.01<p<0.05
Increasing
0.05<p<0.10
No trend
Decreasing
0.05<p<0.10
Decreasing
0.01<p<0.05
Decreasing
p<0.01

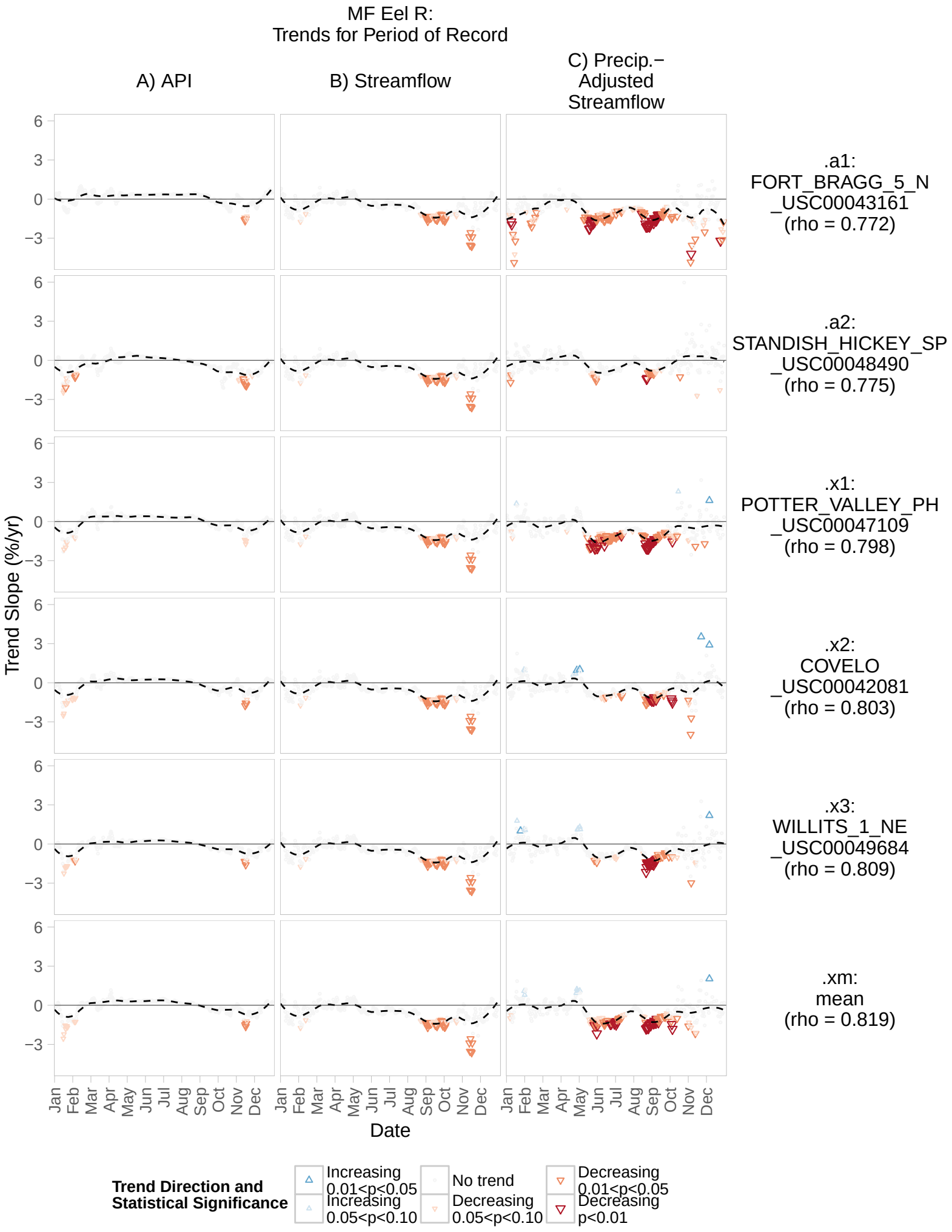
MF Eel R:
Trends for Period of Record
A) API
B) Streamflow
C) Precip.−
Adjusted
Streamflow
.a1:
FORT_BRAGG_5_N
_USC00043161
(rho = 0.772)
.a2:
STANDISH_HICKEY_SP
_USC00048490
(rho = 0.775)
.x1:
POTTER_VALLEY_PH
_USC00047109
(rho = 0.798)
.x2:
COVELO
_USC00042081
(rho = 0.803)
.x3:
WILLITS_1_NE
_USC00049684
(rho = 0.809)
.xm:
mean
(rho = 0.819)
Trend Slope (%/yr)
6
3
0
−3
Jan
Feb
Mar
Apr
May
Jun
Jul
Aug
Sep
Oct
Nov
Dec
Date
Trend Direction and
Statistical Significance
Increasing
0.01<p<0.05
Increasing
0.05<p<0.10
No trend
Decreasing
0.05<p<0.10
Decreasing
0.01<p<0.05
Decreasing
p<0.01

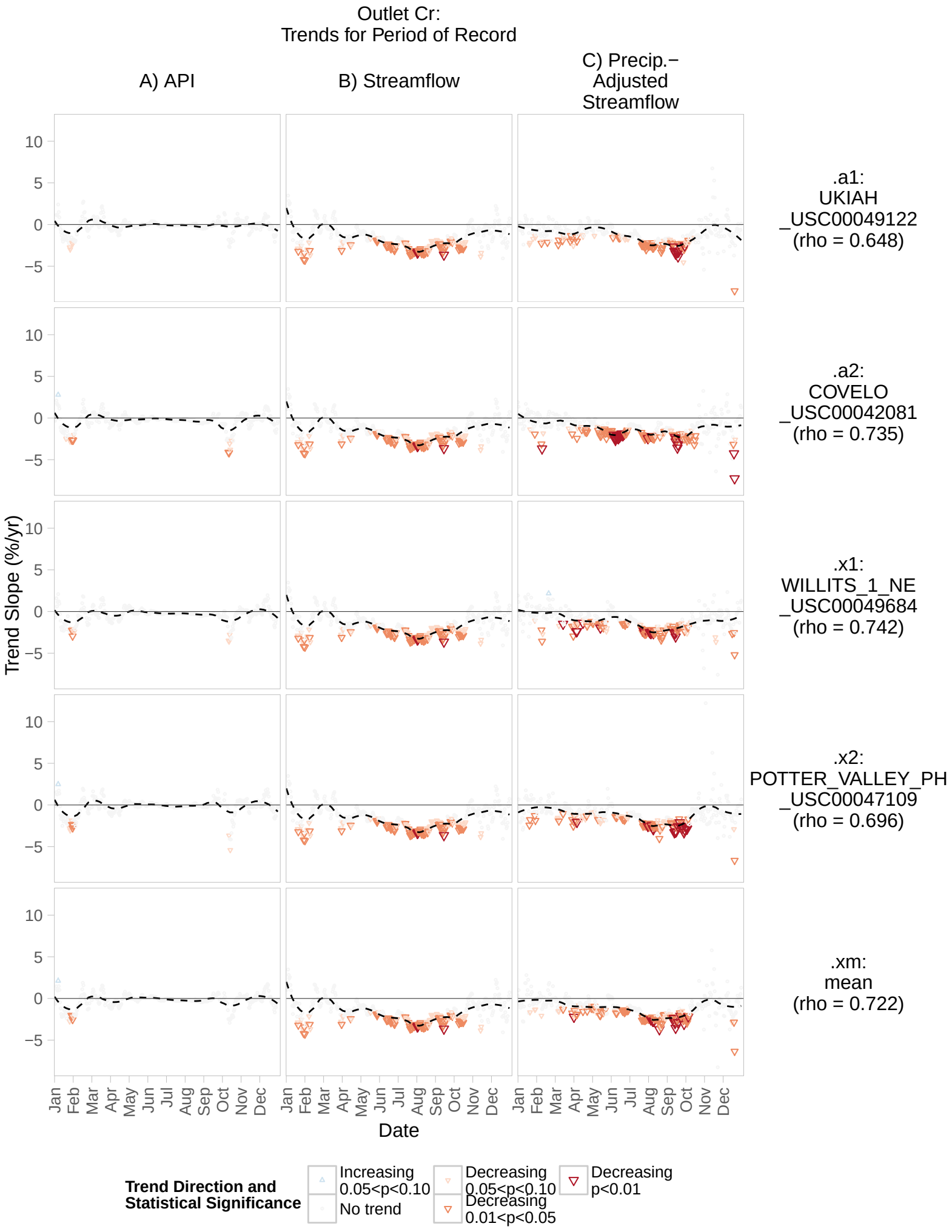
Outlet Cr:
Trends for Period of Record
A) API
B) Streamflow
C) Precip.−
Adjusted
Streamflow
.a1:
UKIAH
_USC00049122
(rho = 0.648)
.a2:
COVELO
_USC00042081
(rho = 0.735)
.x1:
WILLITS_1_NE
_USC00049684
(rho = 0.742)
.x2:
POTTER_VALLEY_PH
_USC00047109
(rho = 0.696)
.xm:
mean
(rho = 0.722)
Trend Slope (%/yr)
10
5
0
−5
Jan
Feb
Mar
Apr
May
Jun
Jul
Aug
Sep
Oct
Nov
Dec
Date
Trend Direction and
Statistical Significance
Increasing
0.05<p<0.10
No trend
Decreasing
0.05<p<0.10
Decreasing
0.01<p<0.05
Decreasing
p<0.01

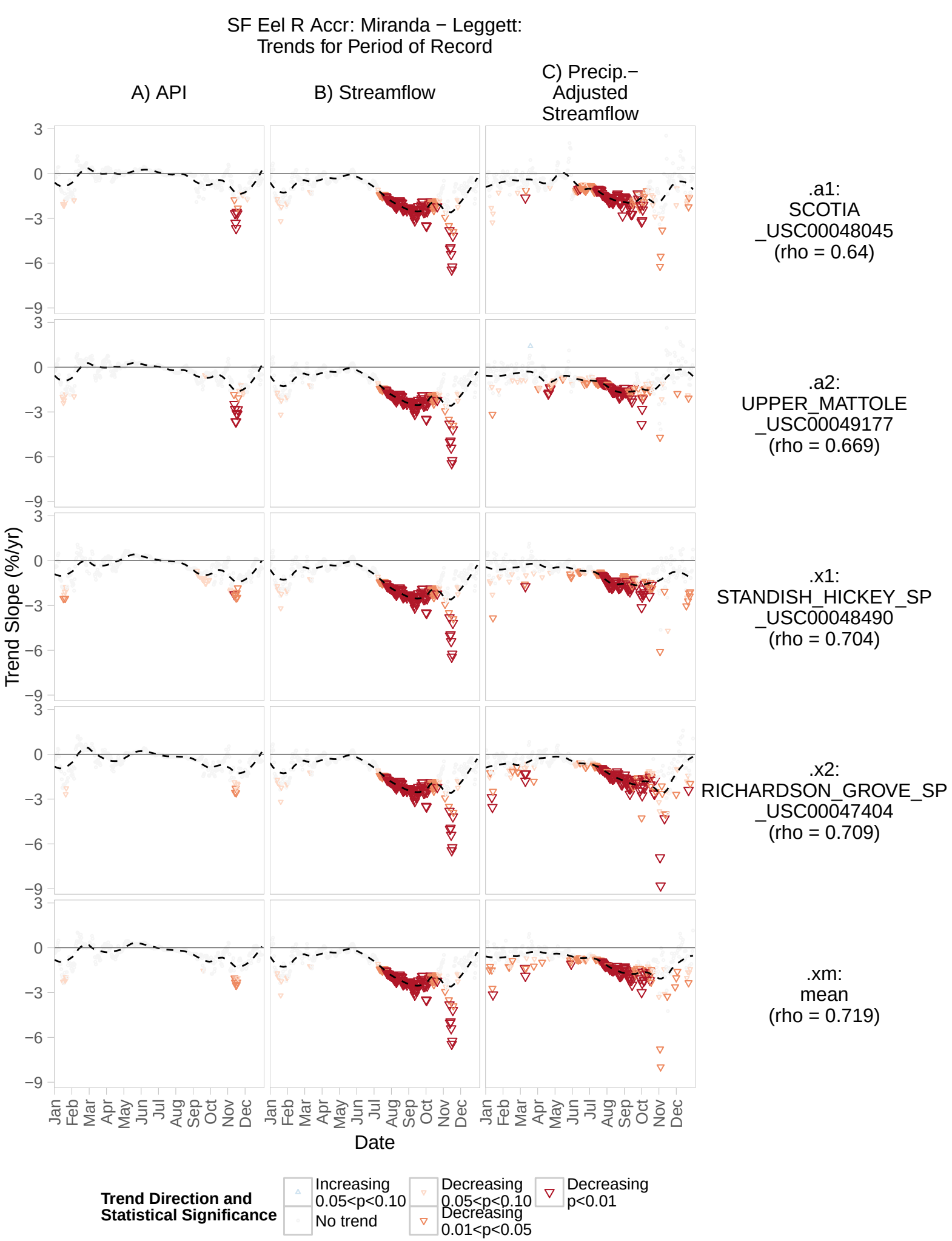
SF Eel R Accr: Miranda − Leggett:
Trends for Period of Record
A) API
B) Streamflow
C) Precip.−
Adjusted
Streamflow
.a1:
SCOTIA
_USC00048045
(rho = 0.64)
.a2:
UPPER_MATTOLE
_USC00049177
(rho = 0.669)
.x1:
STANDISH_HICKEY_SP
_USC00048490
(rho = 0.704)
.x2:
RICHARDSON_GROVE_SP
_USC00047404
(rho = 0.709)
.xm:
mean
(rho = 0.719)
Trend Slope (%/yr)
3
0
−3
−6
−9
Jan
Feb
Mar
Apr
May
Jun
Jul
Aug
Sep
Oct
Nov
Dec
Date
Trend Direction and
Statistical Significance
Increasing
0.05<p<0.10
No trend
Decreasing
0.05<p<0.10
Decreasing
0.01<p<0.05
Decreasing
p<0.01

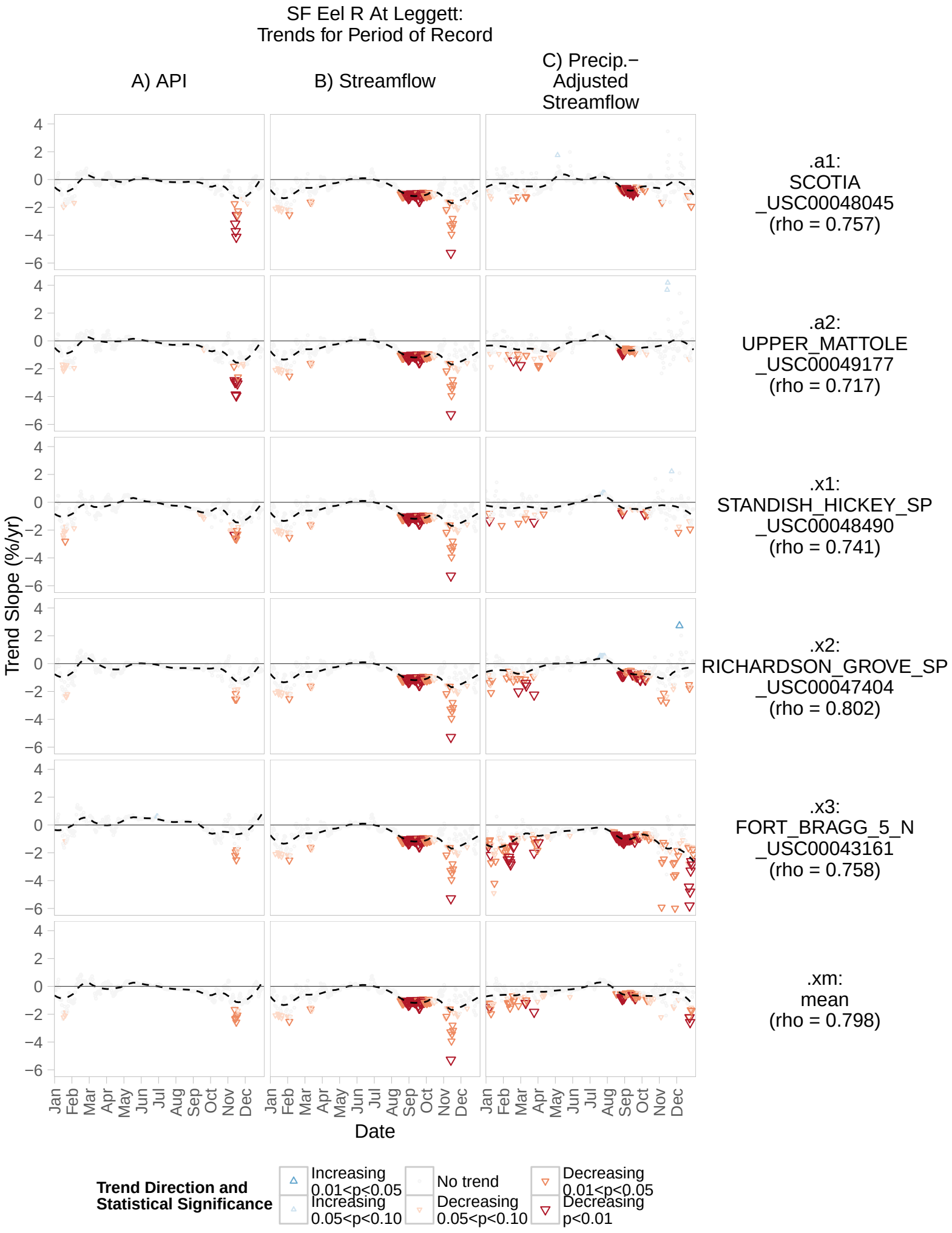
SF Eel R At Leggett:
Trends for Period of Record
A) API
B) Streamflow
C) Precip.−
Adjusted
Streamflow
.a1:
SCOTIA
_USC00048045
(rho = 0.757)
.a2:
UPPER_MATTOLE
_USC00049177
(rho = 0.717)
.x1:
STANDISH_HICKEY_SP
_USC00048490
(rho = 0.741)
.x2:
RICHARDSON_GROVE_SP
_USC00047404
(rho = 0.802)
.x3:
FORT_BRAGG_5_N
_USC00043161
(rho = 0.758)
.xm:
mean
(rho = 0.798)
Trend Slope (%/yr)
4
2
0
−2
−4
−6
Jan
Feb
Mar
Apr
May
Jun
Jul
Aug
Sep
Oct
Nov
Dec
Date
Trend Direction and
Statistical Significance
Increasing
0.01<p<0.05
Increasing
0.05<p<0.10
No trend
Decreasing
0.05<p<0.10
Decreasing
0.01<p<0.05
Decreasing
p<0.01

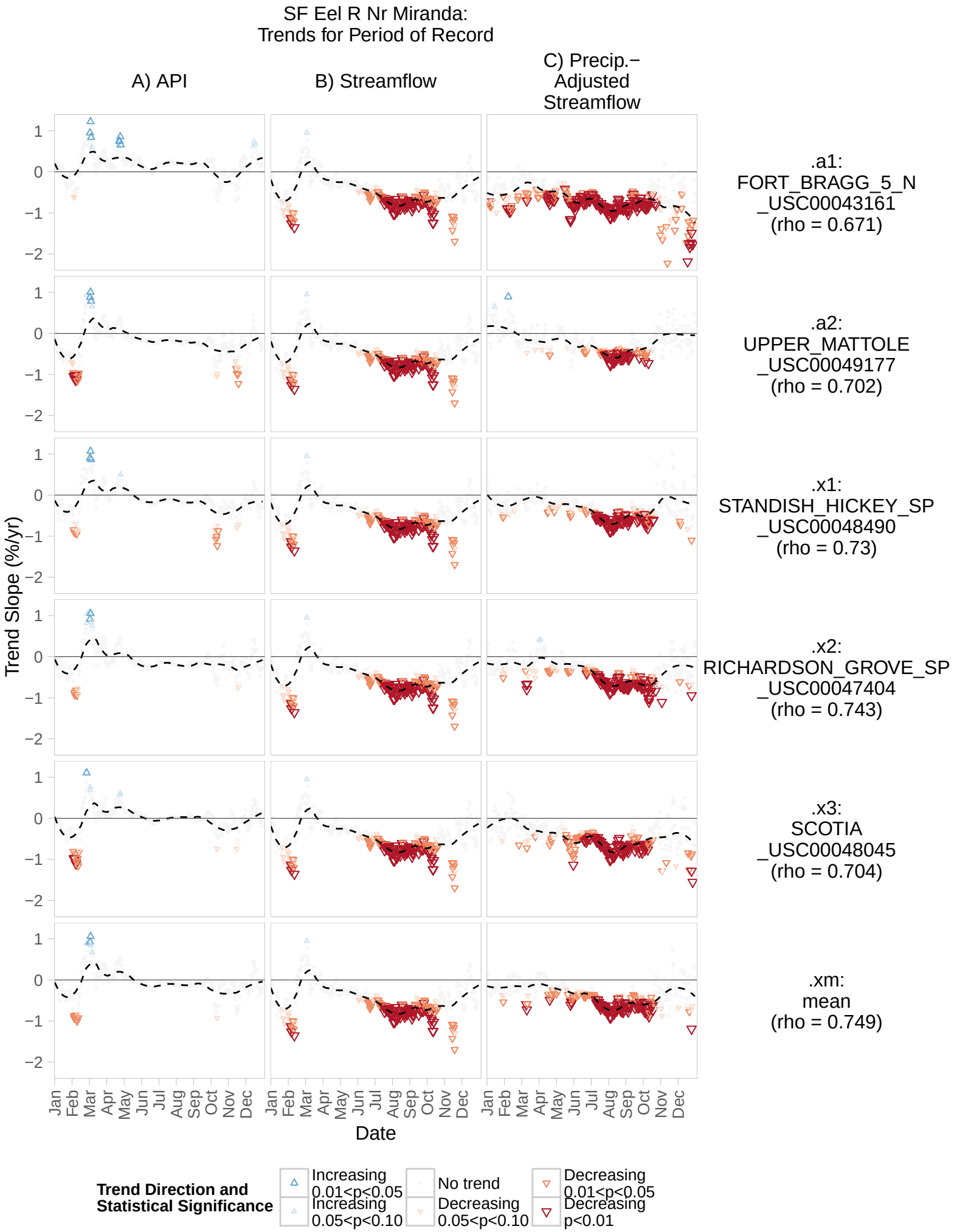
SF Eel R Nr Miranda:
Trends for Period of Record
A) API
B) Streamflow
C) Precip.−
Adjusted
Streamflow
.a1:
FORT_BRAGG_5_N
_USC00043161
(rho = 0.671)
.a2:
UPPER_MATTOLE
_USC00049177
(rho = 0.702)
.x1:
STANDISH_HICKEY_SP
_USC00048490
(rho = 0.73)
.x2:
RICHARDSON_GROVE_SP
_USC00047404
(rho = 0.743)
.x3:
SCOTIA
_USC00048045
(rho = 0.704)
.xm:
mean
(rho = 0.749)
Trend Slope (%/yr)
1
0
−1
−2
Jan
Feb
Mar
Apr
May
Jun
Jul
Aug
Sep
Oct
Nov
Dec
Date
Trend Direction and
Statistical Significance
Increasing
0.01<p<0.05
Increasing
0.05<p<0.10
No trend
Decreasing
0.05<p<0.10
Decreasing
0.01<p<0.05
Decreasing
p<0.01

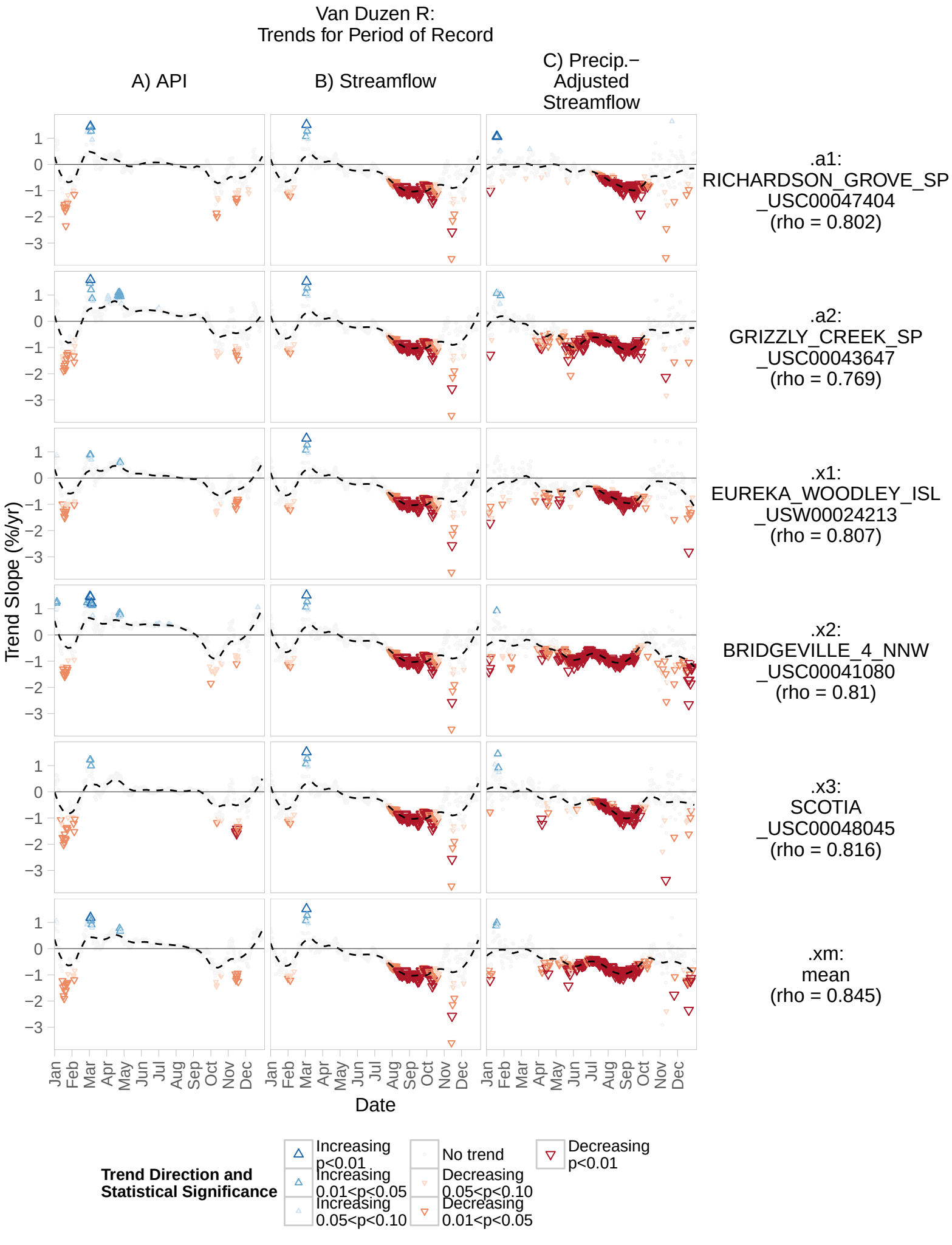
Van Duzen R:
Trends for Period of Record
A) API
B) Streamflow
C) Precip.−
Adjusted
Streamflow
.a1:
RICHARDSON_GROVE_SP
_USC00047404
(rho = 0.802)
.a2:
GRIZZLY_CREEK_SP
_USC00043647
(rho = 0.769)
.x1:
EUREKA_WOODLEY_ISL
_USW00024213
(rho = 0.807)
.x2:
BRIDGEVILLE_4_NNW
_USC00041080
(rho = 0.81)
.x3:
SCOTIA
_USC00048045
(rho = 0.816)
.xm:
mean
(rho = 0.845)
Trend Slope (%/yr)
1
0
−1
−2
−3
Jan
Feb
Mar
Apr
May
Jun
Jul
Aug
Sep
Oct
Nov
Dec
Date
Trend Direction and
Statistical Significance
Increasing
p<0.01
Increasing
0.01<p<0.05
Increasing
0.05<p<0.10
No trend
Decreasing
0.05<p<0.10
Decreasing
0.01<p<0.05
Decreasing
p<0.01